5-1-2019

# Estimation of Stage-Area-Storage Relationships in Reservoirs and Stage-Discharge Relationships in Rivers Using Remotely Sensed Data

Sailuj Shakya
e.sailuz.shakya@gmail.com

# ESTIMATION OF STAGE-AREA-STORAGE RELATIONSHIPS IN RESERVOIRS AND STAGE-DISCHARGE RELATIONSHIPS IN RIVERS USING REMOTELY SENSED DATA

By

Sailuj Shakya

Bachelor's in Civil Engineering
Tribhuwan University
2014

A thesis submitted in partial fulfillment
of the requirements for the

Master of Science in Engineering – Civil and Environmental Engineering

Department of Civil and Environmental Engineering and Construction
Howard R. Hughes College of Engineering
The Graduate College

University of Nevada, Las Vegas
May 2019

UNLV | GRADUATE COLLEGE

## Thesis Approval

The Graduate College
The University of Nevada, Las Vegas

April 15, 2019

This thesis prepared by

Sailuj Shakya

entitled

Estimation of Stage-Area-Storage Relationships in Reservoirs and Stage-Discharge Relationships In Rivers Using Remotely Sensed Data

is approved in partial fulfillment of the requirements for the degree of

Master of Science in Engineering – Civil and Environmental Engineering
Department of Civil and Environmental Engineering and Construction

Sajjad Ahmad, Ph.D.
*Examination Committee Co-chair*

Kathryn Hausbeck Korgan, Ph.D.
*Graduate College Dean*

Haroon Stephen, Ph.D.
*Examination Committee Co-chair*

David James, Ph.D.
*Examination Committee Member*

Pushkin Kachroo, Ph.D.
*Graduate College Faculty Representative*

**Abstract**

This thesis estimates the relationships between the water surface levels and quantities of water in reservoirs and rivers using remotely sensed data without any field measurements. However, the accuracies of the estimates were validated using the field measurements from ground stations. The relationships between the water surface levels and quantities are fundamental for monitoring water quantities for the operation of hydraulic structures, as well as analyzing variability and changes in hydrology. Accessibility and transparency are big issues in establishing a monitoring system that can provide field validation of efforts to model global climate systems. Remote sensing has a capability of global spatial coverage and stable temporal frequency in data acquisition, and hence can be helpful. Two types of remotely sensed data are used: satellite images, and satellite altimeter elevations. The thesis has two parts.

First, the relationships among water surface levels, areas and volumes were estimated for reservoirs. A strategic procedure, which is missing in the current literature, was formulated to estimate the water surface area, and then the water volume. Water levels were derived from Hydroweb, a satellite altimetry database. Areas were estimated from Landsat surface reflectance images by classifying the Modified Normalized Difference Water Index (MDNWI) into binary images using an internally calibrated threshold. Internal calibration of the threshold was performed by computing the overall accuracies of classification from confusion matrices created for selected regions in the classified image. Finally, water surface heights from the lowest levels and areas were used to estimate volumes assuming an inverted pyramidal shape; then, second-order polynomials were fitted to compute relationships. The fits were tested to be statistically significant by performing t-tests for coefficients and F-test for overall significance at $\alpha = 0.05$. Stage-area-storage relationships were developed for Lake Mead (LM) and Lake Powell (LP) that

are reservoirs formed in the Colorado River. The study estimated the areas of LM with a Root Mean Square Difference (RMSD) of 17.8 $km^2$ and LP with an RMSD of 53.7 $km^2$ compared with in-situ measurements. The RMSD in volumes were 699 Million Cubic Meters (MCM) for LM and 1330 MCM for LP. The second-order polynomial fits between water surface heights and volumes were established with $R^2 = 0.999$ for both LM and LP. The coefficients of the fit and the overall fit were tested to be statistically significant at $\alpha = 0.05$. The RMSD is higher in LP than LM and were explained by comparatively more shadows and a higher number of mixed pixels in the LP Landsat images than LM.

Secondly, the relationships between the water surface levels and discharges for rivers were estimated. Two major rivers, the Mississippi River and the Colorado River, representing an alluvial and rocky terrain, were selected to highlight the differences in estimates between varied terrain and size of the river. A variant of Manning's equation was used that required a channel cross-section, water surface slope, and roughness coefficient as input parameters. A parabolic cross-section was fitted for each river using the width of river estimated from the Landsat images at several water levels. Water surface slopes were estimated from water elevations at different locations on each river using two sources. For the Mississippi River, water surface elevations were obtained at virtual stations from the DAHITI database. For the Colorado River, elevations were extracted using the MAPS at river crossings. Roughness coefficients were estimated using empirical models that utilized meander length. Results showed that discharges were estimated to within 31.4% of the average discharge with root mean square error of 5700 cu.m/sec for the Mississippi River. Colorado River discharges were estimated within 30.5% of the average discharge with RMSE of 50 cu.m/sec. A linear relationship was fitted between the water surface elevation and discharges in the Mississippi River with $R^2 = 0.62$. For the Colorado River,

second-order polynomial was fitted for a relationship between water surface elevations and discharges with $R^2 = 0.99$. The coefficients of the fits and the overall significance of the fit were statistically significant at $\alpha = 0.05$ tested by performing t-tests and F-test respectively. It was difficult to estimate a cross-section for rivers with smaller channel widths or smaller changes in width with water level as in the case of the Colorado River. However, estimated accuracies were similar in both the cases in terms of percentage of error.

**Acknowledgements**

This work was supported partly by US-Pakistan Center for Advanced Studies in Water (USPCAS-W).

**This thesis is dedicated to my dear parents for their unconditional love and support, my teachers for their wisdom, and my lovely fiancé for her positive energy.**

Table of Contents

**List of Tables**

**List of Figures**

**List of Abbreviations**

ADCP - Acoustic Doppler Current Profiler

CTOH - Center for Topographic Studies of the Ocean and Hydrosphere

DAHITI-Database for Hydrological Time Series of Inland Waters

DEM-Digital Elevation Model

ERS - European Remote Sensing

GRACE - The Gravity Recovery and Climate Experiment

GRDC - Global Runoff Data Center

G-REALM - Global Reservoirs/Lakes

LEGOS - Laboratoire d'Etudes en Géophysique et Océanographie Spatiales

LM-Lake Mead

LP - Lake Powell

MAPS-Multi-mission Altimetry Processing Software

MCM -Million Cubic Meters

MNDWI – Modified Normalized Difference Water Index

RMSD -Root Mean Square Difference

RMSE -Root Mean Square Error

SWOT - Surface Water and Ocean Topography

USBR -United States Bureau of Reclamation

USGS -United States Geological Survey

WMO - World Meteorological Organization

# CHAPTER 1: Introduction

## 1.1 Research Backgrounds

"When the well is dry, we'll know the worth of water." This quote by Benjamin Franklin ("Benjamin Franklin - Inventions, Quotes & Facts - Biography") highlights two major facts. First, water is a necessity for humankind, and second, times of water scarcity make us realize how essential it is. Stress on available fresh water, due to growing demand is increasing (Ahmad, 2016; Qaiser et al., 2011). The effort to ease this stress has led to adopting two roles: first, storing water in reservoirs for needs during dry seasons (Zhou et al., 2016); and second, trying to improve the capability to predict future trends for water availability in order to increase security (Sagarika et al., 2015; Tamaddun et al., 2019). Both of these efforts require timely and complete information on the amount of available water in the hydrologic features on the surface of the earth. Climate change has affected the stationarity of hydrological processes and increased uncertainty (Milly et al., 2008, 2005; Shakya et al., 2018; Tamaddun et al., 2016, 2017, 2019). This has increased the risk of water shortages in future, and the shortages are expected to be of a larger scale, surpassing our experiences (Barnett and Pierce, 2008; Qaiser et al., 2013). Nevertheless, monitoring has become an essential part of safeguarding the availability of fresh water for the future (Busker et al., 2019; Calmant et al., 2008; Crétaux et al., 2011; Voss et al., 2013). Monitoring involves three specific tasks: acquiring, storing and analyzing data. The monitored information has a great value for modeling efforts, informing on future trends (Achhami et al., 2018; Chen et al., 2017; Moumouni, 2014; Nishat and Rahman, 2009; Westerink and Gray, 1991). Some of the monitored data includes hydrologic, climatic and oceanic variables (Ahmad et al., 2010; Wood, 1991). Hydrologic variables include ground-water levels, discharges in rivers, and volumes in lakes and reservoirs. Climatic variables include

temperature and precipitation, as well as oceanic variables, including oceanic indices, sea surface temperature and air pressure (Bhandari et al., 2018; Sagarika et al., 2015; Tamaddun et al., 2019).

Rivers, lakes/reservoirs and wetlands are the main features of surface water and major parts of the hydrological cycle (Maswood and Hossain, 2015; J. Zhang et al., 2006). Water quantities in each of these features are dynamic and participate in the exchange of moisture between the land and atmosphere. The exchange of moisture is affected by a large array of variables and uncertainties associated with them. Moreover, teleconnections between various variables in diverse regions of the globe coupled with a lagged reaction make it even harder for researchers to make accurate predictions of the amount of water that might circulate in these features (Mallakpour and Villarini, 2016; Sagarika et al., 2015; Tamaddun et al., 2017). Due to the deep integration between hydrologic and climatic factors, they are often analyzed as a single system and referred to as hydro-climatic factors. Tracking changes in water quantities in each of these features is an important source of information. Changes in the volume of water stored in lakes and reservoirs are indicators of climate variability, especially those that are not intervened upon by human activities. Remote lakes have been widely studied in order to detect climate change patterns (Irkett and Birkett, 1995; Keys and Scott, 2018). Lakes formed from snowmelt and glaciers can inform researchers on the changes in temperature as well as precipitation. Similarly, river discharges have been sources of detecting changes in the hydrologic cycle (Ficklin et al., 2016; Kalra et al., 2017). Discharges in rivers and volume in reservoirs are the most accurately measured components of the water cycle (Grabs et al., 1997; Gutowski Jr et al., 1997; Hagemann and Dumenil, 1998). Monitored data on discharge in rivers can inform us on climatic variability and the information is reciprocated to enable researchers to understand the

likely scenario of water availability in the future. A number of studies have investigated trends in river discharge on a continental scale and investigated the relationships of these trends with various climatic and oceanic factors (Pathak et al., 2016; Villarini et al., 2009). The end goal of all of these studies is to improve the prediction of available water in the future.

Current monitoring techniques require physical stations, set on the site, that are equipped with gauges calibrated to measure amounts of water. For reservoirs, volumes of water are measured at several water levels to obtain a calibrated scale (Twichell et al., 2003). Similarly, for rivers, discharges are measured at multiple water surface levels, or elevations, that form the basis of a calibrated scale, which can measure discharge flowing in the river by reading the water level (Herschy, 2014). In both cases, a relationship between the water level and quantity of water is required, and is known as a rating curve. Since water level denotes a stage of a river or reservoir, the relationship is also called stage-storage or stage-discharge curve. These relationships are the foundation for measuring water quantities in the future. Moreover, these relationships transfer the role of monitoring to a person with little expertise and remove the tediousness of measuring water quantities. Meanwhile, the measurement of water quantities requires deploying surveying equipment to estimate reservoir shapes and volumes, as well as cross-sections of the river channels (Furnans and Austin, 2008). In addition, water velocity has to be measured with instruments such as current meters that are essential to estimate discharge. The estimates of water quantities require field-measured data, which needs to be assimilated to establish a monitoring station.

The quantities of water in reservoirs are monitored by various agencies, one of which is the United States Bureau of Reclamation (USBR). The USBR was established in 1902 and is best known for the construction and maintenance of dams, power plants, and canals in 17

western states. Discharges in rivers, on the other hand, are measured and recorded in the United States by the United States Geological Survey (USGS) for more than 28,000 physical stations. The data is acquired, processed, stored and distributed using the National Water Information System (NWIS) and can be accessed via waterdata.usgs.gov/nwis/sw (Goodall et al., 2008). The USGS was created by an act of Congress in 1879 and is the sole science agency of the department of the interior. These are examples of institutions that are responsible for monitoring water quantities in the United States.

Such similar institutional setup is found in almost all other nations in the world. This means monitored data are internationally fractioned, and it is difficult to weave the monitoring efforts into a single framework. The effort becomes more challenging due to transparency issues and the reluctance of nations to participate in such joint efforts. However, efforts are being made to bring the available monitored data into a single framework. One such effort is the establishment of the Global Reservoir and Dam Database, containing 6,862 records of reservoirs (Lehner et al., 2011). Similarly, the Global Runoff Data Center (GRDC) operating under the auspices of the World Meteorological Organization (WMO) is another example (Vörösmarty et al., 2001). The data center has been tasked to collect and archive in-situ earth observations globally. These databases are still reliant on the donors of the data, and often do not receive up-to-date data or do not receive it at all. These efforts are still short in achieving global data. Moreover, the distribution of stations is inadequate in many regions of the world.

## 1.2 Research Motivation

Satellites are capable of global coverage with stable temporal periodicity both of which are favorable qualities required for a monitoring platform (Gleason and Smith, 2014; Irkett and Birkett, 1995; Smith, 1997). Thus, the use of satellite platforms to deploy sensors that can

measure variables capable of estimating water quantities has been a major interest of remote sensing and water resources research communities (McFeeters, 1996; Oubanas et al., 2018). Some of the data gathered with sensors are multi-disciplinary. For example, Operational Land Imager (OLI), mounted on Landsat 8 missions, provides multi-spectral images of the earth's surface. These images have been used to detect various features of the earth including water (Moradi et al., 2017; Stephen, Ahmad, and Piechota, 2010; Zhai et al., 2015). Some of the sensors are specific for measuring variables related to water (Abedin and Stephen, 2019; Puri et al., 2011b, 2011a; Stephen, Ahmad, Piechota, et al., 2010). Radar altimeters are an example of such sensors and have been primarily deployed to measure sea surface elevations (Smith, 1997; Stewart, 1985). The changes in sea surface elevations give vital information to understand global warming impacts on sea level. Some of the satellites have been deployed to track changes in the gravitational force of the earth, such as the Gravity Recovery and Climate Experiment (GRACE). Changes in moisture are the most dynamic aspect of the gravitation of the earth and linked with changes in ground and surface water (Voss et al., 2013). This study will focus on two types of data acquired by satellites: satellite radar elevations, and satellite multispectral images.

Satellite altimetry and imagery has been used to estimate lake and reservoir water elevations and storage variations in diverse regions of the globe (Crétaux et al., 2011; Gao et al., 2012; Schwatke et al., 2015; S. Zhang et al., 2014). There are two general approaches, which have been adopted for two different use cases. First, satellite data has been used in combination with field measured data to develop relationships. These have been termed as at a station hydraulic geometry, or at-many-stations hydraulic geometry based on the number of stations that are being used (Durand et al., 2016). Some of the studies adopted hydrologic model outputs instead of field-measured data to obtain this relationship. However, the models also require field

measured information such as channel cross-section and slope to produce similar water quantities. These relationships are then used to device a monitoring system that is able to measure water quantities. While having some field information is always beneficial to calibrate models or establish boundary conditions, it is not always possible (Durand et al., 2014; Frappart et al., 2015). There are many river systems in diverse regions of the world that have no field measurements available. The second method attempts to measure water quantities independent of any field measurements using only remotely sensed data. Both of the methods are useful and have practical applications in the real world. An example of a study that has been conducted for the first case for reservoirs is the use of the digital bathymetry model and water levels derived from TOPEX/Poseidon (T/P) altimetry data. These data were used to reconstruct water volume variations in the in-land lake Big Aral Sea (Crétaux et al., 2005). Further, an example of a study conducted for the second case is the use of a combination of Satellite radar altimetry and satellite imagery to derive volume variations in the Negro River Basin (Frappart et al., 2008, 2005).

The status of the estimation of discharge in rivers is very similar to reservoirs with two approaches: using field data or information, and without out using any field information. Satellite information has been combined with field data to obtain a monitoring system for rivers (Bogning et al., 2018; Kouraev et al., 2004; Papa et al., 2012). Satellite technology that can measure discharges in rivers directly has not yet been possible. However, efforts have been made to use available satellite-based information to estimate discharge. One such recent study by Bjerklie et al. (2018) estimated discharge in the Yukon River within 21%, with the use of elevation computed from satellite radar and laser altimeters and the width of the river from the Dynamic Water Surface Extent (DWSE), a provisional product computed from Landsat images. Explored satellite-based information includes river morphology from images and water surface slopes

from radar altimeters. The upcoming Surface Water and Ocean Topography (SWOT) mission (http://swot.jpl.nasa.gov/mission/) is targeted to conduct the first global survey of the earth's surface water. It is scheduled to launch in 2021 and will include wide swath radar that provides water surface extent, height, and slope in rivers of 100m or greater width (Biancamaria et al., 2016). This has led the research community to develop algorithms to estimate the discharge in rivers from remote observations of river channels in anticipation of the data from the SWOT mission (Bonnema et al., 2016; Durand et al., 2016). Although, studies have demonstrated completely remotely sensed data approaches to estimate water volumes in reservoirs and discharges in rivers, which can develop relationships between water surface levels and water quantities, certain aspects of the estimation methods and algorithms are still lacking. The goals of these relationships were to monitor water quantities in these features and hence accomplish a single framework for global monitoring. In the case of reservoirs, a specific methodology to address the spatial and temporal variability of the reflectivity of water for estimation of the area is lacking. The estimation of the area from multi-spectral satellite images is an important part. Satellite radar altimeters have been improving in obtaining accurate elevations up to few millimeters but area estimation still lacks a strategic procedure. Similarly, although global monitoring is a major benefit for remotely sensed data, the robustness of the algorithms in diverse regions are still unexplored for many of them. This persists in the estimation of discharge in rivers. Estimation algorithms have not been analyzed for rivers that are diverse in size and nature. This research will focus on highlighting the dependence of accuracy in discharge estimates on the size and nature that is not present in the literature.

## 1.3 Research Objectives

The objective of this research was to estimate water quantities in river and lakes with specific approaches, using only remotely sensed data without any field measurements. Two sources of remotely sensed information were used. One source is water surface elevations, which were acquired with satellite altimeters, and the other is water surface area acquired with satellite imagers. The quantities of water were paired with their corresponding water surface elevations in order to obtain relationships between them. These relationships form the basis for monitoring water quantities from satellite observations that have global coverage and stable temporal frequency. Both of these qualities are favorable for understanding the hydrological cycle of the globe, and its interdependence with climatic and oceanic factors. Reliable estimates of water surface elevations and water surface areas are essential for estimating water levels and water quantity relationships. The understanding of water circulation enlightens the moisture exchange process, and the monitored data can better support modeling efforts. The research has two distinct objectives, and each objective has its specific questions and corresponding hypotheses. The goal of this research is to answer these questions and test the hypotheses.

**Objective 1: Estimation of the stage-area-storage relationships of reservoirs using remotely sensed data**

**Research Questions #1:**

1. How well can the relationships among water surface elevation, area, and storage in reservoirs be estimated from remotely sensed data without the use of any field measurements?
2. What are the types and sources of errors in the estimates?

3. What differences can be found in estimations between different reservoirs, and what is the possible cause of the differences?

**Hypotheses #1:** Estimates of water volumes in reservoirs at various water surface elevations are within reasonable limits. These estimates can be paired to estimate relationships that are reasonably close to the estimates from field measurements. The differences in estimates between field measurements and remote sensing can be explained in the limitations of remotely sensed data such as pixel size, as well as errors due to shadows and human constructions in the water. The features of reservoirs such as shape and size, as well as the presence of shadows due to deep canyons, should affect the estimations.

**Objective 2: Estimation of stage-discharge relationships in rivers using remotely sensed data**

**Research Questions #2:**

1. How well can the relationships between water surface elevation and discharges in the rivers be estimated from remotely sensed data without the use of field measurements?
2. What are the types and sources of errors in the estimates?
3. What differences can be found among the estimates of discharges for different rivers, and what are the possible causes of the differences?

**Hypotheses #2:** Algorithms that utilize hydraulic and morphologic information such as water surface width, slope, and meander length, can estimate discharges within reasonable limits. The accuracy of the estimates of slope and width should play a major role in the discharge estimates and might depend on limitations of remotely sensed data, such as accuracy in water surface elevation from radar altimetry and pixel sizes of Landsat image for detecting changes in

water surface width. The nature of the terrain is expected to influence meander patterns and channel cross-section, and hence, the reliability of the discharge estimates. A river with a larger water surface area and with a higher range of operation should be more favorable for detecting these changes, and hence, lead to more reliable estimates.

## 1.4 Research Tasks

Research tasks are broken into two parts following the objectives that are set out in section 1.3. The research works are presented in a manuscript format. There are four main chapters. This chapter, Chapter 1, provides the background of the research, motivation for this work, formulation of the problem statements and corresponding hypotheses.

Chapter 2 is a section titled "Estimation of Stage-area-storage Relationships of Reservoirs Using Remotely Sensed Data" which addresses Objective 1. Two of the largest reservoirs in the United States, Lake Mead and Lake Powell, which are both formed on the Colorado River, are studied in this chapter. Two types of remotely sensed data are used: 1) Water surface elevations measured by satellite radar altimeters, and satellite multi-spectral images. Fourteen years of data for Lake Mead and 12 years of data for Lake Powell are analyzed in order to obtain sets of elevation and water volume relationships that can be used to develop storage-elevation relationships. Water surface elevations are obtained from the Hydroweb database, which has been developed by the French agency Laboratoire d'Etudes en Géophysique et Océanographie Spatiales (LEGOS). The data are currently accessed via Theia land data services center portal (http://hydroweb.theia-land.fr/). Satellite images from the thematic mappers deployed on the Landsat 5 satellites are used to extract water surface features using spectral indices. The images are downloaded via USGS Earth Explorer (https://earthexplorer.usgs.gov). The accuracy of the estimates is compared with field measurements that are obtained from the

United States Bureau of Reclamation (USBR) websites for the upper and lower Colorado Regions.

Chapter 3 is titled, "Estimating stage-discharge relationship in rivers Using Remotely Sensed Data" and addresses Objective 2. Manning's equation is used to estimate discharges. The equation requires water surface slope, channel cross-section, and roughness coefficient information. Water surface slopes are estimated with elevations at two river channel locations acquired from satellite radar altimeters. Satellite images in combination with water surface elevations are used to estimate a parabolic channel cross-section, and roughness coefficients are estimated from meander length and slope of water surface using empirical models derived by previous studies. Discharges are estimated for the Mississippi River and the Colorado River. Satellite-measured elevations at virtual stations are downloaded from the Database for Hydrological Time Series of Inland Waters (DAHITI) database for the Mississippi River. Multi-mission Altimetry Processing Software (MAPS), developed by the Center for Topographic Studies of the Ocean and Hydrosphere (CTOH), is used to extract water surface elevations at crossings for the Colorado River. Landsat 5, Thematic Mapper (TM) and Landsat 8, Operational Land Imager (OLI) images are used to estimate water surface width. Three years of data are used for the Mississippi River, and 4 years of data are used for the Colorado River depending on the temporal overlap of the satellite missions to acquire a consistent elevation, and image data for the river from the same sensors. Chapter 4 summarizes the results and provides recommendations for future research.

## CHAPTER 2: Estimation of Stage-area-storage Relationships of Reservoirs Using Remotely Sensed Data

### Abstract

Understanding the relationships among the water levels, surface areas, and volumes of reservoirs and lakes are crucial for water management. However, the lack of communication about transboundary water resources and lack of accessibility to remote lakes has affected the availability of data. This has led to the problem in the estimation of these relationships. This study demonstrates the capability of remotely sensed data to estimate reservoir stage-area-storage relationships with a strategic procedure for area estimation that is not available in the current literature. Water levels for two North American lakes were derived from the Hydroweb satellite altimetry database. Areas were estimated from Landsat surface reflectance images by classifying the Modified Normalized Difference Water Index (MDNWI) into binary images using an internally calibrated threshold. Internal calibration of the threshold was performed by computing the overall accuracies of classification from confusion matrices created for selected regions in the classified images. Finally, water surface heights from the lowest levels and areas were used to estimate volume assuming an inverted pyramidal shape, and second-order polynomials were fitted to compute relationships. Stage-area-storage relationships were developed for Lake Mead (LM) and Lake Powell (LP) that are reservoirs formed on the Colorado River. Areas were estimated with the following uncertainties compared to in situ measurements. For LM, a Root Mean Square Difference (RMSD) of 17.8 $km^2$, and for LP with an RMSD of 53.7 $km^2$. The RMSD in volumes were 699 Million Cubic Meters (MCM) for LM and 1330 MCM for LP. The second-order polynomial fits between water surface heights and volumes were established with $R^2 = 0.999$ for both LM and LP. The coefficients of the fit and the

overall fit were tested to be statistically significant at $\alpha = 0.05$. The RMSD is higher in LP than LM and were explained by comparatively more shadows and a higher number of mixed pixels in the LP Landsat images than LM.

## 2.1 Introduction

Estimates of accurate surface levels, areas, and volumes of water stored in reservoirs and lakes are crucial for their regulation, as well as the management of water demands. Estimation of evaporative losses and electric power generation are some of the applications that depend on these estimates. For example, the evaporative loss from Lake Mead (LM), computed to be 7.5 ft. in 1997-99 (Friedrich et al., 2017; Westenburg et al., 2006), was estimated using field measurements of evaporation rates and summing them over the water area. These estimates were tabulated in the form of relationships among elevation, area, and storage (called stage-area-storage relationships) to facilitate reservoir regulation. These relationships are also required for the monitoring of remote inland water bodies that are studied as an indicator of change (Crétaux and Calmant, 2016).

The application of traditional field surveys to estimate stage-area-storage relationships for reservoirs can be a challenge in certain circumstances, such as transboundary basins and remote lakes. A complex web of environmental, political, economic and security interdependencies that complicate basin-wide management link transboundary resources. Sometimes, relationships developed from field measurements may not be accessible due to imposed restrictions on data sharing and lack of co-operation (Hirpa et al., 2013). Moreover, around 60% of the world's international river basins lack cooperative management framework (4$^{th}$ UN World Water Development Report, 2012). There have been 37 acute disputes involving violence in the last 50 years, as well as 150 treaties that involve transboundary water. Countries in regions such as

southeast Asia have failed to reach agreements on sharing the waters of transboundary rivers (Biancamaria et al., 2011; Zhang et al., 2014). This data scarcity and inaccessibility can result in an incomplete understanding of water availability and flood warnings (Crétaux and Calmant, 2016).

The complications related to transparency and the inaccessibility of the information on transboundary or remote water resources require the development of techniques that can estimate these relationships remotely. Satellite remote sensing, particularly altimetry and imagery, is a promising alternative to estimate water surface elevation, area, and volume relationships in reservoirs. Remote sensing has a capability of large spatial coverage that goes beyond the geographical and political limitations. It is capable of long-term data acquisition with consistent temporal and spatial resolutions. The availability of long-term data can be used to formulate or update existing stage-storage relationships for reservoirs with the cost and time of the efficiency. Further, determining the absolute water volume of a lake is not possible with current technologies without precise bathymetry (Lei et al., 2014). However, the determination of the absolute water volume of a lake is not fundamental when the calculation of volume variations within the operating range is of concern (Duan and Bastiaanssen, 2013).

Satellite altimetry and imagery have been used to estimate lake and reservoir water elevation and storage variation worldwide. Additionally, satellite radar altimetry has been combined with satellite imagery to obtain volume variations of surface water in river basins such as the Negro River Basin (Frappart et al., 2008, 2005), the lower Mekong River Basin (Frappart et al., 2006) and the Lower Ob' Basin (Frappart et al., 2010). Similar techniques have been used to reconstruct water volume variations in the in-land lake Big Aral Sea using a digital bathymetry model and water levels derived from TOPEX/Poseidon (T/P) altimetry data (Crétaux

and Calmant, 2016). Further, Peng et al. (2006) used Landsat images to estimate the area of a reservoir and combined it with in-situ water level data to obtain a storage curve. Many studies have illustrated the capability of satellite altimetry for lake surveys in different water bodies around the globe (Birkett, 1995; Coe and Birkett, 2004; Hwang et al., 2005; Kleinherenbrink et al., 2015; Medina et al., 2008; Singh et al., 2012). Although these studies have adopted a combination of remotely sensed and in-situ data, completely remotely sensed data specific approaches to address the spatial and temporal variability of the reflectivity of water for the estimation of area are lacking.

Satellite altimetry is based on the calculation of range, and is estimated based on the time evolution of returned waveform of short radar (or laser) pulses (Birkett and Beckley, 2010; Fu and Cazenave, 2000). Radar altimeters use microwave pulses (e.g., Ku band, C-band and S-band) (Rosmorduc et al., 2011) and are an all-weather measurement system. The resulting altimetry height is with respect to a reference ellipsoid and the height is the mean value within the altimeter footprint. The ellipsoidal height can be further converted into orthometric height by removing a geoid height above the reference ellipsoid. The diameter of the footprint typically ranges between 200m to a few kilometers. Each satellite is placed in a specific repeat orbit and the time series of surface height changes can be constructed for a particular location along the satellite ground track during the lifetime of the mission. The satellite altimetry technology was initially developed for open oceans to monitor sea surface height and polar ice caps (Chelton et al., 2001).

The accuracy of water surface height measurement for a satellite altimeter depends on the length and size of the effective track over a lake (Crétaux et al., 2015), as well as a lake's environment (particularly ice and snow in winter). Large but narrow reservoirs have a lower

accuracy of the measurement. An assessment of 24 lakes of various sizes located in different regions showed sub-decimeter accuracy for big lakes (Crétaux et al., 2016). Despite some limitations, altimetry is a technique that has proven potential for hydrology science since the data are freely available worldwide, and it is the only source of information for most lakes in remote areas.

Satellite imagery has been used to map various features including water, and investigators have developed several different methods to identify water pixels in a satellite image. The methods can be grouped into single-band and multi-band, based on the number of bands used. Both surface reflectance and satellite digital numbers have been used to estimate water extent in practice (Crétaux et al., 2011). A multiband method utilizes the reflective difference in each multi-spectral band (Otsu 1979). Spectral water index is an effective way to obtain a single number derived from an arithmetic operation (e.g., ratio, difference, and normalized difference) of two or more spectral bands. The goal of the arithmetic operation is to enhance the spectral signals by contrasting the reflectance between different wavelengths and cancels out most of the noise components that are common in different wavelength regions. Among various spectral indices used for water pixel identification, the Modified Normalized Difference Water Index (MNDWI) was found to be best for pure water pixel detection and is recommended for use in mapping surfaces affected by mixed pixels. Meanwhile, comparative studies have found other indices using different bands are suitable for various conditions (Boschetti et al., 2014; Ji et al., 2009; McFeeters, 1996; Ouma and Tateishi, 2006; Xu, 2006). An appropriate threshold of the index is required to separate water bodies from other land-cover features based on their spectral characteristics.

The selection of the appropriate threshold affects the estimation of water from spectral index image. Choosing the appropriate threshold can be difficult because of two main issues. First, band ratios that are calculated from different band combinations have different threshold values for the same feature. Additionally, the optical properties of surface objects also vary with time due to factors such as atmospheric or soil conditions, varying sun-target-satellite geometry, water turbidity, sediment load, and sensor degradations. Liu et al. (2012) showed that small threshold variations can occur even daily. Secondly, the band ratio threshold varies depending on the proportion of sub-pixel water/land/vegetation components. Performance of a combination of the band also depends on the instrument used and specific conditions of the study zone (water turbidity/depth, percentage of water present in the pixel). Subjective selection of the threshold value may lead to an over or underestimation of open water area. As an example, longitudinal profiles of MNDWI/NDWI across Lake Zhari Namco showed variation in middle and shore (Lei et al., 2018).

The estimation of water area from the classified MNDWI has been carried out by counting the number of water classified pixels in a region of interest and multiplying this by the pixel area (Busker et al., 2019). The drawback of this approach is that the segregation of the water pixels cannot be tracked. Water bodies such as reservoirs are ideally continuous areas, but could be segregated due to errors in classification or mixed pixels in narrow sections of the water body. Some studies ( e.g., Duan and Bastiaanssen, 2013) have undertaken to inspect and to digitize water areas in the raster data manually, which is more reliable and accurate, but is inefficient.

The goal of this study is to estimate the stage-area-storage relationships for two reservoirs, Lake Mead and Lake Powell, with only remotely sensed data. The satellite altimetry

data product is used for lake surface level elevations and satellite image classification is used to estimate lake surface areas. Satellite altimetry elevations were obtained from the Hydroweb database developed by LEGOS laboratory (Crétaux and Birkett, 2006). The areas of the lakes were estimated from Landsat surface reflectance images. It is noted that the temporally closest Hydroweb data and Landsat images were used to avoid temporal discrepancies between elevation and surface area estimates. The Modified Normalized Difference Water Index (MNDWI), which is a spectral water index computed from Landsat image bands, was computed and classified to obtain a binary image of surface water.

The estimation of water area from images is complex, especially when the classification involves different locations and times. This complexity is addressed in this study with the internal calibration of the MNDWI threshold. Internal calibration involved the computation of the overall accuracy of classification based on selected regions by creating a confusion matrix. Area of the identified water surface was estimated by creating polygons and selecting the largest contiguous polygon. Finally, the combination of area and elevation was used to estimate stage-area-storage relationships. The estimated elevations, areas, and volumes were compared with in-situ measurements and capacity tables in use provided by the United States Bureau of Reclamation (USBR) and the Hydroweb database.

## 2.2 Study Area and Data

The two reservoirs, Lake Mead (LM) and Lake Powell (LP), located in the Colorado River Basin, are paragons of water management in a transboundary river. These reservoirs are formed on the Colorado River flowing through the United States and Mexico and represent the arid and semi-arid regions. LM is the largest reservoir in the United States in terms of water capacity. It is formed by the Hoover Dam in the states of Nevada and Arizona and has a capacity

of 32,236 Million Cubic Meters (MCM). LM receives most of its water from snow-melt in the Colorado, Wyoming, and Utah Rocky Mountains. Inflows to the lake are largely moderated by the upstream Glen Canyon Dam and outflow from the Hoover Dam. The lake has three distinct arms (Figure 2-1). It is divided into several bodies: Boulder Basin in the southwest; Virgin Basin in the mid-area; Temple Basin and Gregg Basin towards the southeast; and Overton Arm towards the north. LP is the second largest reservoir by maximum water capacity in the United States located between the borders of Utah and Arizona. The major tributaries draining into LP are the Colorado, Green, and San Juan Rivers. LP was created by the flooding of Glen Canyon by the Glen Canyon Dam. The reservoir is filamentous in shape and extends through the main corridor of Glen Canyon as well as into over 90 side canyons that extend outward (Figure 2-1). Some of the major parts of LP are Wahweap and Bullfrog, which are popular for marinas and beaches.

Water surface elevations were derived from the Hydroweb database computed from satellite altimetry, which is developed by French agency Laboratoire d'Etudes en Géophysique et Océanographie Spatiales (LEGOS). Elevations for LM were also available from other databases such as ICESat-GLAS and DAHITI. For LP, elevations were also available from DAHITI and G-REALM. However, ICESat-GLAS requires further processing to estimate water surface elevations and is beyond the scope of this study. Moreover, Hydroweb provided water surface elevations for both LM and LP, with information on areas and volume changes for some of the elevations which other databases were lacking. This made Hydroweb the ideal product for this task, and it has been adopted in this study. The lake/reservoir levels in Hydroweb are based on merged T/P, Jason, ERS, ENVISAT and GFO data (Crétaux and Birkett, 2006; Crétaux et al., 2011). The ground track coverage of the satellite radar altimeters over the LM and LP can be located using the Pass Locator at www.avisco.oceanobs.com (Figure 2-1).

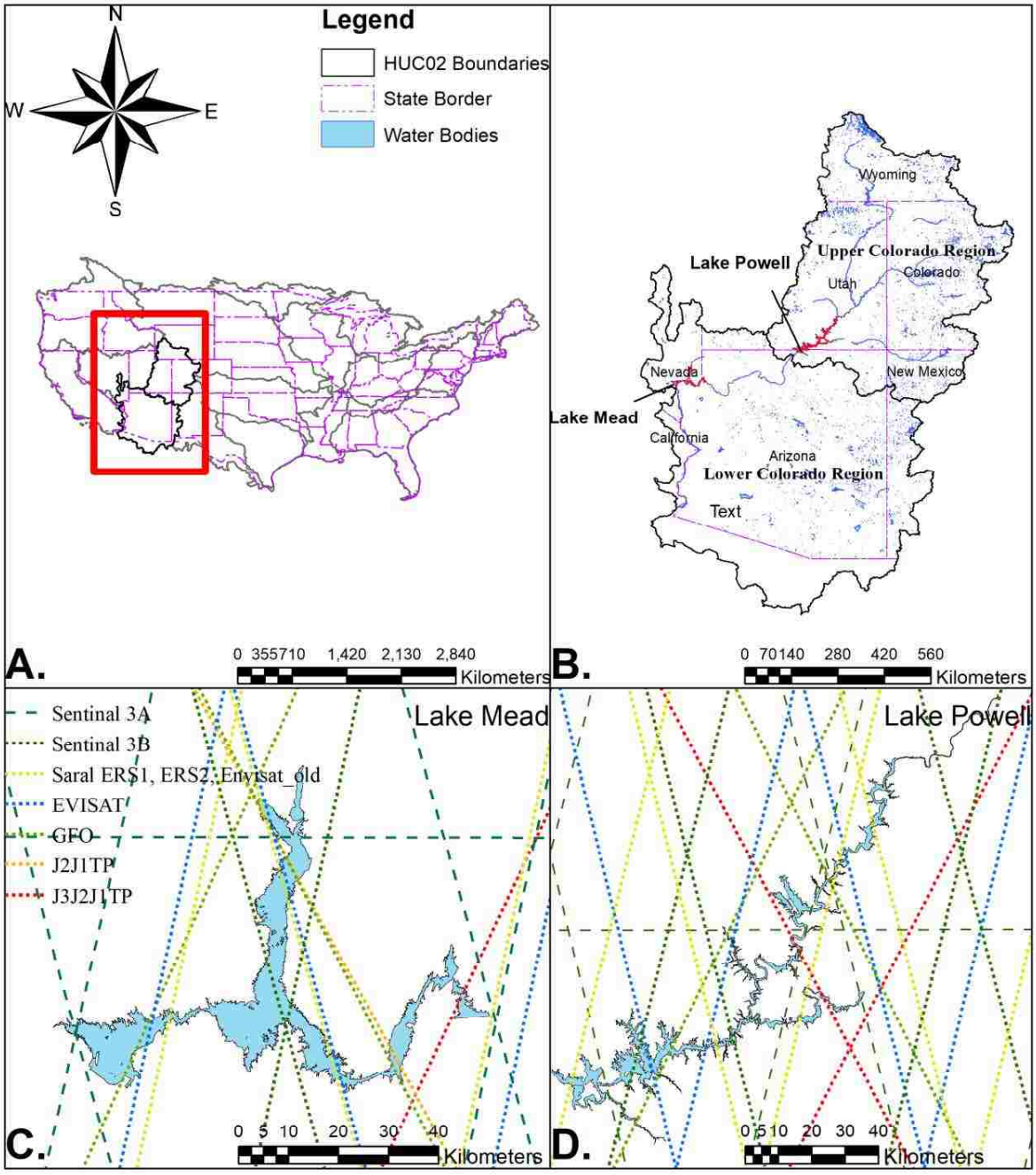


Figure 2-1: Lake Mead and Lake Powell are two major reservoirs in the Colorado River Basin (a & b). The reservoirs are overpassed by several satellite altimeters such as Sentinal 3A and 3B, Saral, ERS 1 & 2, Envisat, GFO, Jason 1-3 and TOPEX-Poseidon (c & d) that are represented by unique dotted lines.

Water surface elevations were downloaded via the website www.hydroweb.theia-land.fr. Fifteen elevations were systematically sampled from the available 119 elevation data for LM and 124 elevation data for LP. It was noted that the temporal spacing of the available elevations was not uniform because of differences in the orbit periods of the satellites used for estimation (Crétaux et al., 2011; Duan and Bastiaanssen, 2013). The choice of altimetry elevation also depended on the availability of a cloud-free image corresponding to the date on which the elevation was sensed. Water surface elevations were available from 2000 to 2014 for LM (14 years), and 1992 to 2010 (18 years) for LP. A series of increasing elevations, representing different stages of the reservoir, were created and numbered from the lowest level to the highest level (Appendix Table A1 & A2). These will be referred to as stage no. throughout this document. One important consideration when using the altimetry elevation product was that the water levels in Hydroweb were referenced to the GRACE GGM02C geoid while the elevations from the USBR were referenced to local datum. Elevations referenced to different datum cannot be compared or computed.

Landsat Surface reflectance level 2 products, corresponding to the selected altimetry elevation data for LM and LP, were download from the Earth Explorer portal of the USGS (https://earthexplorer.usgs.gov). The surface reflectance data product is generated from specialized software called Landsat Ecosystem Disturbance Adaptive Processing System (LEDAPS), which applies atmospheric correction routines to Level-1 Landsat Thematic Mapper (TM) data. Water vapor, ozone, geopotential height, aerosol optical thickness, and digital elevation are input with Landsat data to support simulation of a satellite signal in the solar spectrum radiative transfer models in order to generate surface reflectance, as well as masks for clouds, cloud shadows, adjacent clouds, land, and water (Schmidt et al., 2013). An image search

window of 10 days before and after the altimetry data available was used to get the best available corresponding image. Ideally, the image of the day when the elevation was estimated by radar altimeters is required but factors such as different crossover repeat cycles of Landsat and altimeter satellites, and cloud cover makes it difficult to attain such ideal scenarios. Moreover, analysis of daily in-situ measurements showed a minimal variation of water levels during a short period of times (Duan & Bastiaanssen, 2013). Elevations for LM after 2011 were not used as Thematic Mapper (TM) images discontinued and images from the different sensor would bring discrepancy in the calibration and area estimation. The variance of water reflectance in different bands among the images was noted by calculating the mean reflectance of water pixels in a selected area. It can be noticed that water has low reflectance values in the NIR and SWIR bands (band 4 and band 5 for TM) and high reflectance value in green bands (band 2 for TM). The outliers present in the reflectance for all the images were random and did not persist for a single image, nor did they have any bias or trend present.

The selected altimetry data, dates and the corresponding images from the Landsat that were used are summarized in Appendix Tables A1 for LM and A2 for LP. The difference between the day of acquisition of the elevation data and the day of acquisition of the remotely sensed data for LM ranges between one and 10 days with an average of 4.5 days. For LP, the difference ranges between one and 11 days with an average of four days.

Daily in-situ water levels for the period of 2000 to 2011 for LM, and for the period of 1992 to 2010 for LP, were obtained from the USBR website https://www.usbr.gov (referred as '*USBR values'* after this). The most updated area and capacity tables for LM, also known as 2001/2009 tables, are from the refinement of the LM survey of 1963-1964 by the Coast and Geodetic Survey with an underwater bathymetric survey of LM conducted in 2001 and a Light

Detection and Ranging (LiDAR) survey of LM conducted in 2009 (Tighi and Callejo, 2011). The tables provide the capacities and surface areas between the dead storage elevation of 273m (895.0 ft.) and maximum water surface elevation of 375m (1,229.0 ft.). The elevations in these tables are referenced to the United States Geological Survey datum, adjustment of 1912. The operational water level area and volume relationship for LP used by the USBR were obtained through correspondence and is formulated from a survey in 1986 (Ferrari, 1988) conducted by the USBR. The sediment elevations were determined by a bathymetric survey using sonic depth recording equipment mounted in a power boat. The reservoir capacity was computed based on surface areas determined by a range-line survey.

The shore boundary of a lake/reservoir (termed as "*boundary polygon*" in this document) was obtained from Twichell et al. (2003) for LM and delimits the bounds of LM at full capacity (approximately 375 m elevation). For LP the lake boundary was available from a modified subset of the National Hydrology Database (NHD) and accessed via https://gis.utah.gov/data/water/lakes-rivers-dams but did not represent the shoreline boundary. Instead, a digital elevation model was used to generate the surface extent at the crest level of the dams for both LM and LP. In the case of LM, the boundary polygon matched well with the polygon obtained from Twichell et. al. (2003), and was used to clip the area of the reservoir beyond the upstream location, where the Colorado river joins LM. For LP, the DEM delineated surface area was clearly larger than that of the NHD, and was used for clipping.

## 2.3 Methodology

The estimation of the stage-area-storage relationship from remotely sensed data involved four steps: the computation of the water height from the lowest level; the estimation of the water area, the estimation of the differential volumes, and the estimation of the elevation-area-volume

relationship. A flowchart of the method is presented in Figure 2-2 and is explained in this section. The accuracies of estimates were calculated using the differences between the estimates and the USBR values.

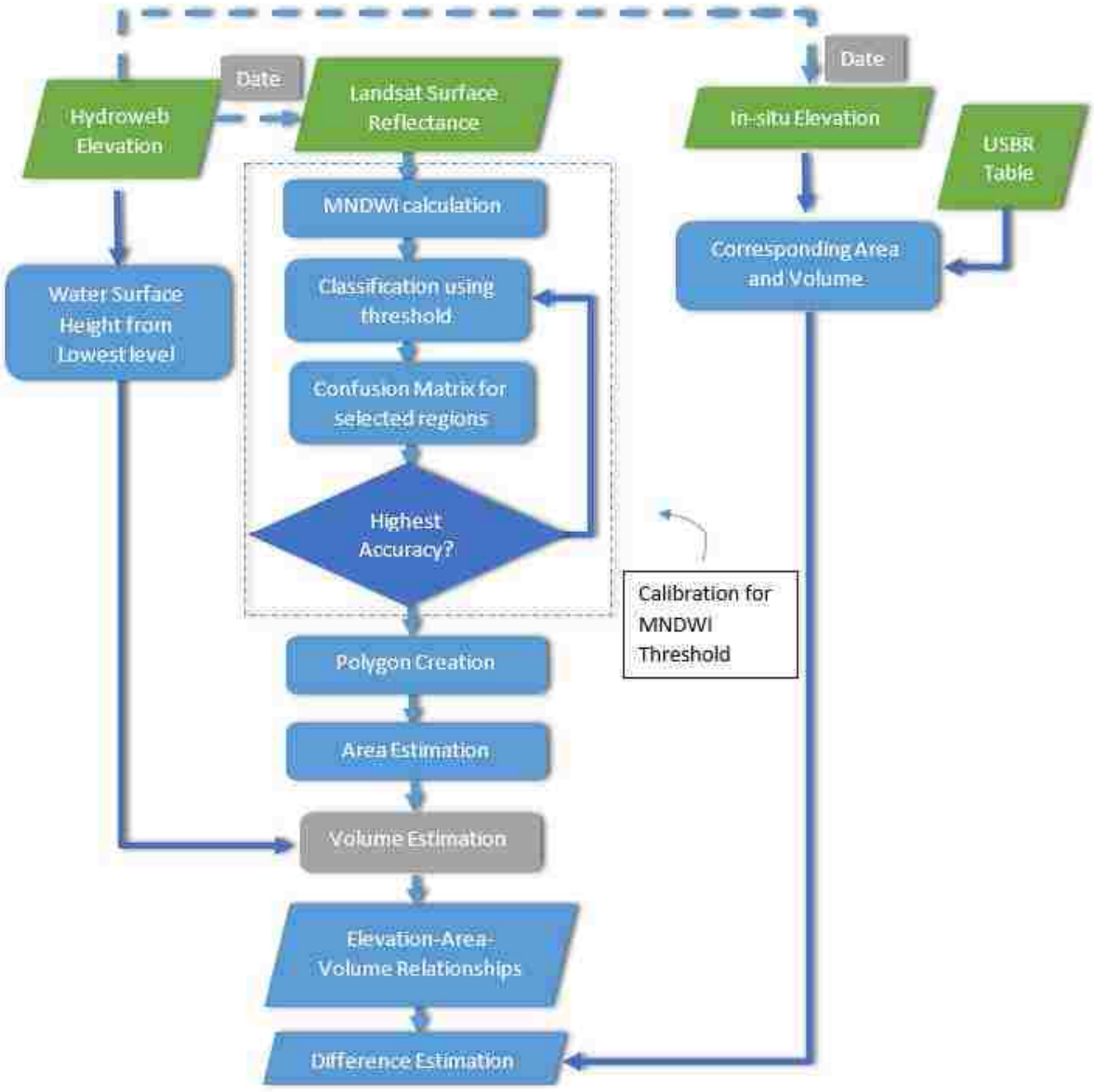


Figure 2-2: Flow Chart for the estimation of water volume from the lowest level using water surface level and area.

Elevations from Hydroweb were used to compute water surface heights from the lowest levels. This assumes a zero level for the first elevation and an increasing height from the lowest to the highest stage of the reservoir. Heights were also calculated using USBR elevations for comparison.

The water surface areas of the reservoirs were estimated from Landsat surface reflectance images. The Modified Normalized Difference Water Index (MNDWI), a spectral water index derived from the normalized difference operation of green and mid-infrared bands (Band 2 and Band 5 for TM) was calculated. The design of a spectral water index is based on the fact that water absorbs more energy at shortwave-infrared (MIR) wavelength than green wavelength as seen in the reflectance curve. The MNDWI is calculated using equation (1).

$$MNDWI = \frac{(b_{green} - b_{MIR})}{(b_{green} - b_{MIR})} \qquad (1)$$

The value of the index is high for water (usually greater than zero) and low for non-water. An appropriate threshold of the index is then established to obtain a binary image of water and non-water pixels. The estimation of the water surface area becomes complex due to the temporal and spatial variance of reflectance, calculated MNDWI values, and the threshold for classification. This is addressed by internally calibrating MNDWI threshold by assessing the accuracy of classification based on testing samples by creating a confusion matrix (Congalton and Green, 2009).

An inspection of the histogram of the MNDWI values calculated was done prior to inferring a suitable range for accuracy assessment. The confusion matrix for the selected testing samples of the classified image was created that indicated the extent of miss-classification.

Errors for misclassification include the error of commission (Error C), and error of omission (Error O). Confusion matrices for five samples were combined and the overall accuracy was calculated. If the classified map versus the reference data error matrix is drawn with the map in the row and reference data in the column. The overall accuracy is given by equation (2):

$$Overall\ Accuracy = \frac{Sum\ of\ the\ major\ diagonals\ of\ the\ error\ matrix}{Total\ sum\ of\ all\ the\ elements\ in\ the\ error\ matrix} \qquad (2)$$

The calibrated MNDWI threshold value from the five sample stages that provided the highest classification accuracies was then used for the remaining of the stages in the group in order to estimate the area. The calibration step was a calculation-intensive job and scripting was done using the Arc Python console and Matlab. Finally, the water pixels were converted into a polygon and the area of the largest contiguous polygon was taken as the estimate of the area of the reservoir. The polygons were simplified using retain-critical points and retain-critical bends techniques inbuilt into the ArcMap.

The estimation of differential volumes with increase in the water surface elevation was done under the hypothesis that between two successive measurements, the morphology of the lake is regular and has an inverted pyramidal shape (Abileah et al., 2011; Crétaux and Calmant, 2016); therefore differential water volumes can be derived from equation (3).

$$\Delta V = \frac{(H_T - H_{T-1}) * (A_T + A_{T-1} + \sqrt{A_T * A_{T-1}})}{3} \qquad (3)$$

where, $\Delta V$ represents the volume variation between two consecutive measurements$H_T$, $H_{T-1}$ and $A_T$, $A_{T-1}$ are levels and areal extents at date $T$ and $T-1$, respectively.

An ensemble of water surface heights from the lowest level derived from Hydroweb, estimated areas, and volumes, was used to fit a second-order polynomial relationship. A second-order polynomial was chosen as a parametric curve because of a good fit with the USBR values that indicate the stage-area-storage relationship was best explained by second-order polynomials for both reservoirs. The estimated values from the remotely sensed technique were compared with USBR values by calculating the Root Mean Square Difference (RMSD). Pearson's correlation coefficient $r$, was used to measure the strength of the relationship between the estimated and the USBR values. The differences are also represented in percentages based on the range for elevation, an average of estimate area for areas, and volume between the lowest and the highest levels for differential and cumulative volumes. The differences between fitted polynomials using estimated and USBR values were also computed to compare between two fits.

## 2.4 Results

The results are presented in four parts; water surface level, area, and volume as well as the relationship between them. Differences in the estimated values and USBR values are also presented.

The RMSD and correlation analysis indicated that elevations computed by the Hydroweb database had minimal errors and were reliable to be used for this analysis. The RMSD of the water surface heights from Hydroweb and USBR for LM was computed to be 1.07 m, which is 3.13% of the range between the highest and the lowest level in this study. The Pearson's correlation coefficient between the Hydroweb and USBR water surface heights for LM was 0.997. For LP, the RMSD difference after the datum adjustment was 1.15 m that is 3.09% of the range between the lowest and highest level. The Pearson's correlation coefficient between the

Hydroweb and USBR water surface heights for LP was 0.996 and showed a strong linear relationship.

Histograms of the MNDWI values for pixels in the images for a reservoir had similar distribution and range. It was noted that the histograms for LM and LP were slightly different. Because of the similar distribution of the histograms for the stages of a reservoir, the histograms of stage 1 for LM and LP are discussed. For LM, MNDWI ranged from -0.75 to 1 with a separation between high and low values that ranged from 0 to 0.3 (Appendix Figure A1 a). For LP, MNDWI ranged from -0.1 to 1 with a separation ranging from -0.1 to 0.3 (Appendix Figure A1 b). This range revealed a positive potential threshold value for LM, and a negative for LP.

The threshold value required for the classification of an MNDWI image into a binary image (water & non-water) was calibrated by assessing the accuracy of classification for the thresholds ranging from -1 to 1 for 5 out of 15 images. The confusion matrix that was computed for these five sample images was combined to compute overall accuracy. At least 10,000 pixels for each water and non-water class were selected to assess the overall accuracy. A second-order polynomial was fitted into the threshold vs. accuracy relation for the optimal threshold with the highest accuracy (Figure 2-3). A threshold value of 0.06 was calculated for LM and -0.05 for LP (Figure 2-3 a & b). The combined confusion matrix for LM and LP for the threshold with the highest accuracy is presented in Appendix Table A3, a & b.

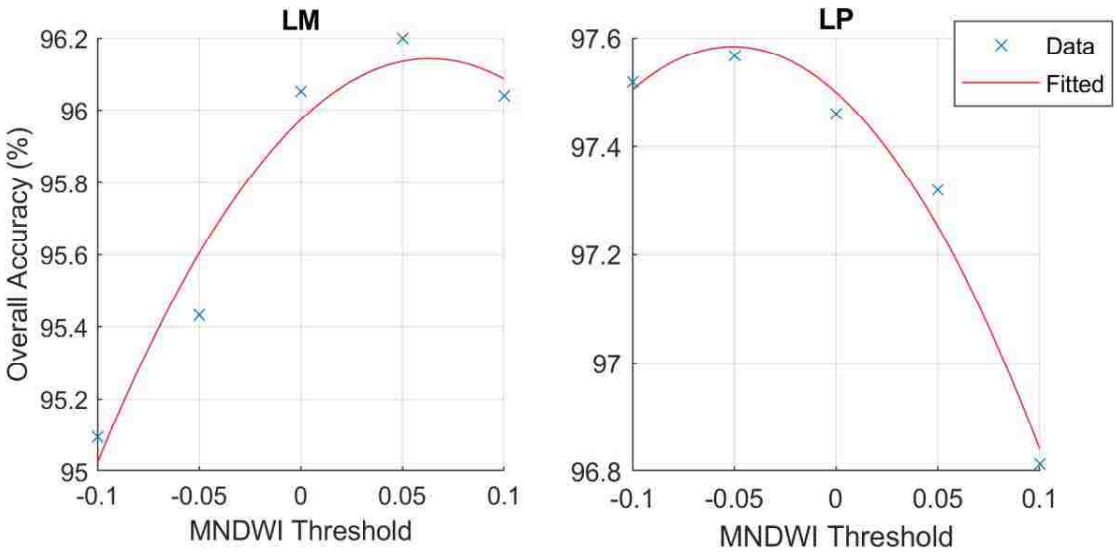


Figure 2-3: Using second-order polynomial to find the maximum accuracy threshold point for a. Lake Mead at 0.06 and b. Lake Powell at -0.05.

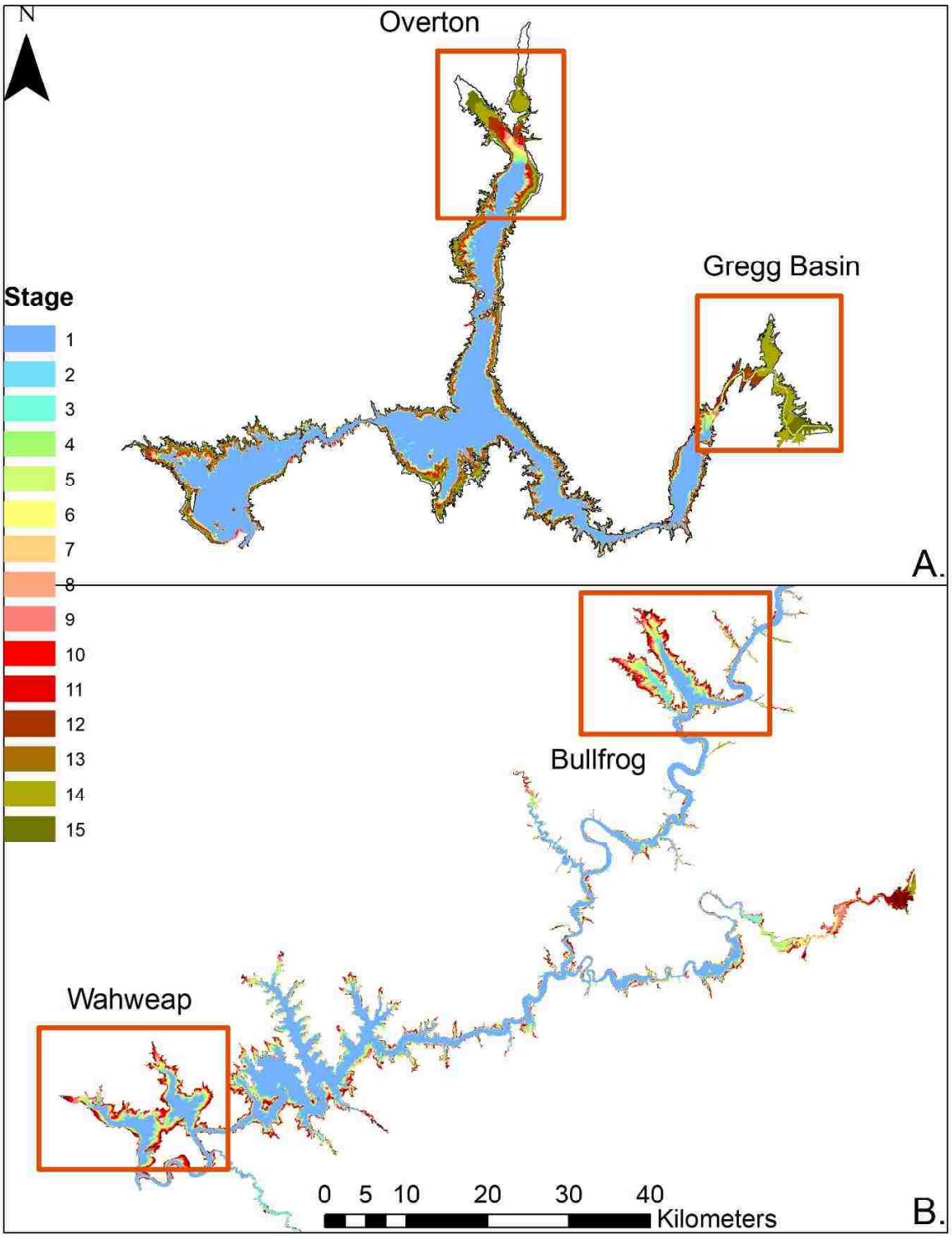


Figure 2-4: Variation in the Lake Mead area (a) for 15 different stages corresponding to elevations ranging from 330 m to 367 m; and Lake Powell area (b) for 15 different stages corresponding to elevations ranging from 1088 m to 1125 m estimated from Landsat images.

The water surface areas of all stages of LM was estimated using MNDWI thresholds of 0.06 for LM and -0.05 for LP. The variations of the reservoir area for LM was pronounced on the northern part of the Overton arm and the Gregg basin in the east arm of the reservoir (Figure 2-4). The area for the lowest level at stage 1 (332.09 m) was estimated to be 322 $km^2$, and for the highest level at stage 15 (366.37 m), it was estimated to be 565.98 $km^2$. The difference between the areas estimated from the Landsat images and reported by USBR lies between 6 $km^2$ (for stage 5) and 37.8 $km^2$ (for stage 15). The RMSD of the estimated area was 17.8 $km^2$, which is 4.5% of the average of the estimated area. The Pearson's correlation coefficient between the estimated and USBR areas was 0.996 and showed a strong linear relationship (Table 2-2). A Comparison plot showed that the areas were underestimated by an average value of 16 $km^2$ (Figure 2-5 a).

For LP, the area variation was high in the Wahweap and Bullfrog sub-basins (Figure 2-4). The area estimated for the lowest level (1089.92 m) was 282.90 $km^2$, and the highest level (1127.06 m) was 577.33 $km^2$. The difference between the areas estimated from the Landsat images and reported by the USBR lies between 26.71 $km^2$ (at stage 5) and 65.18 $km^2$ (at stage 12). The RMSD of the estimated areas was 53.77 $km^2$, which is 12.41% of the average of the estimated areas. The Pearson's correlation coefficient between the estimated and the USBR areas was calculated to be 0.996 and showed a strong linear relationship (Table 2-2). A comparison plot also showed that the areas were largely underestimated with an average of 52.85 $km^2$ (Figure 2-6 a).

A combination of the water surface heights and area information for the 15 stages was used to calculate the differential volumes between each elevation based on the assumptions of an inverted pyramidal shape. For LM, the maximum differential volume that was estimated between

15 stages was 3690 MCM, which was between stages 13 and 14. The maximum differential volume was estimated between an elevation difference of 7.65, and at an end elevation of 360.16 m. The minimum differential volume was 152.55 MCM between stage 6 and 7, within an elevation difference of 0.41 m, and at an end elevation of 342.12 m. The RMSD in the estimated differential volumes was 641.54 MCM, which is 4.41% of the total volume estimated between the lowest and the highest levels. The estimated differential volume and USBR showed a good relationship with $r = 0.918$. The differential volumes were summed from the lowest level to obtain a cumulative volume. The cumulative volume that was estimated between the estimated and USBR had a strong linear relationship $r = 0.996$. The comparison plot showed an underestimation of the estimated cumulative volume compared to USBR.

In the case of LP, the maximum cumulative volume estimated was 2275 MCM, between stages 5 and 6, and within an elevation difference of 5.58, at an end elevation of 1108.44 m. The minimum of the estimated differential volume was 141.03 MCM between stages 14 and 15 within an elevation difference of 0.25m, and at an end elevation of 1127.06m. The RMSD in the estimation of the differential volume for LM was 777.81 MCM which is 5% of the total volume between the highest and lowest levels in this study. Correlation of estimated differential volume and USBR showed a weak relationship with $r = 0.47$. The cumulative volume that was estimated between the estimated and USBR had a strong linear relationship with $r = 0.996$. The comparison plot showed an underestimation of the estimated cumulative volume compared to the USBR, and the errors were greater than those in the case of LM.

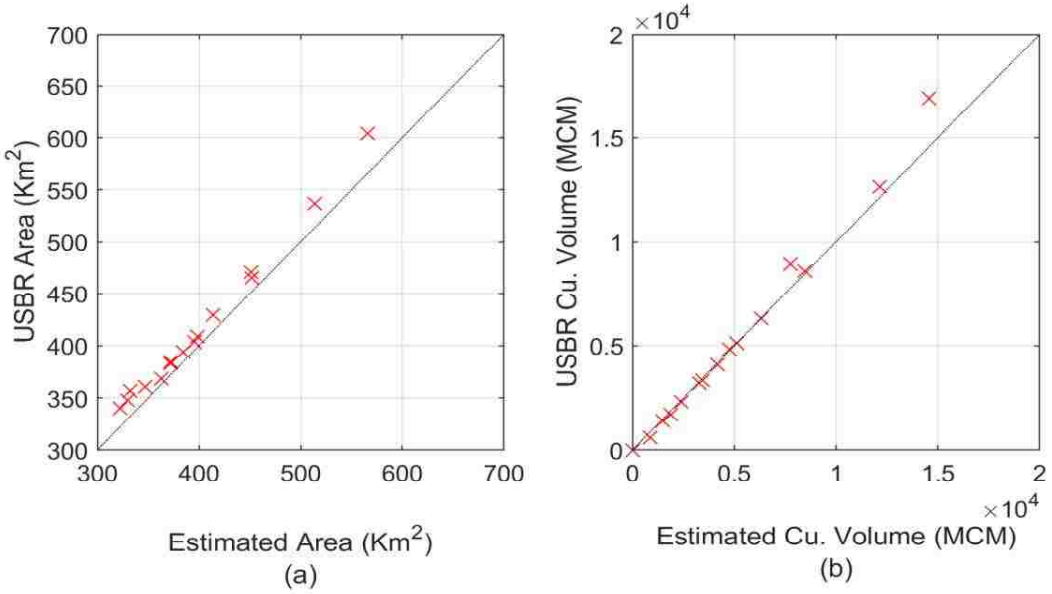


Figure 2-5: Comparison plots for Hydroweb and USBR data a. areas and b. Cumulative differential volumes for Lake Mead.

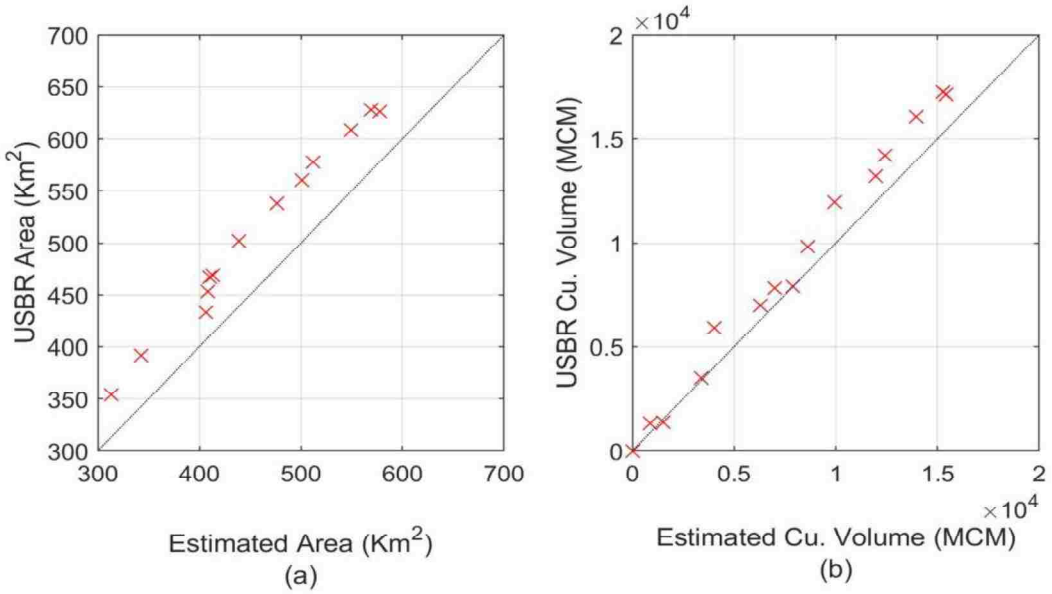


Figure 2-6: Comparison plots for Hydroweb and USBR data **a.** areas and **b.** cumulative differential volumes for Lake Powell.

The second-order polynomial equations were formulated for relationships between water surface heights from the lowest level, and the areas (volumes). For LM, the lowest level (stage 1) is from October 13, 2010, at an elevation of 330.34 m. The second-order polynomial equation between the water surface height ($z$) and area ($A$) was formulated with $R^2 = 0.995$ and an RMSD of 5.25 km$^2$ (Table 2-1, Figure 2-7 a). The equation between water surface height ($z$) and cumulative volume ($V$) was formulated with $R^2 = 0.999$ and RMSD of 21.6 MCM (Table 2-1, Figure 2-7 c). The polynomial fit with no intercept term was selected for water surface heights and volumes because the intercept term was deemed statistically insignificant at α = 0.05. For LP, the lowest level (stage 1) is from September 23, 2004, and at an elevation of 1088.62 m. A second-order polynomial equation between water surface height ($z$) and area ($A$) was formulated with $R^2 = 0.979$ and an RMSD of 15.34 km$^2$ (Table 2-1, Figure 2-7 b). The equation between water surface height ($z$) and cumulative volume ($V$) was formulated with $R^2 = 0.999$ and an RMSD of 38.18 MCM (Table 2-1, Figure 2-7 d). Similar to the case of LM, the intercept term was dropped in the polynomial fit because the coefficient was deemed statistically insignificant at α = 0.05. The second order polynomial fits were all significant overall at α = 0.05 that was tested by performing F-test. Results of significance test performed for LM and LP are tabulated in Appendix Table A4. The RMSD of fit using estimated areas is higher than the fit using USBR areas, and $R^2$ value is lower. In contrast, the RMSD of the fit for estimated volumes is lower than fits to the USBR data for LM and higher for LP.

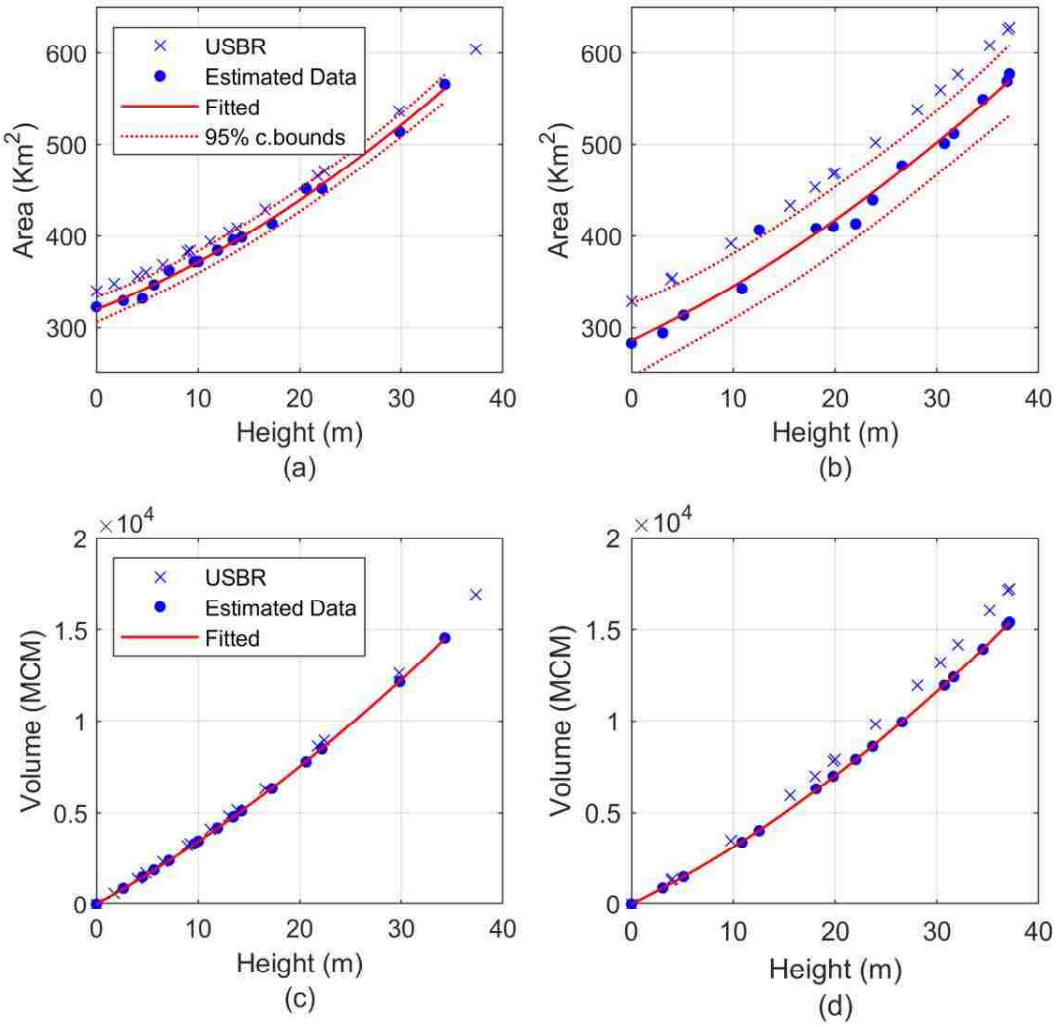


Figure 2-7: Second-order polynomial fits with intercept for height vs areas and second-order polynomial fit without intercept for height vs volume for Lake Mead (a & c) and Lake Powell (b & d) with 95% confidence bounds for areas. The coefficients of the fits and overall fit are statistically significant at $\alpha = 0.05$ tested by t-tests and F-tests. A scatter plot of USBR heights, areas and volumes are plotted in the same graph.

Table 2-1: Second-order polynomial equations fitted for height vs area, and height vs volume for estimated and USBR.

| Variables | Reservoir | Estimated | USBR | Goodness of Fit | | | |
|---|---|---|---|---|---|---|---|
| | | | | R-square | | RMSD | |
| | | | | Estimated | USBR | Estimated | USBR |
| Height vs Area | LM | $A = 0.0765\ z^2 + 4.434\ z + 319.7$ | $A = 0.08125\ z^2 + 4.103\ z + 338.7$ | 0.995 | 0.999 | 5.25 | 1.733 |
| | LP | $A = 0.06252\ z^2 + 5.333\ z + 285.7$ | $A = 0.05971\ z^2 + 5.82\ z + 328.6$ | 0.979 | 0.999 | 15.34 | 0.857 |
| Height Vs Volume | LM | $V = 3.328\ z^2 + 309.2\ z$ | $V = 3.385\ z^2 + 325.1\ z$ | 1 | 1 | 21.6 | 35.76 |
| | LP | $V = 3.729\ z^2 + 275.7\ z$ | $V = 3.964\ z^2 + 316.1\ z$ | 0.999 | 0.999 | 36.56 | 30.57 |

Table 2-2: Pearson's correlation coefficient, root mean square difference and percentage of the difference calculated for the estimated elevation, area and volume compared with the in-situ measurements.

| **Variable (Estimated vs USBR)** | **Pearson Correlation Coefficient r** | | **RMSD** | | **Difference%** | |
|---|---|---|---|---|---|---|
| | **LM** | **LP** | **LM** | **LP** | **LM** | **LP** |
| Height (From Lowest Level) | 0.997 | 0.996 | 1.07 m | 1.15 | 3.13% (of the range of elevation) | 3.09% (of the range of elevation) |
| Area | 0.996 | 0.996 | 17.82 sq.km | 53.77 sq.km | 4.45% of the average estimated area | 12.42% of the average estimated area |
| Differential Volume | 0.918 | 0.474 | 641.54 MCM | 777.81 MCM | 4.41% of the volume between elevation range. | 5.05% of the volume between elevation range. |
| Cumulative Differential Volume | 0.996 | 0.996 | 698.82 MCM | 1330.37 MCM | 4.80% of the volume between elevation range. | 8.63% of the volume between elevation range. |

## 2.5 Discussion

The relationships developed between the heights from the lowest level, areas, and volumes are useful when variation within the operational range is of concern. This methodology was adopted in studies such as Duan and Bastiaanssen (2013) and Tong et al. (2016). It is to be noted that developing a relationship using elevations was attempted, but had high discrepancy and the required conversion of Hydroweb elevations (referenced to GGM02C geoid) to USGS

datum. This involved the use of a mathematical geoid model such as the International Centre for Global Earth Models (Drewes et al., 2016). The discrepancy between the adjusted elevations and USGS elevations on the same day ranged from -2.68 m to 1.29 m for LM and -3.33 to 1.76 m for LP. These difference in elevations, when translated to the volume, would create large errors in the formulation of relationships. The reasons for these discrepancies are likely from the use of a static mathematical model and errors in altimetric measurements.

The estimation of the area from satellite images was challenged by harbors in the lakes, shadows in the canyons, and mixed pixels in the boundaries and narrow sections. Man-made structures in the lakes, such as the Las Vegas Boat Harbor and the Callville Marina in LM, and the Wahweap and Bullfrog Marina in LP created problems in the estimation of areas. These structures are classified as non-water, and thus caused underestimates of the water areas of the reservoirs. The other problem seen in the area estimation was the classification of mixed pixels. These pixels were sensitive to the thresholds. Moreover, these pixels occurred in water boundary and narrow sections of the lake. The narrow sections were prone to errors, as misclassifications would cut off significant parts of water areas. Therefore, care must be taken when using maximum area polygon as an area estimation technique. The correct selection of thresholds for the classification of MNDWI into binary images of water and non-water requires special attention, as suggested by studies such as (Ji et al., 2009; Liu et al., 2012; H. Zhang et al., 2017). The use of a threshold that misclassifies the mixed pixels is an easy pitfall when the estimated areas are overfitted with in-situ measurements. In-fact the thresholds that provided higher accuracies were off by more than 0.1.

The estimates of water surface areas are more accurate for LM than LP. This could be because of the filamentous shape of LP with deep canyons. The image pixels, which are

dominated by shadows, were misclassified as water in experiments conducted in this study. This problem was equally persistent in LM, but the scale was lower than in LP because of the wider shape of the reservoir.

The second-order polynomial fits for height vs area, and height vs volumes were good, with $R^2$ ranging from 0.979 to 1. The RMSD of fit estimated the area and volume higher than the USBR, except for the volume of LM, indicating that second-order polynomial are more suitable fits for USBR relationships. The RMSD for fits are higher for LP compared to LM, which means that the estimated values are more deviated for LP from the fitted curve (Table 2-1). Differences between the fitted values for height vs area for LM is lowest towards the higher stages (30 to 40 meters from the lowest level) (Figure 2-8 a). This is the opposite in the case of LP, where the difference is higher at higher stages. The differences in fitted values of volumes for both LM and LP are higher at the higher stage (Figure 2-8 b).

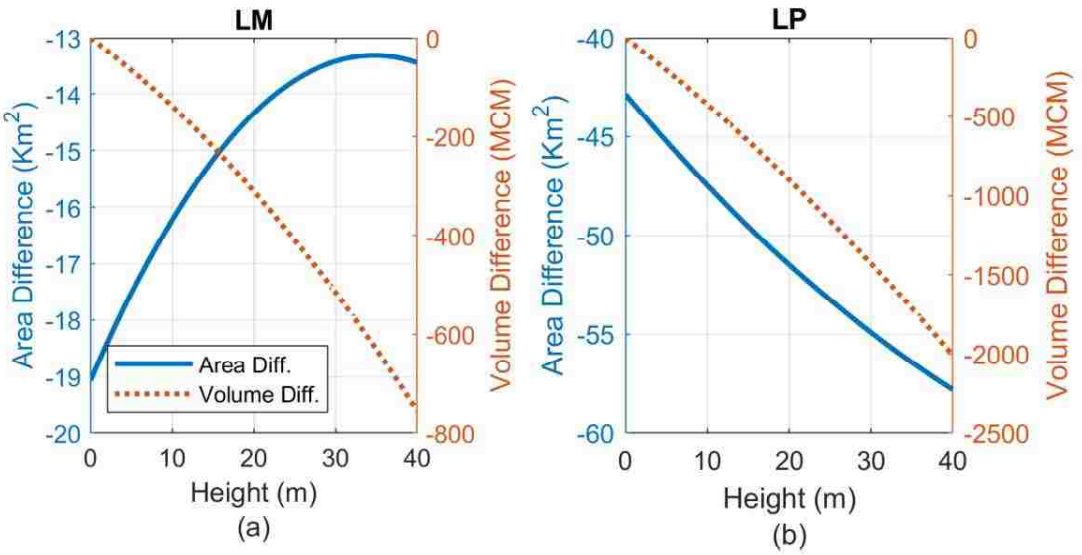


Figure 2-8: Differences in values calculated from fitted second-order polynomials for area and volume for a. LM b. LP

The temporal differences between the elevations from satellite altimetry and areas from satellite imagery were tested for correlation with the differences in area and volume estimates but no significant correlation was found. However, there were correlations between the differences in heights, areas, and volume. For LM, the differences in height between the Hydroweb and the USBR had a significant correlation ($\alpha$=0.05) with differences in volume estimates (r=0.98) and mild correlation with differences in area estimates (r=0.74) (Figure 2-9 a). These correlations are possibly due to the scale at which small differences in height affects the volume when computed for large areas. However, for LP, a significant ($\alpha$=0.05) mild correlation (r=0.67) was found between height differences and volume differences (Figure 2-9 b).

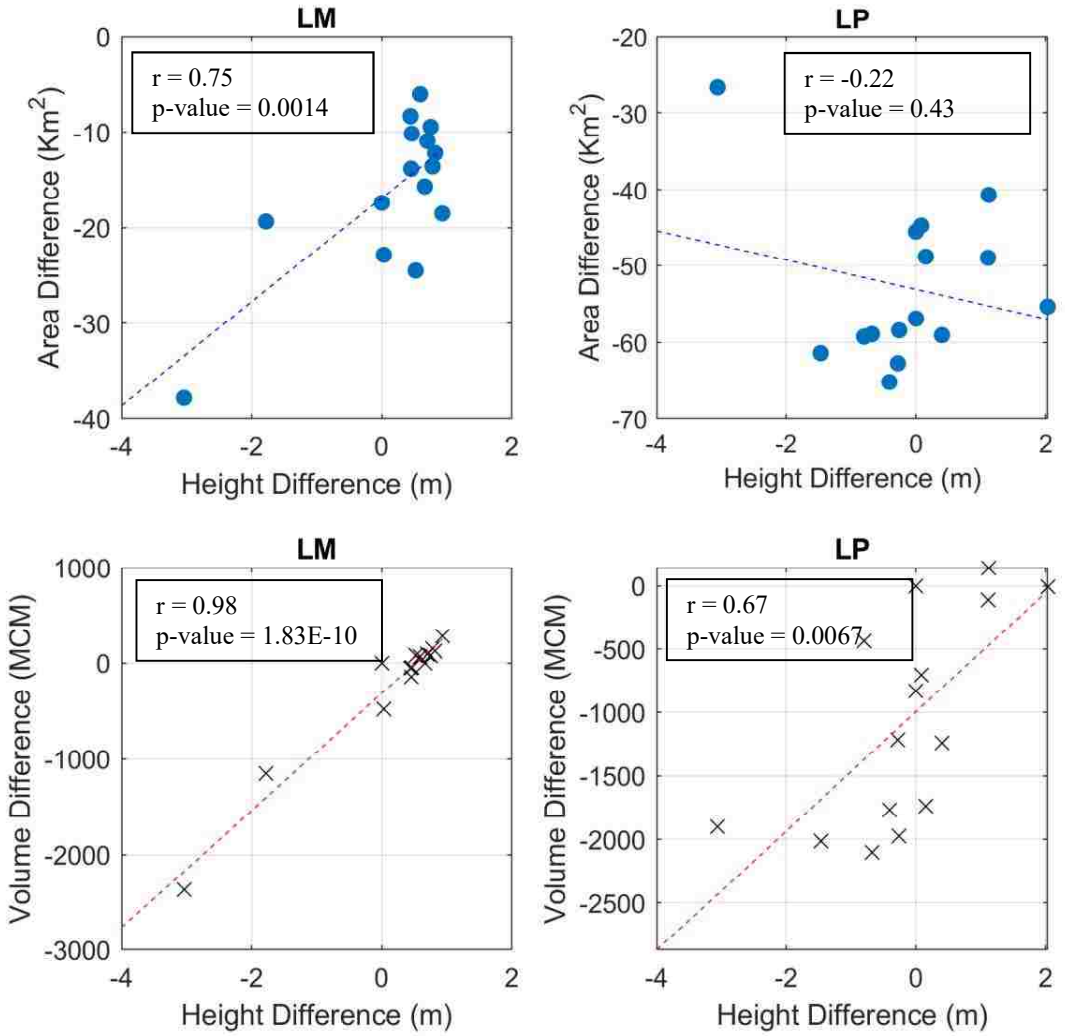


Figure 2-9: Correlations between differences in heights, areas, and volumes between estimated and USBR for LM and LP.

## 2.6 Conclusions

The formulation of the relationships between reservoir heights from the lowest level, areas, and volumes using remotely sensed data were estimated within an operational range, with

a second-order polynomial fit with $R^2$ ranging from 0.97 to 1. The area fits were accurate up 4% and 12% for LM and LP, respectively, compared to the average area in the range while volume fits were accurate up to 3% and 6% for LM and LP, respectively, compared to the volume in between the range of elevation. The formulated relationships under-estimated areas and volumes when compared to USBR values estimated by survey methods. Water surface heights were accurate up to 1.15 m using satellite altimetry. Accurate estimates of the area coming from satellite images were challenged because of mixed pixels in narrow boundaries and the misclassification of shadows. Area estimations were more accurate for LM (5% of the average area) than LP (13% of the average area). Narrow and deeper canyons in LP had mixed pixels and shadows that reduced the accuracy of estimated areas. The estimation of relationship based on remotely sensed data could be a possible alternative for transboundary or remote reservoirs where accessibility or transparency is an issue.

## CHAPTER 3: Estimation of Stage-discharge in Relationship Rivers Using Remotely Sensed Data

### Abstract

Rivers are important features of water circulation on the earth's surface. Estimates of the discharges in rivers are essential for water management and the monitoring of changes due to climate forces. However, global coverage and stable temporal frequency are required for the complete understanding of change and robust modeling. This study focuses on utilizing remotely sensed data to estimate river discharge. Field measurements are used to assess the accuracy of the remote sensing approach. Two major North American rivers, the Mississippi River and the Colorado River, representing alluvial and rocky terrains, were selected to highlight the differences in estimates between varied terrain and size of the rivers. A variant of Manning's equation was used that required channel cross-section, water surface slope, and roughness coefficient as input parameters. A parabolic cross-section was fitted for each river using the river channel widths estimated from the Landsat images at several water levels. The water surface slopes were estimated from water elevations using two sources. For the Mississippi River, water surface elevations were obtained at virtual stations from the DAHITI database. For the Colorado River, elevations were extracted using the MAPS at river crossings. The roughness coefficients were estimated using empirical models that utilized meander lengths. Results showed that discharges were estimated to within 31.4% of the average discharge with a root mean square error of 5700 cu.m/sec for the Mississippi River. Colorado River discharges were estimated within 30.5% of the average discharge with an RMSE of 50 cu.m/sec. A linear relationship was fitted between the water surface elevation and discharges in the Mississippi River with $R^2 = 0.62$. For the Colorado River second-order polynomial was fitted for a relationship between water

surface elevations and discharges with $R^2 = 0.99$. The coefficients of the fits and the overall significance of the fit were statistically significant at $\alpha = 0.05$ tested by performing t-tests and F-test respectively. It was difficult to estimate a cross-section for rivers with smaller channel widths or smaller changes in width with water levels as in the case of the Colorado River. However, the estimated accuracies were similar in both the cases in terms of percentage of error and the results were more stable for the Colorado River than the Mississippi River.

## 3.1 Introduction

Managing fresh water under the pressure of growing demands and climate forcing is increasingly becoming a challenge (Arnell, 1999; Makarigakis and Jimenez-Cisneros, 2019; Vörösmarty, 2000). Forecasting of available fresh water is important to plan and secure water and food (de Vito et al., 2019; Jackson et al., 2001). For forecasting, it is vital to understand the exchange of moisture between the atmosphere and land in order to model future scenarios (Bhandari et al., 2018; Pathak et al., 2016; Song et al., 2019; Tamaddun et al., 2018, 2019). The key to understanding the exchange processes is to monitor changes in surface water storage such as in wetlands, rivers, and lakes (Bjerklie et al., 2018; Crétaux et al., 2016; Yang et al., 2019). The knowledge can then be used in the models that can help the accurate forecast of the quantity of available water. An incomplete understanding of the hydrological cycle and atmospheric exchanges cause majors problem in modeling efforts (Collins et al., 2018; Ghorbani et al., 2019; Granata, 2019; Hussain et al., 2019; Nazari-Sharabian et al., 2019).

A limited number of station-based data that requires a piecewise collection and assembling is a major obstacle in setting a global monitoring system for surface water (Camarillo-Naranjo et al., 2019). Inadequate spatiotemporal coverage is one of the main challenges of hydrological modeling of in situ discharge databases (Tourian et al., 2017).

Moreover, data that might be present are often restricted or prohibited due to transparency issues between international fractions (Nilsson 2005). Remote water bodies, mostly located in higher latitudes and altitudes, with minimum human intervention, are excellent indicators of climate change (Adrian et al., 2009). However, these sources are often unmonitored because of the difficulty in setting up a physical station. Additionally, the physical stations all over the world are decreasing, and that affects monitoring capabilities (Fekete and Vörösmarty, 2007; Shiklomanov et al., 2002). Remote sensing has been an important technology that has proven the immense potential to overcome these challenges and limitations in surface water monitoring.

Rivers around the world contribute to the circulation of fresh water on land and occupy 0.6% of the non-glaciated land surface (Allen et al., 2018). Rivers are major transport for freshwater and vital source of supply to human habitats. It is important to monitor changes in the discharges of rivers forced by climate variability and change. It is equally important to understand the effects of land and water use on water availability in rivers in the future. Estimating discharges and formulating relationships between water levels and discharges were preliminary steps in monitoring. Discharge estimates have traditionally been estimated by measuring the cross-sectional area and measuring velocity at multiple points. A continuity equation that multiplies cross-sectional area and average velocity is then used to estimate discharge at several depths of water. Finally, a stage-discharge curve or a rating curve is established for a station to facilitate easy measurements. Recently more advanced technologies have used acoustics and optics for precise measurement of depths and velocities at several locations along a cross-section to obtain accurate rating curves (Holtschlag and Koschik, 2003; Lant and Boldt, 2018). However, the limitations related to station based monitoring still exists with these new technologies.

Satellite-based measurements have been explored to extend, support and replace the monitoring stations on the site. Satellite multi-spectral images such as the Landsat project have been used for the measurement of surface water extent (Abedin and Stephen, 2019). Satellite radar measurements have been a source to measure water surface elevation and slopes. Recent research includes wide-swath radar imaging for water surface elevation mapping (J.-W. Kim et al., 2014) and GRACE-derived water changes (Milly et al., 2005). Satellite technology that can measure discharges in rivers directly has not yet been possible. However, efforts have been made to use available satellite-based information to estimate discharge. Explored satellite-based information includes river morphology from images and water surface slopes from radar altimeters. Techniques such as optical and near infrared, as well as passive and active microwave-imaging have been used to determine water surface extent and width. Among them, Landsat images are widely used remotely sensed data, and have been tested in diverse regions on the globe (Abedin and Stephen, 2019; Carroll et al., 2016; Jones, 2015; Rind et al., 2018). Water surface extents over the years can generate time series data that helps researchers to understand changes in surface water. Estimating water volumes in reservoirs using such time series data within the operational range is an example of application (Duan and Bastiaanssen, 2013). On the other hand, interferometric SAR (Alsdorf et al., 2001) and radar and laser altimetry have been demonstrated to be useful for water-surface elevation measurements, amongst others. Satellite-based radar altimeters have been used in evaluating river dynamics (Birkett, 1998; Birkett et al., 2002; Michailovsky et al., 2012; Tarpanelli et al., 2017). Radar elevations combined with ground-based measurement (Bogning et al., 2018; Kouraev et al., 2004; Papa et al., 2012) or estimates of discharge from hydrodynamic models (de Paiva et al., 2013; Maswood and Hossain, 2016; Paris et al., 2016) have been used to develop discharge rating curves.

Recent research has been focused on discharge estimation algorithms that are based on remotely sensed data without the use of ground-based measurements. These algorithms are targeted to utilize observations from a future SWOT mission planned to be launched in 2021. The algorithms use information extracted from satellite-observed data as input. Satellite-based information used in the literature includes water surface area (width), slope, and elevation. Gleason and Smith (2014) used reach scale hydraulic geometry to estimate discharge in rivers with a root mean squared error (RMSE) within 30%. While Birkinshaw et al., (2014, 2010) estimated discharge between gages with gage discharge as a boundary condition and utilized satellite-derived stage, slope, and width. Inverse modeling techniques were used to estimate discharge in the Severn River in the United Kingdom (Durand et al., 2014) using a flow resistance equation. Remote observations of the river water surface and morphological features were incorporated by Garambois and Monnier (2015) in inverse methods to estimate the hydraulic properties of the river flow in the Garonne River, France/Spain. Estimates were within 15% of observed discharge for both of the methods. Durand et al. (2016) used modeled river data as representative observations for the upcoming SWOT mission to test various physical and quasi-physical discharge algorithms in a set of rivers around the globe. Reach average widths were derived from the water surface area of the river from models, and water surface height and the slope were used as a measure of the change in flow depth. The tested discharge algorithms varied in accuracy depending on the river as well as reach.

Further, Sichangi et al. (2016) used channel width as well as a stage to derive a rating curve and found it to be superior at the continental scale. Bogning et al. (2018) used Multi-mission Altimetry Processing Software (MAPS) to derive elevation data from drifting orbits and develop a relationship between field-measured discharge and elevation in the ungauged Ogooue

River Basin. Bjerklie et al. (2018) estimated discharge in the Yukon River within 21% with the use of elevation computed from satellite radar and laser altimeters, as well as the width of the river from Dynamic Water Surface Extent (DWSE), a provisional product computed from Landsat images. The ensemble learning regression method, a machine learning model was used to develop a rating curve using elevation from satellite altimeters and in-situ discharge as training data set in the Congo River, which were able to reduce errors in estimates to 2% (Kim et al., 2019). Global monitoring within a single framework is a major benefit of remotely sensed data. However, the robustness of the algorithm in diverse regions are still unexplored for many of them. Moreover, the modeling of channel cross-section is an important part and is dependent on the size of rivers. This study focuses on highlighting some of these dependencies and the accuracy of estimation of discharge for a river that is not present in the literature.

The objective of this study was to estimate discharge in rivers at several water levels (stages) using remotely sensed data without the use of any field measurements. The estimates were then used to formulate relationships between stage and discharge. Manning's equation was used to estimate discharge and required cross-section, water surface slope and roughness coefficient information as input parameters. The discharges were estimated for the Mississippi River and the Colorado River, which represent alluvial and rocky terrain in the continental United States, respectively. Water surface slopes were estimated using water surface elevations at two crossings of satellite altimeters. Elevation data for the Mississippi River was used from the DAHITI database that provided processed data at virtual stations with a consistent datum. However, for the Colorado River, water surface elevations were computed from Jason-2 satellite acquired data using MAPS. An average parabolic cross-section was fitted using widths and water surface elevations at several water levels averaged for the reach. Reach average widths were

estimated using satellite images. Landsat 5 and 8 images were used and the Modified Normalized Difference Water Index (MDNWI) was used to extract water surface area information. The roughness coefficients were estimated using water surface slopes and meander length using empirical models developed from previous studies. Finally, relationships were established by fitting regression lines that were statistically significant. The differences in the estimated discharges were computed against the United States Geologic Survey (USGS) stations using root mean square errors (RMSE).

### 3.2 Study Area and Data

The Mississippi River and the Colorado River are two major North Continental rivers. The two rivers flow in different terrains. The Mississippi River flows through an alluvial plain, and the Colorado River flows through rocky and rugged terrain. The Mississippi River is a much larger river among the two with an average annual discharge of 16,800 cubic meters per second. It drains 2.98 million square kilometers the midwestern and southeastern United States and flows through varied terrain (Kammerer, 1990). The Colorado River drains 0.64 million square kilometers of the western region of the United States, with an annual average discharge of 640 cubic meters per second. The nature of the terrain has a marked effect on channel formation. The Mississippi channel is much less stable and has frequent bends than the Colorado River. The width to height ratio of the Mississippi River channel is larger than that of the Colorado River. Moreover, the Colorado River on average has a much larger vertical elevation change over a shorter channel length compared to the Mississippi River. Due to the differences in cross-sectional shapes, widths and surface area changes with an increase in water level is much larger for the Mississippi River than for the Colorado River.

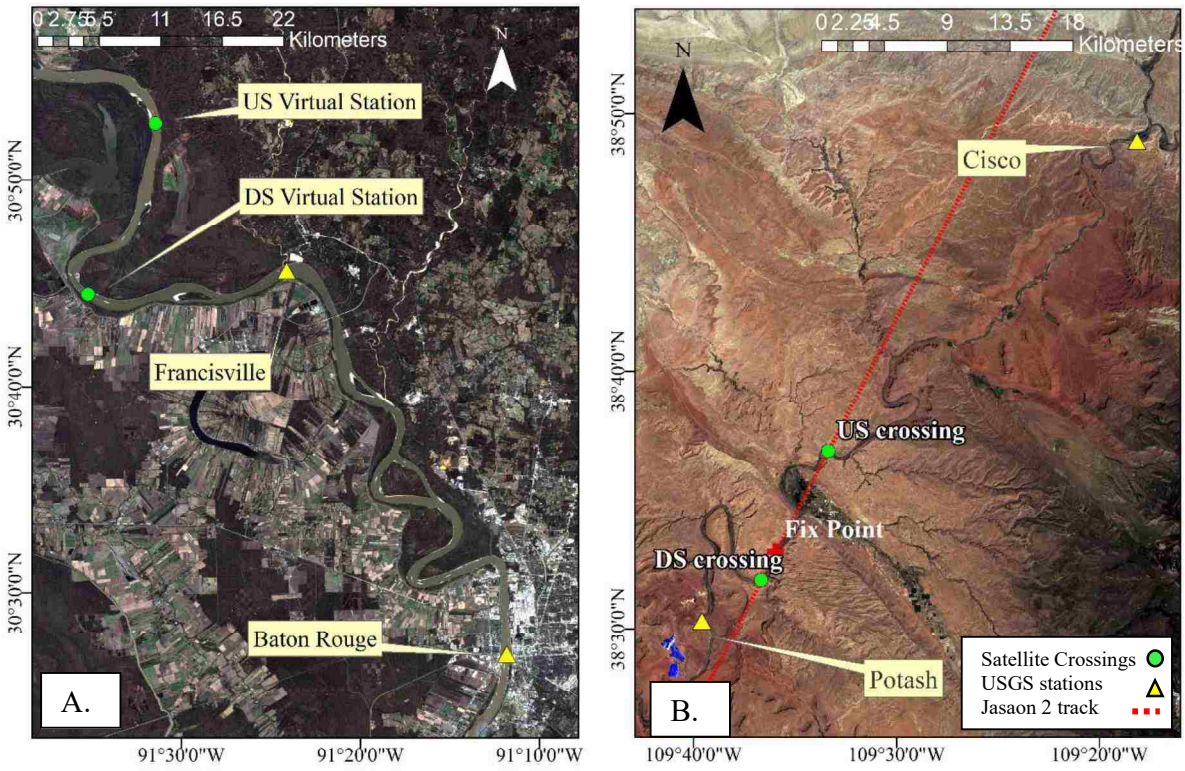


Figure 3-1: Sections of the Mississippi River near Baton Rouge (A) and the Colorado River near Moab (B) between the green dots selected for the study. Green dots are virtual stations for the Mississippi River and crossings for the Colorado River. Yellow triangles are USGS gauging stations that are near the selected river reaches.

Reaches of the rivers were selected based on the crossings of altimeter satellites or the availability of virtual stations in the altimeter database. A reach was identified to be a section between the upstream and downstream points of the altimeter crossings or the locations of virtual stations. A smaller length and the location of a nearby stream gauge were favorable criteria for selection. A 19.4 km section of the river near Baton Rouge, Louisiana was selected for the Mississippi River, and a 13.4 km section of the river near Moab, Utah was selected for the Colorado River.

The Virtual stations are the locations in a river where satellite altimeter ground track crosses the river. These locations are fixed through all of the cycles of the satellite, and a continuous elevation data with a fixed period can be generated for the water surface. The Database for Hydrological Time Series of Inland Waters (DAHITI) (Schwatke et al, 2015) was used for elevation data for the Mississippi River (Figure 3-1 a). DAHITI was developed by the Deutsches Geodätisches Forschungsinstitut der Technischen Universität München (DGFI-TUM). Data were obtained for virtual stations with the DAHITI specific ID 11484 and 11416. Elevation data for the virtual stations were available from 2008, and were calculated based on several satellites. For the Colorado River, Jason 2 satellite data were used. The Jason 2 mission operated from 2008 to 2016. Multi-mission Altimetry Processing Software (MAPS) (Normandin et al., 2018) developed by the Center for Topographic Studies of the Ocean and Hydrosphere (CTOH) was used to obtain elevation at crossings. The Crossings are the locations where the ground track of a satellite altimeter intersects the river (Figure 3-1 b). These locations are ideally fixed, but depends on the stability of the satellites to remain in their designated orbits. Datasets from a single-pass were preferred to eliminate the temporal discrepancy between the readings at crossings. Moreover, the satellite passes were separated by 250 kilometers and were considerably large. The large size of reach is affected by numerous confluences and so was avoided. MAPS software calculated altimetric heights and provided a spatial representation of altimetric heights and help the user to select the data (Frappart et al., 2015).

The Landsat 5 and 8 surface reflectance images were used to estimate the surface area of water within a reach, as well as morphological variables. These are Level 2 on-demand products, and processed using the LEDAPS algorithm. Images were downloaded from earthexplorer.usgs.gov that facilitated image selection with additional criteria such as cloud

cover. A cloud cover criteria of 10% was set in order to obtain cloud-free images. Cloud-free images are important to extract water surface information. The morphological variables included meander length and thalweg length that were constant for a selected river reach. Images acquired on the same date as elevation were ideal for analysis but difficult to achieve. So, the temporally closet elevation and image pairs were used.

It was noted that the use of images from multiple sources could introduce discrepancy in water surface were estimates. Therefore, either Landsat 5 Thematic Mapper (TM) or Landsat 8 Operational Land Imager (OLI) images were used. Landsat 7 images were avoided because of missing pixels which were critical to detect changes in narrow features such as rivers. Landsat 5 images were used for the Mississippi River, as it provides an adequate set of image and elevation pair. Landsat 8 images were used for the Colorado River because of inadequate elevation and cloud-free image pairs. The data pairs used in this study are provided in Appendix B Table B1 & B2. Samples were tested to check the sensor dependence of reflectance values in spectral bands but were found consistent. This supports comparisons that will be made between the two rivers. Moreover, images from multiple sensors were not used for a river that can bring inconsistency in this study.

Field measurements of discharge were obtained for the United States Geological Survey (USGS) stream gauge stations from the National Water Information System. Francisville (ID 07373420) was the nearest gauging station to the selected reach for the Mississippi River and is located 18 kilometers downstream (Figure 3-1 a). However, the station did not have continuous daily discharge data. The closest gauging station with continuous data was located in Baton Rouge (ID 073734000). Discharge data between the two stations were highly correlated and a linear regression line was fitted to estimate discharges at Francisville using Baton Rouge data.

For Colorado River, the closest gauging station was located at Potash (ID 09185600), 17.6 km downstream of the selected reach. The station only had daily discharge data since 2014. Therefore, the gauging station at Cisco (ID 09180500) was used to estimate missing discharge data at Potash.

### 3.3 Methodology

The discharges in the rivers are estimated by Manning's equation. The equation requires the channel cross-section, water surface slope, and roughness coefficient information to estimate discharge. A variant of Manning's Equation (Bjerklie et al., 2018) for flow in channels that includes a shape factor ($b$) is given by equation (1).

$$Q = \frac{[\,W\,((H-B)\left(1-\left(\frac{1}{1+b}\right)\right))^{1.67}S^{0.5}]}{n} \quad (1)$$

where, $Q$ = estimate of discharge.

$W$ = average width of the river channel

$H$ = reach averaged elevation of water surface.

$B$ = bottom of the parabolic section

$b$ = shape factor (e.g. 1.5 for parabolic section)

$S$ = reach averaged slope.

$n$ = channel roughness coefficient.

The estimation of an actual channel cross-section is difficult from remotely sensed data. This is because the channel bed is obstructed by water in the digital elevation model. Additionally, the use of satellite images to estimate the widths and heights is challenging due to the movement of the river channel. Therefore, a representative cross-sectional shape of the channel was assumed and its parameters were estimated. The simplest representative cross-section for the river channel is a parabola. A set of measured maximum and mean flow depths for over 25000 river cross-sections has been made by the USGS across the United States. This was as part of flow measurements made with Acoustic Doppler Current Profilers (ADCPs) (Canova et al., 2016). Bjerklie et al., (2018) estimated the best representative cross-section using a relationship between maximum and mean depth as a governing factor for shape. They indicated a parabolic shape to be the best fit for most of the river with remarkable consistency.

A parabolic section was fitted to a set of reach averaged river widths and elevations. The widths of the rivers, varying from lowest to highest, were estimated from Landsat 5 images. The crossings of the satellite altimeter tracks on the rivers were defined as reaches. The estimated area was divided by thalweg length to obtain a reach average width. The thalweg length was estimated by measuring the length of a line drawn in the image with the lowest water level. The areas of water surfaces within each reach was estimated by creating polygons around the water in a binary image of water and non-water. Polygons were created using the raster-to-polygon tool in Arc-Map that operates by retaining features and bends. Average reach widths and average elevations were used to estimate constants in a parabolic equation represented by equation (2). The equation is

$$H = aW^2 + B \qquad (2)$$

where $a$ and $B$ are parabolic constants that represent the scaling and bottom elevation of the fitted parabola, respectively.

The slopes of the rivers at different stages is estimated by subtracting the elevation at the upstream and downstream virtual stations and dividing the differences by the thalweg lengths. At this point, all of the other variables in equation (1) are known except for the roughness coefficient which is a challenge. It is difficult to estimate the roughness coefficient from satellite observations with the present state of knowledge. A relationship between the bankfull velocity of a river, its meander length, and water surface slope was proposed by Bjerklie (2007). This was based on flume data and a historical observation of a set of rivers in the United States, the United Kingdom, and Canada. The relationship is assimilated to equation (3):

$$V_b = 1.37(\lambda_c S)^{0.32} \qquad (3)$$

where, $V_b$ is the bankfull velocity, $S$ is the slope and $\lambda c$ is the meander length.The meander length was estimated from a Landsat image. The scale at which the meandering of a river changes during the years is insignificant for the estimation of meander length. Therefore, an image with the lowest water level was found to be sufficient to estimate meander length. The estimate of velocity was used to estimate the roughness coefficient using an empirical model for the Froud number ($F_b$) in (Bjerklie et al., 2018) (equation (4)). Finally, the roughness coefficient is then estimated from Manning's velocity equation for wide channel given by equation (5) in combination with equation (4):

$$F_b = 2.85\ (S)^{0.31} = \frac{V_b}{\sqrt{gY_b}} \qquad (4)$$

$$n_b = \frac{Y_b^{0.67} * S^{0.5}}{V_b} \qquad (5)$$

Altimeter elevations in virtual stations were not affected by cloud cover, and therefore were more suitable to estimate discharge for validation purpose in this research. This is also applicable for operational purpose in the applied field. Rearranging equation (2) gives equation (6), which calculates river widths from water surface levels:

$$W^2 = zH + c \qquad (6)$$

where; $z$ is $(1/a)$ and the intercept, c is $-(1/a)B$.

The width was then used in conjunction with a slope to estimate discharge. The Root Mean Square Error ($RMSE$) is used to estimate the difference in estimates and measurements from USGS stations. The schematic diagram for the estimation of discharge from water surface elevation and images is provided in Figure 3-2. Finally, a linear or polynomial line was fitted to a set of water surface elevations and discharges to obtain a rating curve.

Elevations data in the case of DAHITI were designated for virtual stations, which were fixed points. The computation of the average elevation in the reach requires taking an average of the elevations between two virtual stations. The discharge is then attributed to the average elevation in the reach. While this is a straightforward computation in the case of virtual stations, the same is not true when using MAPS. This is because of the drifting of the orbits due to which the crossings of the satellite track change its position in every satellite passes. The elevations measurements points were not for a fixed point, and have to be computed for a fixed point to attribute the discharge estimate to an elevation for several measurements. Therefore, the slope

was computed between the highest point and the lowest measured elevation. The slope was then used to compute the elevation at a fixed point, using the elevation at a known location and the distances between them, with a linear assumption.

Information on water surface features was extracted from surface reflectance images using a spectral index. The Modified Normalized Difference Water Index (MNDWI), a spectral index, was calculated. The value is high for water (greater than zero) and low for non-water. Water features are identified when the value of the index was higher than zero. The design of the spectral water index was based on the fact that water reflects green wavelengths and absorbs infrared (IR) wavelengths. The MNDWI is calculated by the green and mid-infrared bands (MIR) using the following equation (7):

$$MNDWI = \frac{(Surface\ Reflectance_{green} - Surface\ Reflectance_{MIR})}{(Surface\ Reflectance_{green} - Surface\ Reflectance_{MIR})} \quad (7)$$

The pixels classified as water using MNDWI values were converted to a polygon. The polygons were simplified using retain critical points and retain critical bends techniques built into the ArcMap.

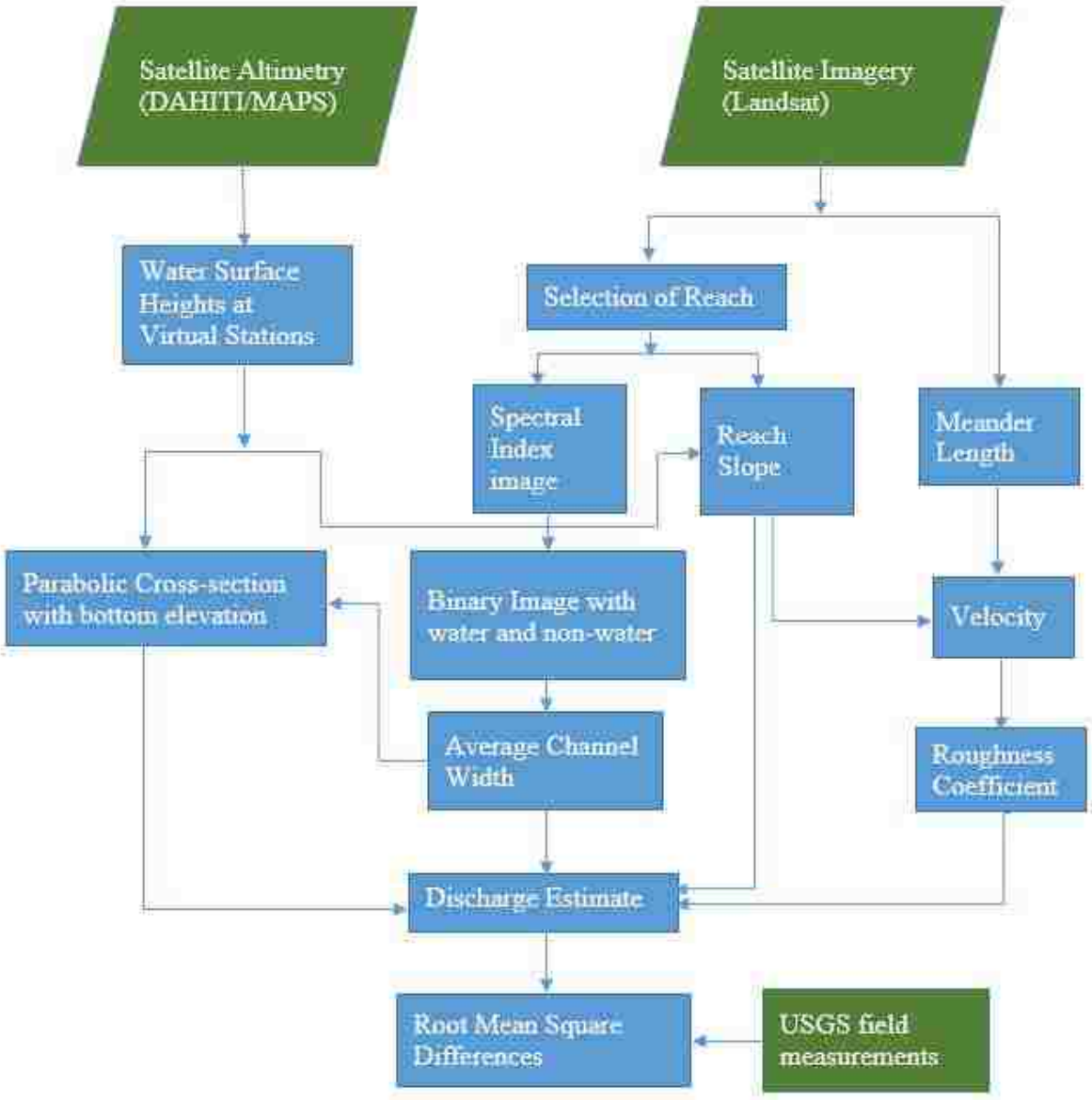


Figure 3-2: Flow chart for the estimation of discharge from satellite acquired water surface elevations and images.

### 3.4 Results

For the Mississippi River, the meander length was estimated to be 21.5 km; thalweg length between upstream and downstream virtual stations was estimated to be 21.4 km. A linear relation between the square of width and elevation of the water surface was well established with $R^2 = 0.87$. The regression coefficients were all statistically significant ($\alpha = 0.05$) that were checked by performing a t-test. Moreover, the fit was significant overall that was tested by performing F-test ($\alpha = 0.05$). The linear equation was obtained to be H = 3.42E-05$W^2$ + 12.659 where H is a dependent variable (y) and $W^2$ is an independent variable (x) in Figure 3-3 a. The bottom elevation of the modeled parabola is 12.7m. For the Colorado River, the meander length was estimated to be 13.4 km. However, a fixed thalweg length could not be defined due to varying crossing points. The crossing points vary due to the drifting of the satellite orbits. Moreover, the measurements were not consistent at a fixed point and varied among the cycles. Therefore, the distance between the two points was determined along the thalweg of the river were used to estimate elevation at a fixed point using the inverse distance method for each cycle. The linear relation between the square of width and elevation was not well defined with $R^2 = 0.32$. The equation of the fit for Colorado River was estimated to be H = 9.72E-05$W^2$ + 1180.5. The bottom elevation of the modeled parabola was estimated to be 1180.5 m. The coefficients of the fit were all statistically significant (α = 0.05) and the fit was significant overall.

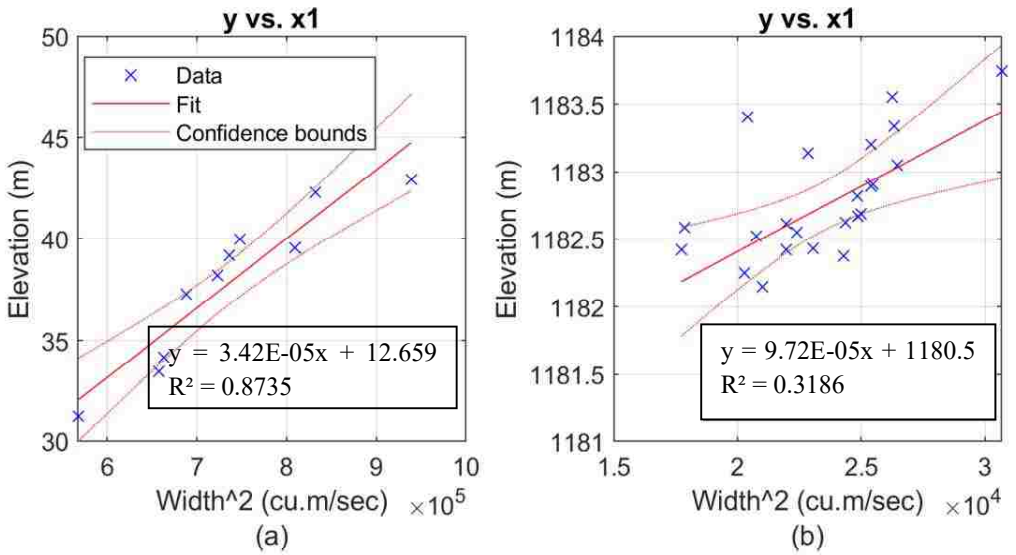


Figure 3-3: Fit of a linear line between the square of width and elevation. The fit is better for Mississippi River (a) with $R^2 = 0.87$ than for Colorado River $R^2 = 0.32$.

The closest gauging station to the selected reach for the Mississippi River was located in Francisville (Figure 1 a). The gauging station in Francisville did not have continuous daily discharge data. However, continuous discharge data is required to compare the estimates of discharge at the date of elevation acquisition. Therefore, a linear relationship was established between the Baton Rouge station, which is the closest gauging station with continuous discharge data, and the Francisville station. The linear relationship was developed using discharge data from 2009 to 2018. The linear fit was estimated with $R^2 = 0.95$. The coefficient of the fit, as well as the overall fit , were statistically significant at α = 0.05. Linear model without an intercept was chosen because the intercept term was deemed statistically insignificant (α = 0.05) from the t-test. The slope of the fit (less than 1) is consistent with the fact that Francisville is located upstream from the Baton Rouge station (Figure 3-4 a).

The estimates of discharges for the Colorado River were close to the discharges in the closest gauging station located in Potash (Figure 3-1 b). Data from the gauging station in Potash was available only from 2014, while the elevation data started from 2013. Therefore, the closest station with continuous data located in Cisco was used to deduce discharge at Potash based on a linear relationship. The linear relationship between discharges was estimated using daily mean discharges from 2014 to 2019. The linear fit without an intercept was estimated with $R^2 = 0.95$. The coefficient of the fit, as well as the overall fit , were statistically significant at $\alpha = 0.05$. A linear fit without an intercept was chosen as a regression model because the intercept was deemed statistically insignificant ($\alpha = 0.05$). The equation is provided in Figure 3-5 and the slope (greater than 1) is consistent with the fact that the Potash station is located downstream of the Cisco station (Figure 3-5 a). A quantile-quantile plot revealed that the distribution of discharge had heavy tails, which represents extreme values. Therefore, the use of the normal distribution assumption for linear modelling is valid for discharges that does not represent extreme values (Figure 3-4 a and 3-5 a).

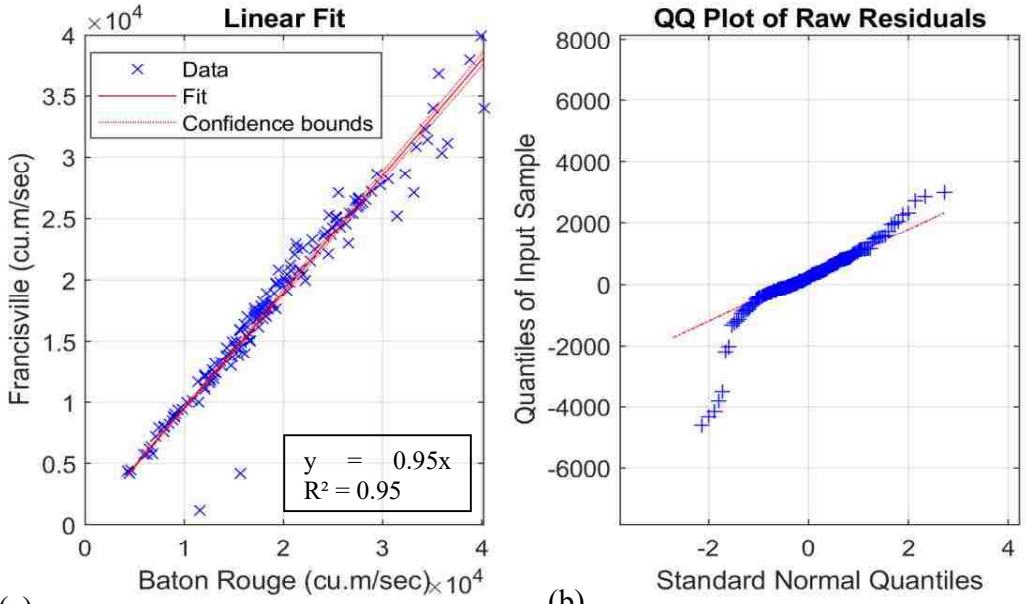


Figure 3-4: Fitting a linear relationship between the Francisville and Baton Rouge station to obtain field-measured discharges at the closest station from the reach for the Mississippi River.

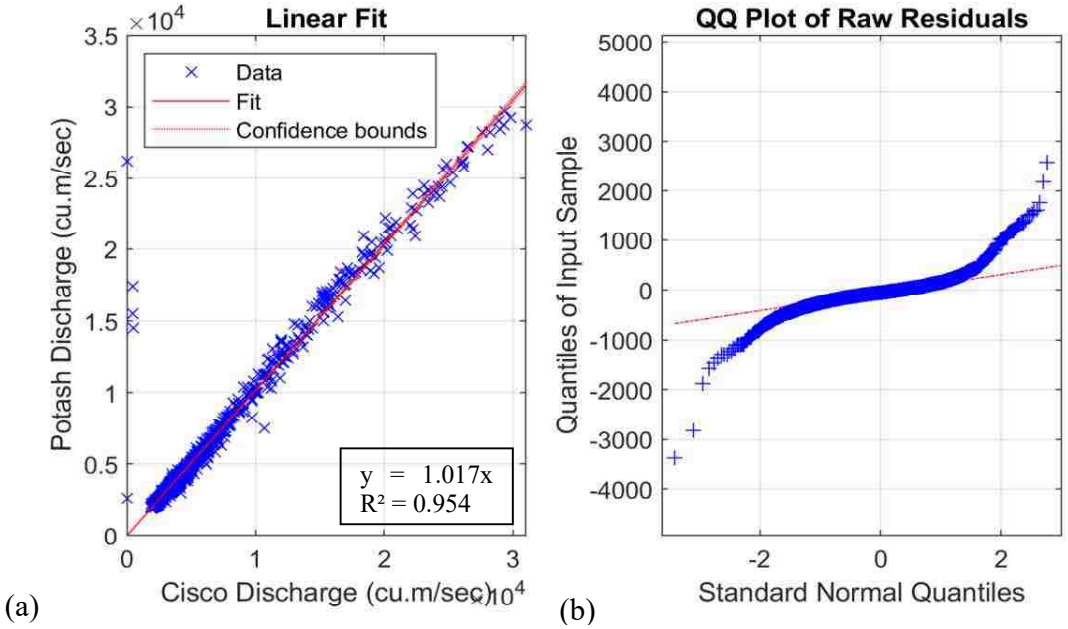


Figure 3-5: Fitting a linear relationship between the Potash and Cisco station to get field discharges at the closest station from the reach for the Colorado River.

Estimated discharges for the Mississippi River, based on the slope of the water surface, the meander length, and a modeled parabolic cross-section using Manning's equation were close to gauge measured discharges at ground stations. Comparison charts between discharge estimates and discharge at the Francisville station showed an RMSE of 7000 cu.m/sec, which is 36% of the gauge-measured discharges for 10 elevation-image sets used to estimate the cross-section (Figure 3-6 a). Discharges were estimated for 290 elevation values obtained from the DAHITI database for the virtual stations. The width of the section was computed using the formulated equation for a parabolic section of the channel. A comparison chart between estimated discharges and ground station-measured discharges revealed the effects of negative and outlier slopes to discharge estimates. These outlying estimates were controlled using a filter for negative slopes and slopes greater than 6E-5, which were considered to be outliers from slope box plots (Figure 3-6 b). The slope values that are greater than three times the quartiles of the slope data were deemed to be the outliers. The estimates were more accurate with an RMSE of 5700 cu.m/sec, which was 31.4% of the average of the discharge values (Figure 3-7 a). Estimates using the continuity equation that utilizes velocity and cross-section in the method were found to be biased, especially in the higher range, and with higher errors. The RMSE in the estimates using the continuity equation was 6.0129E+03 cu.m/sec and that is 33.2% of the average estimated values (Figure 3-7 b).

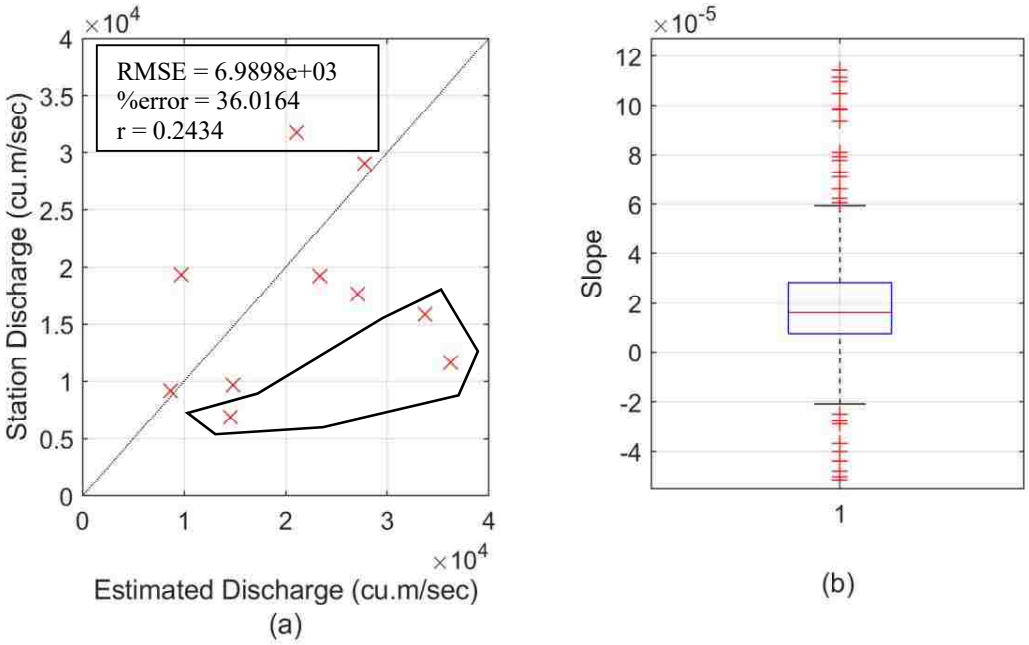


Figure 3-6: Scatter plot for estimates of discharge and discharge at Francisville for 10 elevation image sets (a). Box plots of slopes computed for all of the elevation data available for the virtual station from DAHITI show outliers starting from 6E-05. The black polygon in (a) shows the data points that were estimated with slopes that were deemed outliers in (b).

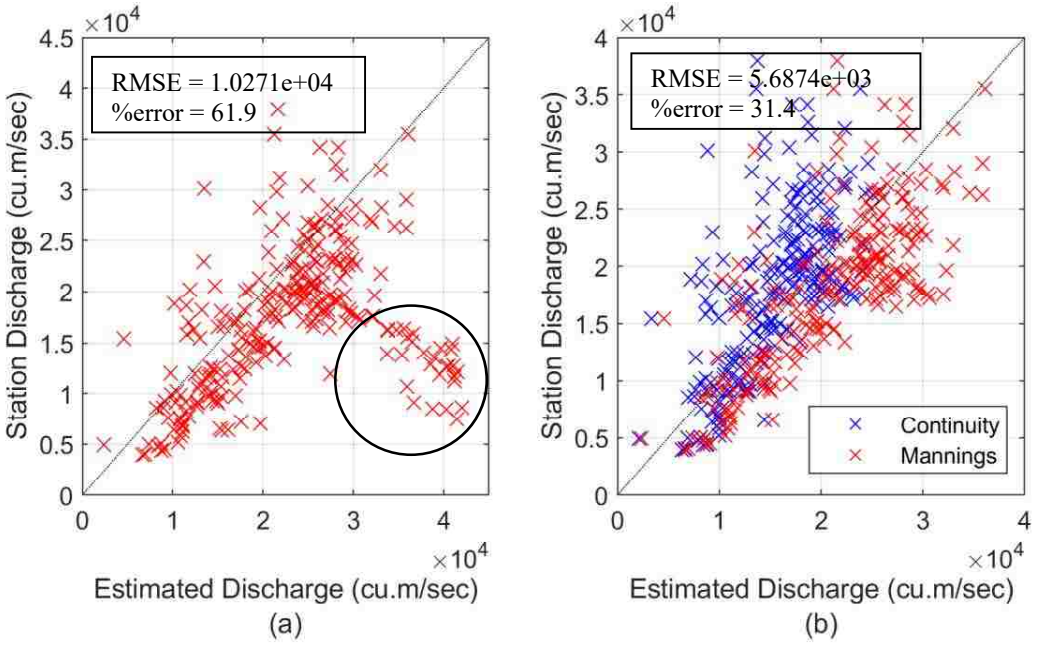


Figure 3-7: Comparison between estimated discharges from elevations and discharge at Francisville gauging station. The estimates were highly affected by negative as well as the high slope values (a) (shown with a circle) which when filtered out controlled estimates with high errors (b). The blue points are estimates from a using continuity equation in (b).

For the Colorado River, the estimates of discharge were close to the field measured discharges at the closest gauging station located in Potash as seen from the comparison plot (Figure 3-8 a). The RMSE of the discharge estimates was 36.6 cu.m/sec, which is 25.2% of the average of the gauge-measured discharges for 24 elevation-image sets used to estimate the parabolic section. Discharge estimates were also computed using 128 elevation values computed from Jason-2 altimeter data using the MAPS. This required calculation of water surface widths using the parabolic equation that was modeled for the channel section. The outlying estimates were not as severe as in the case of the Mississippi River. A filter was used for negative slopes

and slopes that exceeded 3.5E-4 for identifying slope outliers from slope box plots (Figure 3-8 b). The RMSE of the discharge estimates was 50.36 cu.m/sec, which was 30.42% of the average of discharge values (Figure 3-9 a). Estimates using the continuity equation that utilizes velocity and cross-section were found to be positively biased with higher errors (Figure 3-9 b). The RMSE of the estimates using continuity was 204.53 cu.m/sec that is 123.55% of the average estimated values.

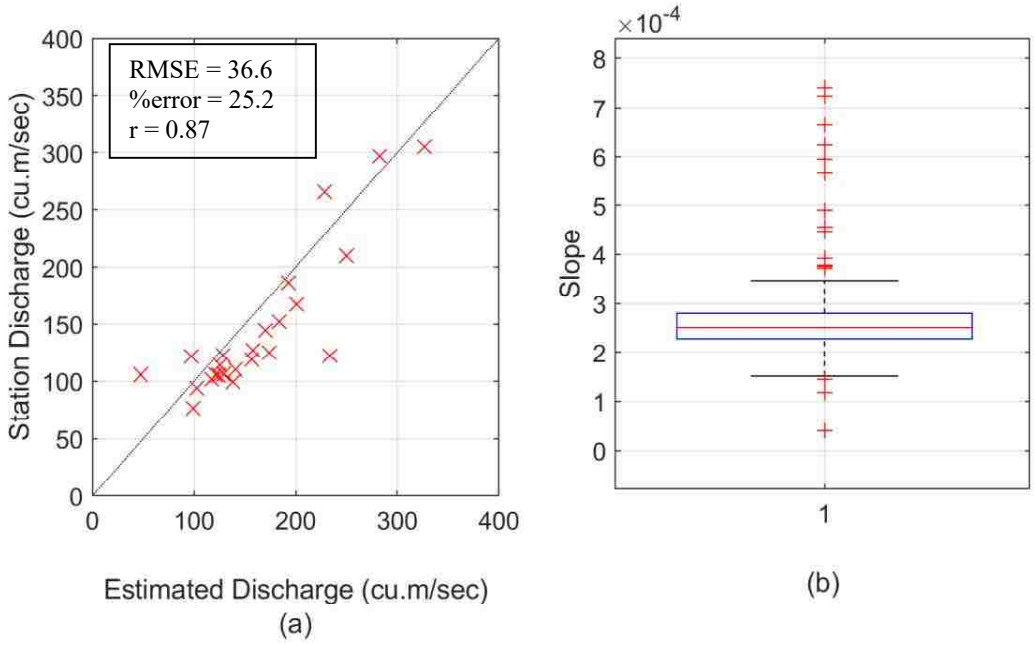


Figure 3-8: Scatter plot for estimates of discharge and discharge at Potash for 24 elevation image sets (a). Box plot of slopes computed for all of the elevation data from Jason-2 satellite extracted using MAPS shows outliers starting from 3.5E-04.

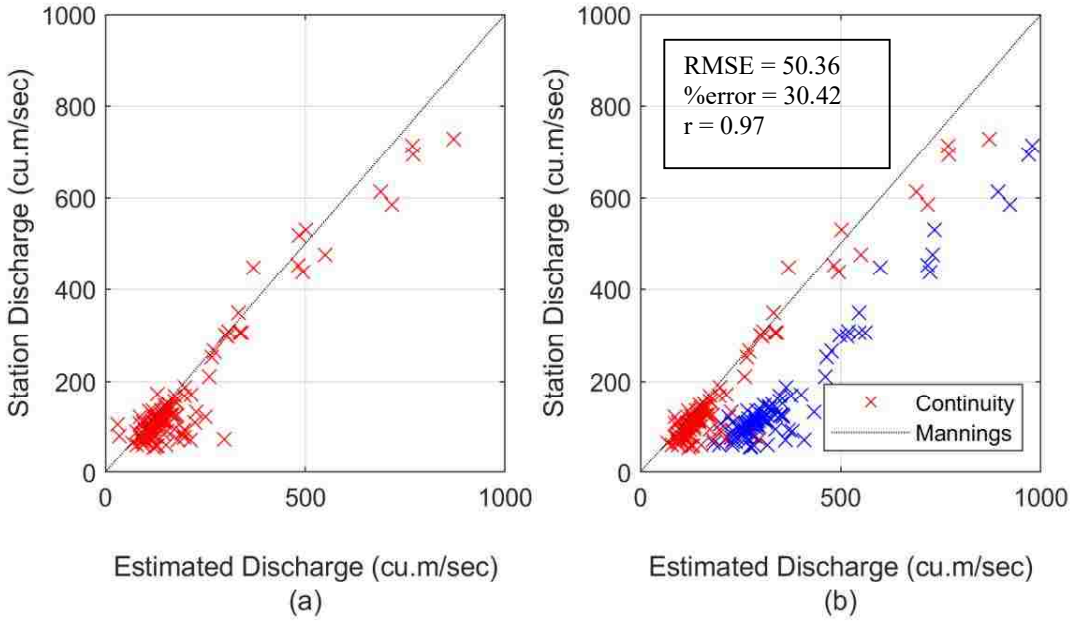


Figure 3-9: (a) The estimated discharges plotted against station discharge at Potash shows a good agreement with an RMSE = 36.65 cu.m/sec which is 24.4% of the average discharge. (b) The blue crosses are the discharge estimates using continuity equation shows higher errors.

The modeled channel cross-section for the Mississippi River and the Colorado River is shown in Figure 3-10. The Colorado River flows in a small range of elevation within 10 meters of height from the bottom. The cross-sectional shape of the Mississippi River is wider and larger than the Colorado River which is consistent with the field measurements. The equations of parabola, using the square of width and elevation that governs the property of shape, are presented in Figure 3-3 a.

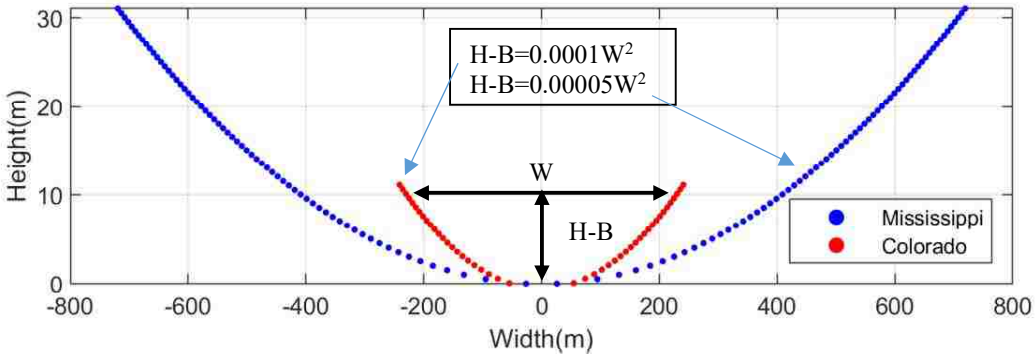


Figure 3-10: Modelled cross-section of the Mississippi and the Colorado River showing differences in size and shape. Mississippi River is wider and larger than Colorado, which is steeper.

The roughness coefficient was back-calculated based on available discharge but no linear relationship or any stage-based pattern in increment or decrement of the roughness coefficient was found in either of the rivers. (Figure 3-11 a and b) However, it was found that the roughness coefficients computed to match the discharge were overfitted and sometimes were beyond normal values for a natural river channel that is typically between 0.2 and 0.4.

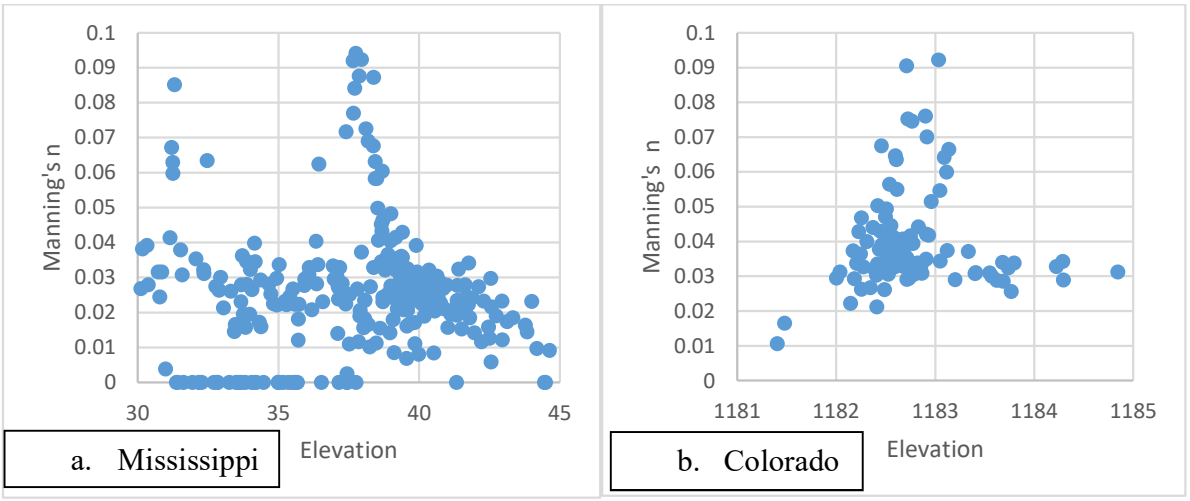


Figure 3-11: Scatter plot of elevation vs a calibrated Manning's roughness coefficient showed no strong correlation or relationship for either (a) the Mississippi River or (b) the Colorado River.

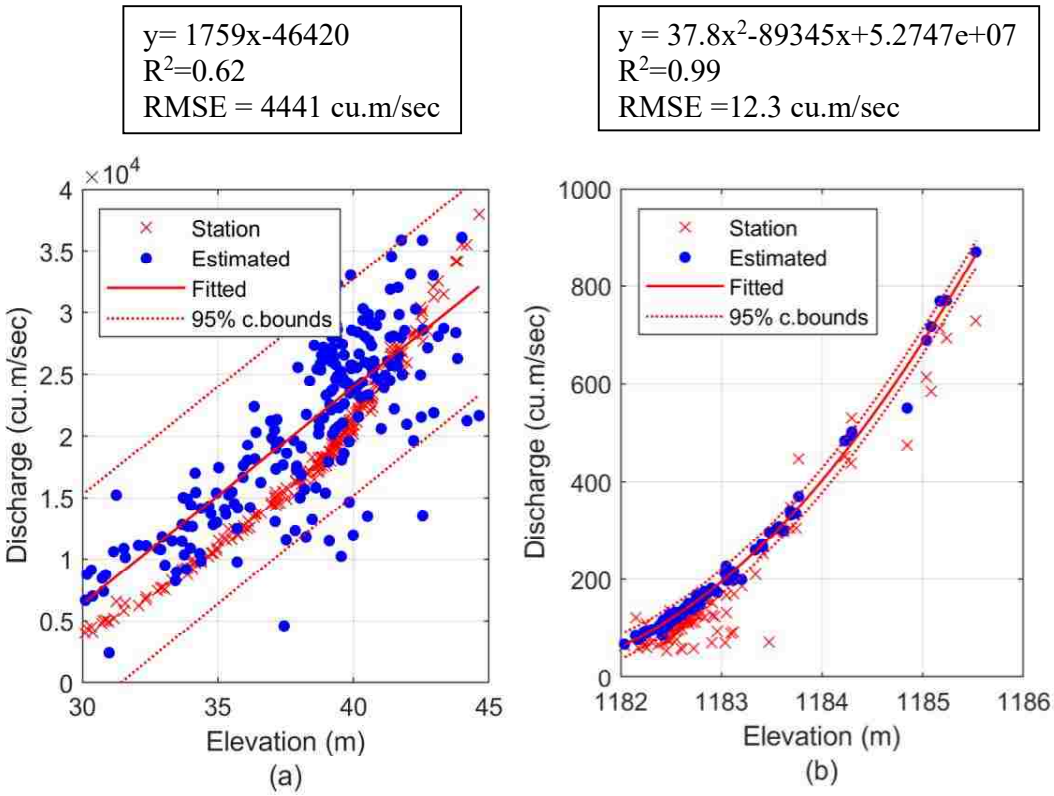


Figure 3-12: Fitted linear line (red line) for the Mississippi River (a) and second-order polynomial for the Colorado River (b) between water surface elevation and estimated discharge (blue dots) overlapped with discharge at the closest USGS station (red cross). The fit coefficients and the overall fits are statistically significant (α = 0.05). This shows that the estimated discharge and the formulated curve is more realistic for the Colorado River than for the Mississippi River.

Second-order polynomial curves were tested to fit the data with elevation as the independent variable $(x)$ and estimated discharge as the dependent variable $(y)$. Statistical significance of the estimated coefficients were tested by performing t-test, and overall significance of the fit were tested by performing F-test. But the coefficient for the second-degree term was statistically insignificant (α = 0.05) in the case of the Mississippi River. So, a linear fit

with significant coefficients and a overall fit was used. For the Colorado River, a second-order polynomial was fitted with coefficients that were statistically significant ($\alpha = 0.05$). Results of the significance tests for the final models are summarized in Appendix Table B 3. The coefficient of determination for the fitted curve for the Mississippi River was moderate with $R^2 = 0.62$ and $RMSE$ of 4441 cu.m/sec (Figure 3-12 a). The estimated discharge has a large variability and includes field-measured discharges on the same day at USGS station within 95% confidence bounds. However, the characteristics of the stage-discharge curve represented by the elevation and station discharge could not be captured. The nature of the curve is concave while the estimated fit is linear. For the Colorado River, the fit of the polynomial curve to elevation and estimated discharges was very good with coefficient of determination $R^2 = 0.99$ and $RMSE$ of 12.3 cu.m/sec (Figure 3-12 b). The coefficients and overall fits are statistically significant. The nature of polyline well captures the USGS station data. However, station data were outside of 95% confidence bounds in many instances.

### 3.5 Discussion

The use of Manning's equation required estimates of three major components: the slope of the water surface, cross-sectional shape, and roughness coefficient. The slope of the water surface is a major component in estimating discharge. The estimates were found to be heavily dependent on slope estimates compared to other components. The use of empirical equations for velocity to estimate water depth were intermediate steps to estimate the channel roughness coefficient. The assumption of wide channel flow for the estimate of roughness coefficients in equation (6) is to be noted when using the algorithm for narrow channels. It was noted that the roughness coefficient of a channel is dynamic and depends on the regime and depth of water in

the channel. However, the roughness coefficient was sensitive to the elevation and slope of water while the velocity and depth of water remained less affected in the procedure.

Wider channels with the larger width-to-height ratios are favorable for estimating parameters for cross-sectional shape. The Colorado River has a narrow cross-sectional profile. Therefore, the change in the width of the river within a small range of change in elevation of the water surface also becomes small. These minor changes might be hard to detect with satellite images with relatively large pixel sizes. The maximum width for 10-m height is 400 meters for the Colorado River. The 400 m width is equivalent to 13 pixels of Landsat 8 OLI images. In fact, the change of water surface elevation is so small that discerning a change within a 30-m pixel increment is difficult in some instances. A very low coefficient of determination for linear relationship for the Colorado River is indicated by $R^2 = 0.32$ . It is not surprising that the Mississippi River on the other hand, with a larger elevation change in the water surface within a reach, and a marked increase in width has better co-efficient of determination for shape parameters.

The bottom elevation of the river channel was an important shape parameter in terms of dependency in discharge estimates. The accuracy of estimated discharges for the Colorado River could exist because of suitable estimates of bottom elevation even with a low coefficient of determination. A low coefficient of determination means that the estimate of bottom elevation is less reliable for the Colorado River because of a width-to-height ratio than the Mississippi River. This result conforms to limitations discussed in Bjerklie et al., (2003). However, the range of accuracy is higher than what might be expected from ground-based indirect measurements of discharge (Rantz, 1982).

The estimation of shape parameters was more reliable for the Mississippi River. However, the accuracy of the identification of cross-sectional shape cannot be stated. In fact, the shape of the river cross-sections obtained from the ADCP at the Francisville and Baton Rouge stations were considerably different. The estimates of discharge were more accurate and stable for the Colorado River. This result is not necessarily counterintuitive to estimates of shape parameters. Even though channel section estimates were less accurate and reliable, the stability of the channel section due to rocky terrain is greater. A stable cross-section ensures that a similar discharge is flowing in the section at the same water surface elevation. This might have increased the accuracy of the discharge estimates for 128 elevation data. On the other hand, the Mississippi River has a dynamic cross-section and roughness coefficients that have more variability of discharge at similar water surface elevations. However, the plot of elevation and USGS station discharge is counterintuitive. The plot is more stable for the Mississippi River than the Colorado River. This might occur for two reasons. First, the estimation of discharge is largely dependent on slope estimates. Slope estimates might be more stable for the Colorado River and is an indication of less flooding and backwater curves. The second reason could be that the algorithm is less reliable for wide channel rivers. Estimating discharge from slope and channel cross-section parameters might be inaccurate for wide channels than for steeper channels. Apart from these two reasons, the discrepancies between the station discharge and estimated discharge for Colorado River might be because of errors in the extraction of slopes and elevations at fixed points from MAPS using the procedure adopted in this study. However, this could be due to accuracy limitations of radar altimeters. Radar altimeters have a footprint that is larger than the width of the river and can pick up elevations that are not related to the water surface.

The steeper shape of the modeled parabola for the Colorado River in comparison to the Mississippi River conforms to the nature of the terrain. The Colorado River flows through rugged and rocky terrain for most of its path. A well-defined channel cross-section of the Colorado River barely changes throughout the year. The channels, formed by eroding rocks, are more stable. On the other hand, the Mississippi River flows through alluvial plains and receives multiple floods in a year. The impact of the floods and, fluctuating discharge volume, coupled with a more mobile channel bed brings larger and more frequent changes to the channel cross-section than occurs for the Colorado River.

The mean squared error was much better and ranged between 5 to 21% in the case of the Yukon River for un-calibrated estimates. Moreover, results improved drastically when calibrated using field-measured discharges with mean error within 2%. The biases in the high and low end, as well as the mean of the estimates, were improved. These accuracies could not be obtained in either of the rivers in this study for un-calibrated discharges. Surprisingly, no definite nature of bias in the estimates was found in this study as in the case of the Yukon River (Figure 3-7 and 3-9).

## 3.6 Conclusions

Discharges in the Mississippi River and the Colorado River were estimated within 31% of the average discharges in each river. Results showed that discharges were estimated with a root mean square error of 5600 cu.m/sec for the Mississippi River. For the Colorado River discharges were estimated with an RMSE of 50 cu.m/sec. It was difficult to estimate a cross-section for rivers with a smaller width and/or smaller change in width with water level as in the case of the Colorado River. However, the accuracies of estimates were similar in both the cases in terms of the percentage of error. Results were more stable for the Colorado River than for the

Mississippi River. Estimates of discharge in the Colorado River were overestimated, due to errors in the computation of elevations and/or transferring elevations at a fixed point.

This study provides a method for estimating the discharge in rivers from the use of only remotely sensed data. The methods were tested for two different rivers, the Mississippi River that represents an alluvial river, and the Colorado River representing a river flowing through rocky terrain. The method used the Modified Normalized Difference Water Index, a spectral index, computed from Landsat Surface Reflectance data to extract water surface extents for computing channel widths. Water surface widths and water surface elevations were used to model a parabolic cross-section of each river. Manning's equation was used to estimate discharges. The following general conclusions can be drawn from this research:

a. A set of satellite altimeter data matched with the temporally closest Landsat image can successfully estimate discharge in rivers with reasonable accuracy.
b. The estimation of the cross-sectional shape is an important step and depends on the accuracy of the width estimation from the Landsat images. Rivers with smaller widths and/or small changes in width with water level are difficult to evaluate because of resolution limits of the images to detect change.
c. A combination of remote sensing image and radar altimetry data can provide a global framework for monitoring flows in river networks that will provide a better understanding of the changes in surface water.

Results of the estimation procedure provide insights on how remotely sensed data can be sufficient to estimate discharges in rivers under a reasonable range. However, the goal of achieving reliable estimates can be difficult to attain due to insufficient discharge computation

algorithms. Empirical models were found to be inadequate to estimate discharge in varied terrains. Meanwhile, it is exciting how the SWOT mission scheduled for 2020 that will acquire width information along with more reliable and accurate elevations that can improve estimates of discharges.

## CHAPTER 4: Contributions and Recommendations

### 4.1 Summary

Remote sensing is a promising technology for the future due to its capability of global coverage and stable frequency in data acquisition. Both of these qualities have great potential for establishing a monitoring framework for tracking water features on the surface of the earth. Exploring the available data, as well as formulating the algorithms and techniques, to estimate water quantities in rivers and lakes are important to achieve the goal of a single and complete monitoring system. Moreover, this research could also guide the type of data to be acquired in future satellite missions. These new sources of data are likely to enhance the estimation capabilities.

In this study, satellite acquired data were used to estimate volume in reservoirs and discharge in rivers. These estimates were paired with water surface elevations to obtain stage-area-storage relationships for reservoirs and stage-discharge relationship for rivers. Two primary data sources were used in this study to accomplish the objectives set out in Chapter 1. Water surface elevations acquired with a satellite radar altimeter were obtained from opensource databases. Water surface extents (area and width) and morphological features such as meander length were extracted from satellite multi-spectral images obtained from Landsat missions. Two tasks were performed to address the questions and the hypotheses proposed in the study.

The first task investigated Research Question #1: How well can the relationships among water surface elevations, areas, and storages in reservoirs be estimated from remotely sensed data without the use of any field measurements? What are the types and sources of error in the estimates? What differences can be found in the estimates between different reservoirs, and what

can the possible cause of the differences be? It was hypothesized that the estimates of water volume in reservoirs at various water surface elevations would be within reasonable limits. These estimates could be paired to estimate relationship that was reasonably close to the estimates from field measurements. The differences in estimates between field measurements and remote sensing could be explained with the limitations of remotely sensed data such as pixel size and errors due to shadow and human constructions, such as marinas, in water. The features of reservoirs such as shape and size and presence of shadow due to deep canyons should affect the estimates in some manner.

Research Question #1 was addressed by formulating a strategic procedure to estimate water surface area and water volume that was missing in the current literature. Water levels were derived from Hydroweb, which is an open-access satellite altimetry database. Areas were estimated from Landsat 5 surface reflectance images by classifying the Modified Normalized Difference Water Index (MDNWI). The MNDWI is a spectral index calculated using green and infrared bands. The classification converts the index image into binary images using an internally calibrated threshold. Internal calibration of the threshold was done by computing the overall accuracies of classification by forming confusion matrices. These matrices were created for selected regions in the classified image. Finally, water surface heights from the lowest levels and areas were used to estimate volume assuming pyramidal shape, and second-order polynomials were fitted to compute relationships.

Stage-area-storage relationships were developed for Lake Mead (LM) and Lake Powell (LP). The study estimated the areas of LM with a Root Mean Square Difference (RMSD) of 17.8 $km^2$ and LP with 53.7 $km^2$ compared with in-situ measurements. The RMSD in volumes were 699 Million Cubic Meters (MCM) for LM and 1330 MCM for LP. LM estimates were more

accurate than LP. This was found to be because of three reasons: first, LP is filamentous and has more land and water interface where mixed pixels are located. Mixed pixels are sources of error for misclassification and the resolution of the image (30 meters) accumulates substantial errors during each miss-classification. Second, LP has deeper and narrower canyons that are dominated by shadow. Shadows are prone to classification as water, and hence, were another source of error. Third, human construction in the lake, such as marinas, obscures the water surface that is acquired by the satellites, and hence, introduces artificial islands in the image.

The second task addressed Research Question #2: How well can the relationship between water surface elevations and discharges in the river be estimated from remotely sensed data without the use of any field measurements? What are the types and sources of error in the estimates? What differences can be found among estimates of discharges for different rivers, and what are the possible causes of differences? It was hypothesized that algorithms utilizing hydraulic and morphologic information such as water surface width, slope, and meander length can estimate discharges within reasonable limits. The accuracy of estimates of slope and width should play a major role in estimates. The accuracy might depend on limitations of remotely sensed data such as accuracy in water surface elevations, as well as pixel size for detecting a change in water surface width. The nature of the terrain was expected to influence meander patterns, and channel cross-section, and hence, the reliability of estimates of discharge.

The study addressed Research Question #2 by using an algorithm that uses Manning's equation for estimating the discharge, and empirical models to estimate the roughness coefficient. Two rivers, the Mississippi and Colorado, representing an alluvial and rocky terrain, respectively, were selected to highlight the differences in estimates in varied terrain, as well as the size of the river. A variant of Manning's equation was used, which required channel cross-

section, water surface slope, and roughness coefficient as input parameters. A parabolic cross-section was fitted for each river using the width of the river estimated from Landsat images at several water levels. The water surface slopes were estimated from water elevations using two sources. For the Mississippi River, water surface elevations provided at virtual stations from the DAHITI database were utilized. For the Colorado River, elevations were extracted using the MAPS at river crossings. The roughness coefficients were estimated using empirical models that utilized meander length. The results showed that discharges were estimated within 31.4% of the average discharge with root mean square error (RMSE) of 5700 cu.m/sec for Mississippi River. For the Colorado River, discharges were estimated within 30.4% of the average discharge with an RMSE of 50 cu.m/sec. It was difficult to estimate a cross-section for rivers with a smaller width, and/or smaller change in width with water level as in the case of the Colorado River. However, the accuracies in estimates were similar in both the rivers in terms of percentage of error and results were more stable for the Colorado River than the Mississippi River.

## 4.2 Contributions

An appreciable number of studies have used remotely sensed data to estimate the water quantities in rivers and lakes around the globe. It is acknowledged that many of the studies have developed relationships among the variables (water surface level, area, and water quantity) although not as an explicit objective of the study. However, this study is the first to bring focus on the estimation of the relationships that are vital before making any comments on climate change or variability. The major contributions of this research are as follows. First, this study provides a strategic procedure to estimate water surface areas from satellite images with the calibration of the thresholds for spectral indices computed for images. Few studies have acknowledged the temporal and sensor dependency of the threshold used for classification. This

leads to estimates of water extent that either is under-estimated or over-estimated because of an uncalibrated value chosen based on other studies. This study also highlights that the shapes of reservoirs influence the presence of mixed pixels that are prone to be miss-classified by using two reservoirs. Shadows that are dominant in canyons were also found to reduce the accuracy in the estimation of water surface area.

Second, studies that estimate discharges in rivers in the continental United States are very few, and this study adds valuable insights on the Mississippi River and the Colorado River, both of which are unexplored in this area. Moreover, the use of an open-source database for satellite-acquired elevations such as the DAHITI and elevation extraction tools such as MAPS have not been used in any of the previous studies. These sources have the advantage of being freely available and save computational time and cost. The classification of the MNDWI to estimate river widths is also a unique application for estimating water extent in rivers.

### 4.3 Limitations

Although this study attempts to address the challenges of estimating water quantities in the water bodies, some still exist. The accuracies of water surface elevations were compromised when the shape of the water surface was narrow such as in narrow canyons. The reflected radar waveforms might be a combination of adjoining land and water, instead of only water. This problem was noted in the case of the Colorado River. The resolution of the image was a major challenge in both of the tasks. Higher resolution images could reduce the effect of mixed pixels that were present in the interface between land and water (boundaries). Moreover, the higher resolution could increase the accuracy in detecting changes in the water area and width in narrow rivers, which was a dominant problem noted in the case of the Colorado River. The algorithms for the estimation of discharge were based on empirical models rather than physical and were

developed from a set of data among many rivers. A physical interpretation was difficult for such relationships and algorithms that might lead to incorrect estimates in rivers not having similar features. Additionally, the volumes of water in the reservoirs within an operational range were estimated in this study and is adequate for volume monitoring in most of the application. However, determining the complete shape of the reservoir with remotely sensed data is still an area of research.

### 4.4 Recommendations for future work

This study covers the estimation of water quantities in the reservoirs and rivers and highlights the differences in the estimates in different water bodies. However, it is acknowledged that a set of two rivers and reservoirs can provide limited information regarding the implementation of algorithms and techniques. The availability of data was a major obstacle, and an additional number of rivers and reservoirs could add more insights. Apart from this, other recommendations for similar future research are listed below:

1. Availability of data especially for water surface elevations of rivers was limited in the North American Continent. However, the database such as Hydroweb and DAHITI both are continuously extending their scope. They are including a greater number of virtual stations and reservoirs as the collection and processing of data is progressing. New data sets at additional locations will be very helpful to test these algorithms for other locations.
2. A combination of multi-satellite data can provide a longer time series of elevation. Although this idea has been adopted by the databases used in this study, extraction of elevation values from MAPS relied on Jason-2 data. This limited the use of data pairs within a few years. Although connecting elevation values from multi-satellite data

might require additional steps to verify the conjunction, the effort might be worth the increment in the accuracies.

3. The use of elevations at two crossings to estimate slope has higher changes of being erroneous if there are errors in the readings between any one of them. Synthetic Aperture Radar (SAR) images are able to capture a complete state of water surface that might be very helpful to estimate correct slopes if the images are of adequate resolution.
4. The resolution of images (Pixel sizes) was a major hurdle to achieve higher accuracies in area estimation. However, if high-resolution images can be used, and accuracy can be compared with the existing data, it could be helpful.

The satellite images from different sensors and at taken at different times lead to variability in surface reflectances. There has not been a concrete way to eliminate these temporal and sensor dependencies. Although a method of calibrating threshold is proposed in this study, a method to remove these dependencies is still an active area of research.

**Appendix A: Supplemental information for Chapter 2.**

Table A-1: Details of 15 selected stages based on altimetry elevation for the Lake Mead. The columns from left to right shows the date and time of the measurement of the elevation; elevation values; the date of acquisition of satellite imagery for the estimation of area and the difference in days between the elevation measurement and the images used for area estimation.

| **Stage** | **Date of elevation acquisition** | **Height above GGM02C geoid (m)** | **Date of Image acquisition** | **Difference in Days** |
|---|---|---|---|---|
| 1 | October 13, 2010 | 330.75 | October 14, 2010 | 1 |
| 2 | July 1, 2010 | 333.41 | July 10, 2010 | 9 |
| 3 | January 6, 2010 | 335.28 | January 15, 2010 | 9 |
| 4 | June 11, 2011 | 336.42 | June 11, 2011 | 0 |
| 5 | September 2, 2008 | 337.90 | September 6, 2008 | 4 |
| 6 | July 12, 2007 | 340.37 | July 18, 2007 | 6 |
| 7 | September 3, 2011 | 340.78 | August 30, 2011 | -4 |
| 8 | May 3, 2007 | 342.67 | April 29, 2007 | -4 |
| 9 | November 8, 2006 | 344.21 | November 4, 2006 | -4 |
| 10 | January 17, 2007 | 345.04 | January 7, 2007 | -10 |
| 11 | April 13, 2006 | 348.03 | April 10, 2006 | -3 |
| 12 | August 16, 2002 | 351.39 | August 21, 2002 | 5 |
| 13 | October 30, 2002 | 352.94 | October 24, 2002 | -6 |
| 14 | July 20, 2001 | 360.59 | July 17, 2001 | -3 |
| 15 | June 14, 2000 | 365.03 | June 12, 2000 | -2 |

Table A-2: Details of 15 selected stages based on altimetry elevation for the Lake Powell. The columns from left to right shows the date and time of measurement of the elevation; elevation values; the date of acquisition of the satellite imagery for the estimation of area and the differences in days between the elevation measurement and the images used for area estimation.

| **Stage** | **Date of elevation acquisition** | **Height above GGM02C geoid (m)** | **Date of Image acquisition** | **Difference in Days** |
|---|---|---|---|---|
| 1 | September 23, 2004 | 1088.38 | September 13, 2004 | -10 |
| 2 | July 15, 2004 | 1091.46 | July 11, 2004 | -4 |
| 3 | March 20, 2004 | 1093.50 | March 21, 2004 | 1 |
| 4 | September 1, 2005 | 1099.24 | August 31, 2005 | -1 |
| 5 | October 15, 1992 | 1100.93 | October 14, 1992 | -1 |
| 6 | August 28, 2008 | 1106.52 | August 23, 2008 | -5 |
| 7 | August 21, 2010 | 1108.20 | August 13, 2010 | -8 |
| 8 | September 16, 2009 | 1110.41 | September 27, 2009 | 11 |
| 9 | March 6, 2002 | 1112.08 | February 28, 2002 | -6 |
| 10 | October 26, 2001 | 1114.98 | October 23, 2001 | -3 |
| 11 | June 2, 2001 | 1119.13 | June 1, 2001 | -1 |
| 12 | April 29, 2000 | 1120.04 | April 27, 2000 | -2 |
| 13 | August 2, 1996 | 1122.92 | August 6, 1996 | 4 |
| 14 | June 24, 1997 | 1125.27 | June 22, 1997 | -2 |
| 15 | September 27, 1999 | 1125.52 | October 2, 1999 | 5 |

Table A-3: Confusion matrix and overall accuracy for classification using a threshold of 0.06 for the Lake Mead and -0.05 for the Lake Powell.

| **(a)** Lake Mead (Threshold 0.05) | | Reference Data | |
|---|---|---|---|
| | | Non-Water | Water |
| Classified Data | Non-Water | 59582 | 2675 |
| | Water | 1964 | 57814 |
| Overall Accuracy = 96.19% | | | |

| **(b)** Lake Powell (Threshold -0.05) | | Reference Data | |
|---|---|---|---|
| | | Non-Water | Water |
| Classified Data | Non-Water | 80222 | 6714 |
| | Water | 272 | 67745 |
| Overall Accuracy = 95.49% | | | |

Table A-4: Regression statistics for polynomial fits (with and without intercept) for the Lake Mead and Lake Powell.

| Reservoirs | Variables (A/V ~ z model) | Coefficients (Confidence interval) | T-stat and P-value | Overall Significance F-stat and P-value |
|---|---|---|---|---|
| Lake Mead | Area ($\mathbf{A} = a\mathbf{z}^2+b\mathbf{z}+c$) | a = 0.07648 (0.04629, 0.1067)<br>b = 4.434 (3.371, 5.498)<br>c = 319.7 (312.1, 327.2) | 5.519592, 0.000132<br>9.088298, 9.96E-07<br>5.519592, 0.000132 | 1220.24, 1.37E-14 |
| | Volume ($\mathbf{V} = a\mathbf{z}^2+b\mathbf{z}$) | a = 3.328 (3.234, 3.423)<br>b = 309.2 (306.7, 311.7) | 76.21698, 1.27E-18<br>271.1802, 8.80E-26 | 411046.3, 1.22E-30 |
| Lake Powell | Area ($\mathbf{A} = a\mathbf{z}^2+b\mathbf{z}+c$) | a = 0.06257 (-0.006616, 0.1318)<br>b = 5.333 (2.569, 8.097)<br>c = 285.7 (262.3, 309.1) | 1.970463, 0.072299<br>4.203724, 0.001224<br>26.60873, 4.87E-12 | 274.67, 9.54E-11 |
| | Volume ($\mathbf{V} = a\mathbf{z}^2+b\mathbf{z}$) | a = 3.729 (3.608, 3.85)<br>275.7 (271.9, 279.5) | 66.39664, 7.61E-18<br>157.4234, 1.03E-22 | 2.84E+05, 1.34E-29 |

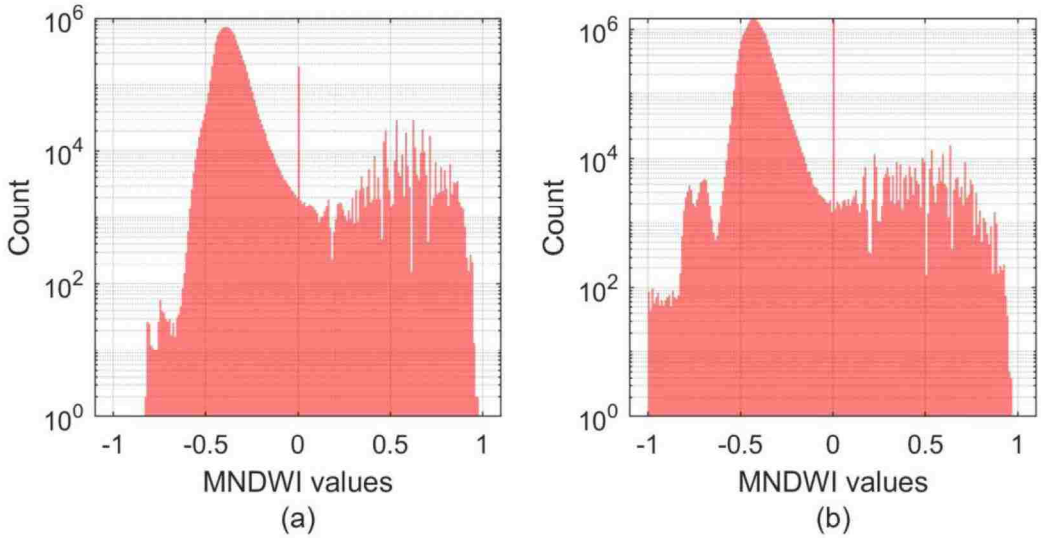


Figure A-1: Histogram of Modified Normalized Difference Water Index (MNDWI) values for the first stage (lowest water level) of the Lake Mead (a) and the Lake Powell (b) showing a separation between water and non-water near the value of zero.

**Appendix B: Supplemental information for Chapter 3**

Table B-1: Elevation and Image pairs used for the Mississippi River to estimate the relationship between water surface elevation and width. Some of the data were discarded to filter out negative and outlier slope as discussed in the main text

| (i) | Upstream Virtual Station | | Downstream Virtual Station | | | | (iv) | (v) | (vi) |
|---|---|---|---|---|---|---|---|---|---|
| Stage | (ii) Date of Elevation (mm/dd/yyyy) | Elevation, E1 (m) | (iii) Date of Elevation (mm/dd/yyyy) | Elevation, E2 (m) | The difference in Height (E1-E2) | Average Elevation (E1+E2)/2 | Image Date | Days differences ((iv)-(ii)) | Discharge at Francisville (cu.m/sec) |
| **1** | 10/19/2011 | 31.828 | 10/19/2011 | 30.676 | 1.152 | 31.252 | 10/17/2011 | -2 | 6731.63 |
| **2** | 10/27/2010 | 32.993 | 10/27/2010 | 32.788 | 0.205 | 32.8905 | 10/30/2010 | 3 | 7021.53 |
| **3** | 8/27/2009 | 33.52 | 8/27/2009 | 33.429 | 0.091 | 33.4745 | 8/24/2009 | -3 | 8971.76 |
| **4** | 12/6/2010 | 33.546 | 12/6/2010 | 33.794 | -0.248 | 33.67 | 12/1/2010 | -5 | 7390.49 |
| **5** | 8/30/2011 | 34.397 | 8/30/2011 | 33.97 | 0.427 | 34.1835 | 8/30/2011 | 0 | 9472.49 |
| **6** | 10/7/2010 | 34.113 | 10/7/2010 | 34.239 | -0.126 | 34.176 | 10/14/2010 | 7 | 8075.71 |
| **7** | 8/29/2010 | 39.052 | 8/29/2010 | 35.493 | 3.559 | 37.2725 | 8/27/2010 | -2 | 11370.01 |
| **8** | 3/1/2009 | 39.259 | 3/1/2009 | 37.127 | 2.132 | 38.193 | 3/1/2009 | 0 | 15560.37 |
| **9** | 7/10/2010 | 39.236 | 7/10/2010 | 38.198 | 1.038 | 38.717 | 7/10/2010 | 0 | 16904.45 |
| **10** | 1/11/2009 | 39.583 | 1/11/2009 | 38.756 | 0.827 | 39.1695 | 1/12/2009 | 1 | 17299.76 |
| **11** | 4/22/2010 | 39.562 | 4/22/2010 | 39.539 | 0.023 | 39.5505 | 4/21/2010 | -1 | 18986.45 |
| **12** | 6/18/2009 | 40.173 | 6/18/2009 | 39.752 | 0.421 | 39.9625 | 6/21/2009 | 3 | 18854.67 |
| **13** | 2/11/2010 | 41.659 | 2/11/2010 | 41.065 | 0.594 | 41.362 | 2/16/2010 | 5 | 27419.87 |
| **14** | 5/19/2009 | 42.495 | 5/19/2009 | 42.095 | 0.4 | 42.295 | 5/20/2009 | 1 | 28474.05 |
| **15** | 6/12/2011 | 43.022 | 6/12/2011 | 42.904 | 0.118 | 42.963 | 6/11/2011 | -1 | 31109.49 |

Table B-2: Elevation and image pairs used for the Colorado River to estimate the relationship between water surface elevation and width. The elevations are extracted from Jason 2 satellite data using MAPS. Elevations at a fixed point were computed instead of average elevation due to the drifting of crossings. Some of the data were discarded to filter out negative and outlier slopes as discussed in the main text.

| (i) Stage | (ii) Cycle Date (mm/dd/yy) | (iii) Elevation at a fixed point (m) | (iv) Water Surface Slope | (v) Image Date | (vi) Days differences ((v) – (ii)) | (vii) Discharge at Potash (cu.m/sec) |
|---|---|---|---|---|---|---|
| 1 | 6/1/2013 | 1183.336 | 0.00025 | 5/26/2013 | -6 | 209.76 |
| 2 | 6/11/2013 | 1183.551 | 0.00026 | 6/11/2013 | 0 | 296.36 |
| 3 | 7/1/2013 | 1182.418 | 0.00023 | 6/27/2013 | -4 | 93.82 |
| 4 | 9/28/2013 | 1182.821 | 0.00024 | 10/1/2013 | 3 | 144.45 |
| 5 | 10/18/2013 | 1182.667 | 0.00027 | 10/17/2013 | -1 | 126.90 |
| 6 | 1/25/2014 | 1182.248 | 0.00026 | 1/21/2014 | -4 | 76.27 |
| 7 | 4/14/2014 | 1183.403 | 0.00025 | 4/11/2014 | -3 | 265.28 |
| 8 | 5/14/2014 | 1183.74 | 0.00023 | 5/13/2014 | -1 | 304.99 |
| 9 | 8/21/2014 | 1182.685 | 0.00025 | 8/17/2014 | -4 | 118.56 |
| 10 | 8/31/2014 | 1182.907 | 0.00024 | 9/2/2014 | 2 | 151.93 |
| 11 | 9/20/2014 | 1182.892 | 0.00021 | 9/18/2014 | -2 | 124.89 |
| 12 | 9/30/2014 | 1183.202 | 0.00015 | 10/4/2014 | 4 | 186.46 |
| 13 | 10/10/2014 | 1183.051 | 0.00022 | 10/4/2014 | -6 | 167.47 |
| 14 | 11/9/2014 | 1182.373 | 0.00029 | 11/5/2014 | -4 | 113.96 |
| 15 | 11/18/2014 | 1182.586 | 0.00024 | 11/21/2014 | 3 | 105.90 |
| 16 | 1/7/2015 | 1181.407 | 0.00074 | 1/8/2015 | 1 | 105.61 |
| 17 | 2/6/2015 | 1182.549 | 0.00023 | 2/9/2015 | 3 | 106.19 |
| 18 | 3/17/2015 | 1182.611 | 0.00025 | 3/13/2015 | -4 | 99.28 |
| 19 | 3/27/2015 | 1182.52 | 0.00027 | 3/29/2015 | 2 | 122.87 |
| 20 | 4/16/2015 | 1182.42 | 0.00024 | 4/14/2015 | -2 | 101.30 |
| 21 | 7/5/2015 | 1183.683 | 0.00027 | 7/3/2015 | -2 | 304.99 |
| 22 | 9/22/2015 | 1182.147 | 0.00032 | 9/21/2015 | -1 | 121.72 |
| 23 | 10/12/2015 | 1183.139 | 0.00038 | 10/7/2015 | -5 | 122.30 |
| 24 | 11/10/2015 | 1599.438 | 0.01923 | 11/8/2015 | -2 | 115.68 |
| 25 | 2/18/2016 | 1182.621 | 0.00021 | 2/12/2016 | -6 | 109.93 |
| 26 | 2/28/2016 | 1182.43 | 0.00026 | 2/28/2016 | 0 | 105.04 |

Table B-3: Regression statistics for linear fit for the Mississippi River and 2nd order polynomial fit for Colorado River.

| **River Name** (Q ~ z model) | **Coefficients** (Confidence interval) | **Significance of the coefficients** t-statistic and P-value | **Overall Significance** F-statistic and P-value |
|---|---|---|---|
| The Mississippi River (**Q** = a**z** + b) | a = 1759 (1575, 1943)<br>b = -4.642E+04 (-5.347E+04, -3.938E+04) | 18.88205, 1.09E-47<br>-12.9845, 6.62E-29 | 356.532, 1.09E-47 |
| The Colorado River (**Q** = a$z^2$+b**z**+c) | a = 37.83 (34.2, 41.46)<br>b = -8.934e+04 (-9.794e+04, -8.075e+04)<br>c = 5.275e+07 (4.766e+07, 5.783e+07) | 20.66456, 2.00E-38<br>-20.6148, 2.44E-38<br>20.56526, 2.98E-38 | 8432.035, 6.86E-115 |

**References**


Abedin, S., Stephen, H. (2019). GIS Framework for Spatiotemporal Mapping of Urban Flooding. *Geosciences*, *9*(2), 77. https://doi.org/10.3390/geosciences9020077

Abileah, R., Vignudelli, S., Scozzari, A. (2011). A completely remote sensing approach to monitoring reservoirs water volume. *Int. Water Technol. J*, *1*, 63–77.

Achhami, A., Kalra, A., Ahmad, S. (2018). Dynamic Simulation of Lake Mead Water Levels in Response to Climate Change and Varying Demands. *World Environmental and Water Resources Congress 2018*, 260–268. https://doi.org/10.1061/9780784481400.023

Adrian, R., O'Reilly, C. M., Zagarese, H., Baines, S. B., Hessen, D. O., Keller, W., … Van Donk, E. (2009). Lakes as sentinels of climate change. *Limnology and Oceanography*, *54*(6part2), 2283–2297.

Ahmad, S. (2016). Managing Water Demands for a Rapidly Growing City in Semi-Arid Environment: Study of Las Vegas, Nevada. *Int. J. Water Resour. Arid Env*, *5*(1), 35–42.

Ahmad, S., Kalra, A., Stephen, H. (2010). Estimating soil moisture using remote sensing data: A machine learning approach. *Advances in Water Resources*, *33*(1), 69–80. https://doi.org/10.1016/j.advwatres.2009.10.008

Allen, G. H., David, C. H., Andreadis, K. M., Hossain, F., Famiglietti, J. S. (2018). Global Estimates of River Flow Wave Travel Times and Implications for Low-Latency Satellite Data. *Geophysical Research Letters*, *45*(15), 7551–7560. https://doi.org/10.1029/2018GL077914

Alsdorf, D., Birkett, C., Dunne, T., Melack, J., Hess, L. (2001). Water level changes in a large Amazon lake measured with spaceborne radar interferometry and altimetry. *Geophysical Research Letters*, *28*(14), 2671–2674.

Arnell, N. W. (1999). Climate change and global water resources. *Global Environmental Change*, *9*, S31–S49. https://doi.org/https://doi.org/10.1016/S0959-3780(99)00017-5

Barnett, T. P., Pierce, D. W. (2008). When will Lake Mead go dry? *Water Resources Research*, *44*(3). https://doi.org/10.1029/2007WR006704

Benjamin Franklin - Inventions, Quotes & Facts - Biography. (n.d.). Retrieved April 20, 2019, from https://www.biography.com/scholar/benjamin-franklin#citation

Bhandari, S., Kalra, A., Tamaddun, K. A., Ahmad, S. (2018). Relationship between Ocean-Atmospheric Climate Variables and Regional Streamflow of the Conterminous United States. *Hydrology*, *5*(2), 30. https://doi.org/10.3390/hydrology5020030

Biancamaria, S., Hossain, F., Lettenmaier, D. P. (2011). Forecasting transboundary river water elevations from space. *Geophysical Research Letters*, *38*(11). https://doi.org/10.1029/2011GL047290

Biancamaria, S., Lettenmaier, D. P., Pavelsky, T. M. (2016). The SWOT Mission and Its Capabilities for Land Hydrology. In *Remote Sensing and Water Resources* (pp. 117–147). https://doi.org/10.1007/978-3-319-32449-4_6

Birkett, C. M. (1995). The contribution of TOPEX/POSEIDON to the global monitoring of climatically sensitive lakes. *Journal of Geophysical Research: Oceans*, *100*(C12), 25179–25204.

Birkett, C. M. (1998). Contribution of the TOPEX NASA Radar Altimeter to the global monitoring of large rivers and wetlands. *Water Resources Research*, *34*(5), 1223–1239. https://doi.org/10.1029/98WR00124

Birkett, C. M., Beckley, B. (2010). Investigating the Performance of the Jason-2/OSTM Radar Altimeter over Lakes and Reservoirs. *Marine Geodesy*, *33*(sup1), 204–238. https://doi.org/10.1080/01490419.2010.488983

Birkett, C. M., Mertes, L. A. K., Dunne, T., Costa, M. H., Jasinski, M. J. (2002). Surface water dynamics in the Amazon Basin: Application of satellite radar altimetry. *Journal of Geophysical Research: Atmospheres*, *107*(D20), LBA-26. https://doi.org/https://doi.org/10.1029/2001JD000609

Birkinshaw, S J, Moore, P., Kilsby, C. G., O'Donnell, G. M., Hardy, A. J., Berry, P. A. M. (2014). Daily discharge estimation at ungauged river sites using remote sensing. *Hydrological Processes*, *28*(3), 1043–1054. https://doi.org/10.1002/hyp.9647

Birkinshaw, Stephen J, O'Donnell, G. M., Moore, P., Kilsby, C. G., Fowler, H. J., Berry, P. A. M. (2010). Using satellite altimetry data to augment flow estimation techniques on the Mekong River. *Hydrological Processes*, *24*(26), 3811–3825. https://doi.org/10.1002/hyp.7811

Bjerklie, D. M. (2007). Estimating the bankfull velocity and discharge for rivers using remotely sensed river morphology information. *Journal of Hydrology*, *341*(3–4), 144–155. https://doi.org/https://doi.org/10.1016/j.jhydrol.2007.04.011

Bjerklie, D. M., Birkett, C. M., Jones, J. W., Carabajal, C., Rover, J. A., Fulton, J. W., Garambois, P.-A. (2018). Satellite remote sensing estimation of river discharge: Application to the Yukon River Alaska. *Journal of Hydrology*, *561*, 1000–1018. https://doi.org/10.1016/j.jhydrol.2018.04.005

Bjerklie, D. M., Lawrence Dingman, S., Vörösmarty, C. J., Bolster, C. H., Congalton, R. G. (2003). Evaluating the potential for measuring river discharge from space. *Journal of Hydrology*, *278*(1–4), 17–38. https://doi.org/10.1016/S0022-1694(03)00129-X

Bogning, S., Frappart, F., Blarel, F., Niño, F., Mahé, G., Bricquet, J.-P., … Braun, J.-J. (2018). Monitoring Water Levels and Discharges Using Radar Altimetry in an Ungauged River Basin: The Case of the Ogooué. *Remote Sensing*, *10*(3), 350. https://doi.org/10.3390/rs10020350

Bonnema, M. G., Sikder, S., Hossain, F., Durand, M., Gleason, C. J., Bjerklie, D. M. (2016). Benchmarking wide swath altimetry-based river discharge estimation algorithms for the Ganges river system. *Water Resources Research*, *52*(4), 2439–2461. https://doi.org/10.1002/2015WR017296

Boschetti, M., Nutini, F., Manfron, G., Brivio, P. A., Nelson, A. (2014). Comparative Analysis of Normalised Difference Spectral Indices Derived from MODIS for Detecting Surface Water in Flooded Rice Cropping Systems. *PLoS ONE*, *9*(2), e88741. https://doi.org/10.1371/journal.pone.0088741

Busker, T., de Roo, A., Gelati, E., Schwatke, C., Adamovic, M., Bisselink, B., … Cottam, A. (2019). A global lake and reservoir volume analysis using a surface water dataset and satellite altimetry. *Hydrology and Earth System Sciences*, *23*(2), 669–690. https://doi.org/10.5194/hess-23-669-2019

Calmant, S., Seyler, F., Crétaux, J.-F. (2008). Monitoring continental surface waters by satellite altimetry. *Surveys in Geophysics*, *29*(4–5), 247–269. https://doi.org/https://doi.org/10.1007/s10712-008-9051-1

Camarillo-Naranjo, J. M., Álvarez-Francoso, J. I., Limones-Rodríguez, N., Pita-López, M. F., Aguilar-Alba, M. (2019). The global climate monitor system: from climate data-handling to knowledge dissemination. *International Journal of Digital Earth*, *12*(4), 394–414. https://doi.org/10.1080/17538947.2018.1429502

Carroll, M., Wooten, M., DiMiceli, C., Sohlberg, R., Kelly, M. (2016). Quantifying Surface Water Dynamics at 30 Meter Spatial Resolution in the North American High Northern Latitudes 1991–2011. *Remote Sensing*, *8*(8), 622. https://doi.org/10.3390/rs8080622

Chelton, D. B., Ries, J. C., Haines, B. J., Fu, L. L., Callahan, P. S. (2001). Chapter 1 Satellite Altimetry. *International Geophysics*, *69*(C), 1–ii. https://doi.org/10.1016/S0074-6142(01)80146-7

Chen, C., Ahmad, S., Kalra, A., Xu, Z. (2017). A dynamic model for exploring water-resource management scenarios in an inland arid area: Shanshan County, Northwestern China. *Journal of Mountain Science*, *14*(6), 1039–1057. https://doi.org/https://doi.org/10.1007/s11629-016-4210-1

Coe, M. T., Birkett, C. M. (2004). Calculation of river discharge and prediction of lake height from satellite radar altimetry: Example for the Lake Chad basin. *Water Resources Research*, *40*(10), W10205. https://doi.org/10.1029/2003WR002543

Collins, M., Minobe, S., Barreiro, M., Bordoni, S., Kaspi, Y., Kuwano-Yoshida, A., … Sutton, R. (2018). Challenges and opportunities for improved understanding of regional climate dynamics. *Nature Climate Change*, 1. https://doi.org/https://doi.org/10.1016/S0074-6142(01)80146-7

Crétaux, J.-F., Abarca-del-Río, R., Berge-Nguyen, M., Arsen, A., Drolon, V., Clos, G., Maisongrande, P. (2016). Lake volume monitoring from space. *Surveys in Geophysics*,

*37*(2), 269–305. https://doi.org/https://doi.org/10.1007/s10712-016-9362-6

Crétaux, J.-F., Biancamaria, S., Arsen, A., Bergé-Nguyen, M., Becker, M. (2015). Global surveys of reservoirs and lakes from satellites and regional application to the Syrdarya river basin. *Environmental Research Letters*, *10*(1), 15002.

Crétaux, J.-F., Birkett, C. (2006). Lake studies from satellite radar altimetry. *Comptes Rendus Geoscience*, *338*(14–15), 1098–1112. https://doi.org/https://doi.org/10.1016/j.crte.2006.08.002

Crétaux, J.-F., Calmant, S. (2016). Spatial Altimetry and Continental Waters. In *Land Surface Remote Sensing in Continental Hydrology* (pp. 183–229). https://doi.org/10.1016/B978-1-78548-104-8.50006-1

Crétaux, J.-F., Jelinski, W., Calmant, S., Kouraev, A., Vuglinski, V., Bergé-Nguyen, M., … Cazenave, A. (2011). SOLS: A lake database to monitor in the Near Real Time water level and storage variations from remote sensing data. *Advances in Space Research*, *47*(9), 1497–1507. https://doi.org/https://doi.org/10.1016/j.asr.2011.01.004

Crétaux, J.-F., Kouraev, A. V., Papa, F., Bergé-Nguyen, M., Cazenave, A., Aladin, N., Plotnikov, I. S. (2005). Evolution of sea level of the Big Aral Sea from satellite altimetry and its implications for water balance. *Journal of Great Lakes Research*, *31*(4), 520–534. https://doi.org/10.1016/S0380-1330(05)70281-1

de Paiva, R. C. D., Buarque, D. C., Collischonn, W., Bonnet, M., Frappart, F., Calmant, S., Mendes, C. A. B. (2013). Large-scale hydrologic and hydrodynamic modeling of the Amazon River basin. *Water Resources Research*, *49*(3), 1226–1243. https://doi.org/10.1002/wrcr.20067

de Vito, R., Pagano, A., Portoghese, I., Giordano, R., Vurro, M., Fratino, U. (2019). Integrated Approach for Supporting Sustainable Water Resources Management of Irrigation Based on the WEFN Framework. *Water Resources Management*, 1–15. https://doi.org/https://doi.org/10.1007/s11269-019-2196-5

Drewes, H., Kuglitsch, F., Adám, J., Rózsa, S. (2016). The Geodesist's Handbook 2016. *Journal of Geodesy*, *90*(10), 907–1205. https://doi.org/10.1007/s00190-016-0948-z

Duan, Z., Bastiaanssen, W. G. M. (2013). Estimating water volume variations in lakes and reservoirs from four operational satellite altimetry databases and satellite imagery data. *Remote Sensing of Environment*, *134*, 403–416. https://doi.org/10.1016/j.rse.2013.03.010

Durand, M., Gleason, C. J., Garambois, P. A., Bjerklie, D., Smith, L. C., Roux, H., … Vilmin, L. (2016). An intercomparison of remote sensing river discharge estimation algorithms from measurements of river height, width, and slope. *Water Resources Research*, *52*(6), 4527–4549. https://doi.org/10.1002/2015WR018434

Durand, M., Neal, J., Rodríguez, E., Andreadis, K. M., Smith, L. C., Yoon, Y. (2014). Estimating reach-averaged discharge for the River Severn from measurements of river

water surface elevation and slope. *Journal of Hydrology*, *511*, 92–104. https://doi.org/10.1016/j.jhydrol.2013.12.050

Fekete, B. M., Vörösmarty, C. J. (2007). The current status of global river discharge monitoring and potential new technologies complementing traditional discharge measurements. *IAHS Publ*, *309*, 129–136.

Ferrari, R. L. (1988). Lake Powell survey. *US Bureau of Reclamation*.

Ficklin, D. L., Robeson, S. M., Knouft, J. H. (2016). Impacts of recent climate change on trends in baseflow and stormflow in United States watersheds. *Geophysical Research Letters*, *43*(10), 5079–5088. https://doi.org/10.1002/2016GL069121

Foody, G. (2010). Assessing the accuracy of remotely sensed data: principles and practices. *The Photogrammetric Record*, *25*(130), 204–205.

Frappart, F., Minh, K. Do, L'Hermitte, J., Cazenave, A., Ramillien, G., Le Toan, T., Mognard-Campbell, N. (2006). Water volume change in the lower Mekong from satellite altimetry and imagery data. *Geophysical Journal International*, *167*(2), 570–584. https://doi.org/10.1111/j.1365-246X.2006.03184.x

Frappart, F., Papa, F., Famiglietti, J. S., Prigent, C., Rossow, W. B., Seyler, F. (2008). Interannual variations of river water storage from a multiple satellite approach: A case study for the Rio Negro River basin. *Journal of Geophysical Research*, *113*(D21), D21104. https://doi.org/10.1029/2007JD009438

Frappart, F., Papa, F., Güntner, A., Werth, S., Ramillien, G., Prigent, C., … Bonnet, M.-P. (2010). Interannual variations of the terrestrial water storage in the Lower Ob' Basin from a multisatellite approach. *Hydrology and Earth System Sciences*, *14*(12), 2443–2453. https://doi.org/10.5194/hess-14-2443-2010

Frappart, F., Papa, F., Marieu, V., Malbeteau, Y., Jordy, F., Calmant, S., … Bala, S. (2015). Preliminary assessment of SARAL/AltiKa observations over the Ganges-Brahmaputra and Irrawaddy Rivers. *Marine Geodesy*, *38*(sup1), 568–580. https://doi.org/https://doi.org/10.1080/01490419.2014.990591

Frappart, F., Seyler, F., Martinez, J.-M., León, J. G., Cazenave, A. (2005). Floodplain water storage in the Negro River basin estimated from microwave remote sensing of inundation area and water levels. *Remote Sensing of Environment*, *99*(4), 387–399. https://doi.org/10.1016/j.rse.2005.08.016

Friedrich, K., Grossman, R. L., Huntington, J., Blanken, P. D., Lenters, J., Holman, K. D., … Kowalski, T. (2017). Reservoir Evaporation in the Western United States: Current Science, Challenges, and Future Needs. *Bulletin of the American Meteorological Society*, *99*(1), 167–187. https://doi.org/10.1175/bams-d-15-00224.1

Fu, L.-L., Cazenave, A. (2000). *Satellite altimetry and earth sciences: a handbook of techniques and applications* (Vol. 69). Elsevier.

Furnans, J., Austin, B. (2008). Hydrographic survey methods for determining reservoir volume. *Environmental Modelling & Software*, *23*(2), 139–146. https://doi.org/10.1016/j.envsoft.2007.05.011

Gao, H., Birkett, C., Lettenmaier, D. P. (2012). Global monitoring of large reservoir storage from satellite remote sensing. *Water Resources Research*, *48*(9). https://doi.org/10.1029/2012WR012063

Garambois, P.-A., Monnier, J. (2015). Inference of effective river properties from remotely sensed observations of water surface. *Advances in Water Resources*, *79*, 103–120. https://doi.org/10.1016/j.advwatres.2015.02.007

Ghorbani, K., Salarijazi, M., Abdolhosseini, M., Eslamian, S., Ahmadianfar, I. (2019). Evaluation of Clark IUH in rainfall-runoff modelling (case study: Amameh Basin). *International Journal of Hydrology Science and Technology*, *9*(2), 137. https://doi.org/10.1504/IJHST.2019.098131

Gleason, C. J., Smith, L. C. (2014). Toward global mapping of river discharge using satellite images and at-many-stations hydraulic geometry. *Proceedings of the National Academy of Sciences*, *111*(13), 4788–4791. https://doi.org/10.1073/pnas.1317606111

Goodall, J. L., Horsburgh, J. S., Whiteaker, T. L., Maidment, D. R., Zaslavsky, I. (2008). A first approach to web services for the National Water Information System. *Environmental Modelling & Software*, *23*(4), 404–411. https://doi.org/https://doi.org/10.1016/j.envsoft.2007.01.005

Grabs, W., Daamen, K., Gellens, D., Kwadijk, J. C. J., Lang, H., Middelkoop, H., … Wilke, K. (1997). *Impact of climate change on hydrological regimes and water resources management in the Rhine basin*. https://doi.org/https://doi.org/10.1023/A:1010784727448

Granata, F. (2019). Evapotranspiration evaluation models based on machine learning algorithms—A comparative study. *Agricultural Water Management*, *217*, 303–315. https://doi.org/10.1016/j.agwat.2019.03.015

Gutowski Jr, W. J., Chen, Y., Ötles, Z. (1997). Atmospheric Water Vapor Transport in NCEP-NCAR Reanalyses: Comparison with River Discharge in the Central United States. *Bulletin of the American Meteorological Society*, *78*(9), 1957–1969. https://doi.org/10.1175/1520-0477(1997)078<1957:AWVTIN>2.0.CO;2

Hagemann, S., Dumenil, L. (1998). Hydrological discharge model. In *Technical report No 17, MPI, Hamburg.* (p. 42).

Herschy, R. W. (2014). *Streamflow measurement*. CRC Press.

Hirpa, F. A., Hopson, T. M., De Groeve, T., Brakenridge, G. R., Gebremichael, M., Restrepo, P. J. (2013). Upstream satellite remote sensing for river discharge forecasting: Application to major rivers in South Asia. *Remote Sensing of Environment*, *131*, 140–151. https://doi.org/10.1016/j.rse.2012.11.013

Holtschlag, D. J., Koschik, J. A. (2003). *An acoustic Doppler current profiler survey of flow velocities in St. Clair River, a connecting channel of the Great Lakes*. https://doi.org/https://doi.org/10.3133/ofr03119

Hussain, A., Singh, J. K., Kumar, A. R. S., Harne K R. (2019). Rainfall-Runoff Modeling of Sutlej River Basin (India) Using Soft Computing Techniques. *International Journal of Agricultural and Environmental Information Systems*, *10*(2), 1–20. https://doi.org/10.4018/IJAEIS.2019040101

Hwang, C., Peng, M.-F., Ning, J., Luo, J., Sui, C.-H. (2005). Lake level variations in China from TOPEX/Poseidon altimetry: data quality assessment and links to precipitation and ENSO. *Geophysical Journal International*, *161*(1), 1–11. https://doi.org/10.1111/j.1365-246X.2005.02518.x

Irkett, C. M. B., Birkett, C. M. (1995). The contribution of TOPEX/POSEIDON to the global monitoring of climatically sensitive lakes. *Journal of Geophysical Research*, *100204*(15), 179–25. https://doi.org/10.1029/95JC02125

Jackson, R. B., Carpenter, S. R., Dahm, C. N., McKnight, D. M., Naiman, R. J., Postel, S. L., Running, S. W. (2001). Water in a changing world. *Ecological Applications*, *11*(4), 1027–1045. https://doi.org/https://doi.org/10.1890/1051-0761(2001)011[1027:WIACW]2.0.CO;2

Ji, L., Zhang, L., Wylie, B. (2009). Analysis of Dynamic Thresholds for the Normalized Difference Water Index. *Photogrammetric Engineering & Remote Sensing*, *75*(11), 1307–1317. https://doi.org/10.14358/PERS.75.11.1307

Jones, J. (2015). Efficient Wetland Surface Water Detection and Monitoring via Landsat: Comparison with in situ Data from the Everglades Depth Estimation Network. *Remote Sensing*, *7*(9), 12503–12538. https://doi.org/10.3390/rs70912503

Kalra, A., Sagarika, S., Pathak, P., Ahmad, S. (2017). Hydro-climatological changes in the Colorado River Basin over a century. *Hydrological Sciences Journal*, *62*(14), 2280–2296. https://doi.org/10.1080/02626667.2017.1372855

Kammerer, J. C. (1990). Largest rivers in the United States. *Open-File Report*, 2. Retrieved from http://pubs.usgs.gov/of/1987/ofr87-242/pdf/ofr87242.pdf

Keys, T. A., Scott, D. T. (2018). Monitoring volumetric fluctuations in tropical lakes and reservoirs using satellite remote sensing. *Lake and Reservoir Management*, *34*(2), 154–166. https://doi.org/10.1080/10402381.2017.1402226

Kim, D., Yu, H., Lee, H., Beighley, E., Durand, M., Alsdorf, D. E., Hwang, E. (2019). Ensemble learning regression for estimating river discharges using satellite altimetry data: Central Congo River as a Test-bed. *Remote Sensing of Environment*, *221*, 741–755. https://doi.org/10.1016/j.rse.2018.12.010

Kim, J.-W., Lu, Z., Jones, J. W., Shum, C. K., Lee, H., Jia, Y. (2014). Monitoring Everglades freshwater marsh water level using L-band synthetic aperture radar backscatter. *Remote*

*Sensing of Environment*, *150*, 66–81. https://doi.org/10.1016/j.rse.2014.03.031

Kleinherenbrink, M., Lindenbergh, R. C., Ditmar, P. G. (2015). Monitoring of lake level changes on the Tibetan Plateau and Tian Shan by retracking Cryosat SARIn waveforms. *Journal of Hydrology*, *521*, 119–131. https://doi.org/10.1016/j.jhydrol.2014.11.063

Kouraev, A. V, Zakharova, E. A., Samain, O., Mognard, N. M., Cazenave, A. (2004). Ob' river discharge from TOPEX/Poseidon satellite altimetry (1992–2002). *Remote Sensing of Environment*, *93*(1–2), 238–245. https://doi.org/10.1016/j.rse.2004.07.007

Lant, J. G., Boldt, J. A. (2018). *River meander modeling of the Wabash River near the Interstate 64 Bridge near Grayville, Illinois*. https://doi.org/https://doi.org/10.3133/sir20175117

Lehner, B., Reidy Liermann, C., Revenga, C., Vörösmarty, C. J., Fekete, B., Crouzet, P., … Magome, J. (2011). Global reservoir and dam database, version 1 (GRanDv1): Dams, revision 01. *Data Distributed by the NASA Socioeconomic Data and Applications Center (SEDAC)*.

Lei, Y., Yang, K., Wang, B., Sheng, Y., Bird, B. W., Zhang, G., Tian, L. (2014). Response of inland lake dynamics over the Tibetan Plateau to climate change. *Climatic Change*, *125*(2), 281–290. https://doi.org/10.1007/s10584-014-1175-3

Lei, Y., Yao, T., Yang, K., Bird, B. W., Tian, L., Zhang, X., … Wang, L. (2018). An integrated investigation of lake storage and water level changes in the Paiku Co basin, central Himalayas. *Journal of Hydrology*, *562*, 599–608. https://doi.org/10.1016/j.jhydrol.2018.05.040

Liu, Y., Song, P., Peng, J., Ye, C. (2012). A physical explanation of the variation in threshold for delineating terrestrial water surfaces from multi-temporal images: effects of radiometric correction. *International Journal of Remote Sensing*, *33*(18), 5862–5875. https://doi.org/10.1080/01431161.2012.675452

Makarigakis, A., Jimenez-Cisneros, B. (2019). UNESCO's Contribution to Face Global Water Challenges. *Water*, *11*(2), 388. https://doi.org/10.3390/w11020388

Mallakpour, I., Villarini, G. (2016). Investigating the relationship between the frequency of flooding over the central United States and large-scale climate. *Advances in Water Resources*, *92*, 159–171. https://doi.org/10.1016/j.advwatres.2016.04.008

Maswood, M., Hossain, F. (2015). International Journal of River Basin Management Advancing river modelling in ungauged basins using satellite remote sensing: the case of the Ganges-Brahmaputra-Meghna basin Advancing river modelling in ungauged basins using satellite remote sensing: the c. *International Journal of River Basin Management*, *14*(1), 103–117. https://doi.org/10.1080/15715124.2015.1089250org/10.1080/15715124.2015.1089250

Maswood, M., Hossain, F. (2016). Advancing river modelling in ungauged basins using satellite remote sensing: the case of the Ganges–Brahmaputra–Meghna basin. *International Journal of River Basin Management*, *14*(1), 103–117.

https://doi.org/10.1080/15715124.2015.1089250

McFeeters, S. K. (1996). The use of the Normalized Difference Water Index (NDWI) in the delineation of open water features. *International Journal of Remote Sensing*, *17*(7), 1425–1432. https://doi.org/https://doi.org/10.1080/01431169608948714

Medina, C. E., Gomez-Enri, J., Alonso, J. J., Villares, P. (2008). Water level fluctuations derived from ENVISAT Radar Altimeter (RA-2) and in-situ measurements in a subtropical waterbody: Lake Izabal (Guatemala). *Remote Sensing of Environment*, *112*(9), 3604–3617. https://doi.org/10.1016/j.rse.2008.05.001

Michailovsky, C. I., McEnnis, S., Berry, P. A. M., Smith, R., Bauer-Gottwein, P. (2012). River monitoring from satellite radar altimetry in the Zambezi River basin. *Hydrology and Earth System Sciences*, *16*(7), 2181–2192. https://doi.org/10.5194/hess-16-2181-2012

Milly, P. C. D., Betancourt, J., Falkenmark, M., Hirsch, R. M., Kundzewicz, Z. W., Lettenmaier, D. P., Stouffer, R. J. (2008). Stationarity Is Dead: Whither Water Management? *Science*, *319*(5863), 573–574. https://doi.org/10.1126/science.1151915

Milly, P. C. D., Dunne, K. A., Vecchia, A. V. (2005). Global pattern of trends in streamflow and water availability in a changing climate. *Nature*, *438*(7066), 347–350. https://doi.org/10.1038/nature04312

Moradi, M., Sahebi, M., Shokri, M. (2017). Modified optimization water index (MOWI) for Landsat-8 OLI/TIRS. *International Archives of the Photogrammetry, Remote Sensing and Spatial Information Sciences*, *42*(4/W4).

Moumouni, Y. (2014). A System Dynamics Model for Energy Planning in Niger. *International Journal of Energy and Power Engineering*, *3*(6), 308. https://doi.org/10.11648/j.ijepe.20140306.14

Nazari-Sharabian, M., Taheriyoun, M., Ahmad, S., Karakouzian, M., Ahmadi, A. (2019). Water Quality Modeling of Mahabad Dam Watershed–Reservoir System under Climate Change Conditions, Using SWAT and System Dynamics. *Water*, *11*(2), 394. https://doi.org/10.3390/w11020394

Nishat, B., Rahman, S. M. M. (2009). Water Resources Modeling of the Ganges-Brahmaputra-Meghna River Basins Using Satellite Remote Sensing Data1. *Journal of the American Water Resources Association*, *45*(6), 1313–1327. https://doi.org/DOI 10.1111/j.1752-1688.2009.00374.x

Normandin, C., Frappart, F., Diepkilé, A. T., Marieu, V., Mougin, E., Blarel, F., … Ba, A. (2018). Evolution of the Performances of Radar Altimetry Missions from ERS-2 to Sentinel-3A over the Inner Niger Delta. *Remote Sensing*, *10*(6), 833. https://doi.org/10.3390/rs10060833

Oubanas, H., Gejadze, I., Malaterre, P.-O., Mercier, F. (2018). River discharge estimation from synthetic SWOT-type observations using variational data assimilation and the full Saint-

Venant hydraulic model. *Journal of Hydrology*, *559*, 638–647. https://doi.org/10.1016/j.jhydrol.2018.02.004

Ouma, Y. O., Tateishi, R. (2006). A water index for rapid mapping of shoreline changes of five East African Rift Valley lakes: an empirical analysis using Landsat TM and ETM+ data. *International Journal of Remote Sensing*, *27*(15), 3153–3181. https://doi.org/10.1080/01431160500309934

Papa, F., Bala, S. K., Pandey, R. K., Durand, F., Gopalakrishna, V. V, Rahman, A., Rossow, W. B. (2012). Ganga-Brahmaputra river discharge from Jason-2 radar altimetry: An update to the long-term satellite-derived estimates of continental freshwater forcing flux into the Bay of Bengal. *Journal of Geophysical Research: Oceans*, *117*(C11), n/a-n/a. https://doi.org/10.1029/2012JC008158

Paris, A., Dias de Paiva, R., Santos da Silva, J., Medeiros Moreira, D., Calmant, S., Garambois, P., … Seyler, F. (2016). Stage-discharge rating curves based on satellite altimetry and modeled discharge in the Amazon basin. *Water Resources Research*, *52*(5), 3787–3814. https://doi.org/10.1002/2014WR016618

Pathak, P., Kalra, A., Ahmad, S., Bernardez, M. (2016). Wavelet-aided analysis to estimate seasonal variability and dominant periodicities in temperature, precipitation, and streamflow in the Midwestern United States. *Water Resources Management*, *30*(13), 4649–4665. https://doi.org/https://doi.org/10.1007/s11269-016-1445-0

Peng, D., Guo, S., Liu, P., Liu, T. (2006). Reservoir storage curve estimation based on remote sensing data. *Journal of Hydrologic Engineering*, *11*(2), 165–172. https://doi.org/https://doi.org/10.1061/(ASCE)1084-0699(2006)11:2(165)

Puri, S., Stephen, H., Ahmad, S. (2011a). Relating TRMM Precipitation Radar backscatter to water stage in wetlands. *Journal of Hydrology*, *401*(3–4), 240–249. https://doi.org/10.1016/j.jhydrol.2011.02.026

Puri, S., Stephen, H., Ahmad, S. (2011b). Relating TRMM precipitation radar land surface backscatter response to soil moisture in the Southern United States. *Journal of Hydrology*, *402*(1–2), 115–125. https://doi.org/10.1016/j.jhydrol.2011.03.012

Qaiser, K., Ahmad, S., Johnson, W., Batista, J. (2011). Evaluating the impact of water conservation on fate of outdoor water use: A study in an arid region. *Journal of Environmental Management*, *92*(8), 2061–2068. https://doi.org/10.1016/j.jenvman.2011.03.031

Qaiser, K., Ahmad, S., Johnson, W., Batista, J. R. (2013). Evaluating Water Conservation and Reuse Policies Using a Dynamic Water Balance Model. *Environmental Management*, *51*(2), 449–458. https://doi.org/10.1007/s00267-012-9965-8

Rantz, S. E. (1982). *Measurement and computation of streamflow* (Vol. 2175). US Department of the Interior, Geological Survey.

Rind, M. A., Ansari, K., Saher, R., Shakya, S., Ahmad, S. (2018). Watershed. *World Environmental and Water Resources Congress 2018*, 468–482. https://doi.org/10.1061/9780784481400.044

Rosmorduc, V., Benveniste, J., Lauret, O., Maheu, C., Milagro, M., Picot, N. (2011). Radar altimetry tutorial. *ESA, Europe*, 112–128.

Sagarika, S., Kalra, A., Ahmad, S. (2015). Interconnections between oceanic-atmospheric indices and variability in the U.S. streamflow. *Journal of Hydrology*, *525*, 724–736. https://doi.org/10.1016/j.jhydrol.2015.04.020

Schmidt, G., Jenkerson, C. B., Masek, J., Vermote, E., Gao, F. (2013). *Landsat ecosystem disturbance adaptive processing system (LEDAPS) algorithm description*. https://doi.org/https://doi.org/10.3133/ofr20131057

Schwatke, C., Dettmering, D., Bosch, W., Seitz, F. (2015). DAHITI – an innovative approach for estimating water level time series over inland waters using multi-mission satellite altimetry. *Hydrology and Earth System Sciences*, *19*(10), 4345–4364. https://doi.org/10.5194/hess-19-4345-2015

Shakya, S., Kalra, A., Ahmad, S. (2018). A Dynamic Simulation Approach to Analyze Hydro-Electric Energy Production under Variable Flow and Demand Conditions. *World Environmental and Water Resources Congress 2018*, 244–259. https://doi.org/10.1061/9780784481400.022

Shiklomanov, A. I., Lammers, R. B., Vörösmarty, C. J. (2002). Widespread decline in hydrological monitoring threatens Pan-Arctic Research. *Eos, Transactions American Geophysical Union*, *83*(2), 13. https://doi.org/10.1029/2002EO000007

Sichangi, A. W., Wang, L., Yang, K., Chen, D., Wang, Z., Li, X., … Kuria, D. (2016). Estimating continental river basin discharges using multiple remote sensing data sets. *Remote Sensing of Environment*, *179*, 36–53. https://doi.org/10.1016/j.rse.2016.03.019

Singh, A., Seitz, F., Schwatke, C. (2012). Inter-annual water storage changes in the Aral Sea from multi-mission satellite altimetry, optical remote sensing, and GRACE satellite gravimetry. *Remote Sensing of Environment*, *123*, 187–195. https://doi.org/10.1016/j.rse.2012.01.001

Smith, L. C. (1997). Satellite remote sensing of river inundation area, stage, and discharge: A review. *Hydrological Processes*, *11*(10), 1427–1439.

Song, X., Zhang, J., Zhang, C., Zou, X. (2019). A Comprehensive Analysis of the Changes in Precipitation Patterns over Beijing during 1960–2012. *Advances in Meteorology*, *2019*, 1–22. https://doi.org/10.1155/2019/6364040

Stephen, H., Ahmad, S., Piechota, T. C. (2010). Land Surface Brightness Temperature Modeling Using Solar Insolation. *IEEE Transactions on Geoscience and Remote Sensing*, *48*(1), 491–498. https://doi.org/10.1109/TGRS.2009.2026893

Stephen, H., Ahmad, S., Piechota, T. C., Tang, C. (2010). Relating surface backscatter response from TRMM precipitation radar to soil moisture: results over a semi-arid region. *Hydrology and Earth System Sciences*, *14*(2), 193–204. https://doi.org/10.5194/hess-14-193-2010

Stewart, R. H. (1985). *Methods of satellite oceanography*.

Tamaddun, K. A., Kalra, A., Ahmad, S. (2016). Identification of Streamflow Changes across the Continental United States Using Variable Record Lengths. *Hydrology*, *3*(2), 24. https://doi.org/10.3390/hydrology3020024

Tamaddun, K. A., Kalra, A., Ahmad, S. (2017). Wavelet analyses of western US streamflow with ENSO and PDO. *Journal of Water and Climate Change*, *8*(1), 26–39. https://doi.org/10.2166/wcc.2016.162

Tamaddun, K. A., Kalra, A., Ahmad, S. (2018). Potential of rooftop rainwater harvesting to meet outdoor water demand in arid regions. *Journal of Arid Land*, *10*(1), 68–83. https://doi.org/10.1007/s40333-017-0110-7

Tamaddun, K. A., Kalra, A., Ahmad, S. (2019). Spatiotemporal Variation in the Continental US Streamflow in Association with Large-Scale Climate Signals Across Multiple Spectral Bands. *Water Resources Management*, 1–22. https://doi.org/10.1007/s11269-019-02217-8

Tarpanelli, A., Amarnath, G., Brocca, L., Massari, C., Moramarco, T. (2017). Discharge estimation and forecasting by MODIS and altimetry data in Niger-Benue River. *Remote Sensing of Environment*, *195*, 96–106. https://doi.org/10.1016/j.rse.2017.04.015

Tighi, S., Callejo, R. (2011). *Lake Mead Area and Capacity Tables*. (September), 153.

Tong, X., Pan, H., Xie, H., Xu, X., Li, F., Chen, L., … Jin, Y. (2016). Estimating water volume variations in Lake Victoria over the past 22 years using multi-mission altimetry and remotely sensed images. *Remote Sensing of Environment*, *187*, 400–413. https://doi.org/10.1016/j.rse.2016.10.012

Tourian, M. J., Schwatke, C., Sneeuw, N. (2017). River discharge estimation at daily resolution from satellite altimetry over an entire river basin. *Journal of Hydrology*, *546*, 230–247. https://doi.org/10.1016/j.jhydrol.2017.01.009

Twichell, D. C., Cross, V. A., Belew, S. D. (2003). *Mapping the floor of Lake Mead (Nevada and Arizona): Preliminary discussion and GIS data release*.

Villarini, G., Serinaldi, F., Smith, J. A., Krajewski, W. F. (2009). On the stationarity of annual flood peaks in the continental United States during the 20th century. *Water Resources Research*, *45*(8). https://doi.org/10.1029/2008WR007645

Vörösmarty, C. J. (2000). Global Water Resources: Vulnerability from Climate Change and Population Growth. *Science*, *289*(5477), 284–288. https://doi.org/10.1126/science.289.5477.284

Vörösmarty, C. J., Askew, A., Grabs, W., Barry, R. G., Birkett, C., Doll, P., … Webster, F. (2001). Global water data: A newly endangered species. *Eos, Transactions American Geophysical Union*, *82*(5), 54–54. https://doi.org/10.1029/01EO00031

Voss, K. A., Famiglietti, J. S., Lo, M., de Linage, C., Rodell, M., Swenson, S. C. (2013). Groundwater depletion in the Middle East from GRACE with implications for transboundary water management in the Tigris-Euphrates-Western Iran region. *Water Resources Research*, *49*(2), 904–914. https://doi.org/10.1002/wrcr.20078

Westenburg, C. L., DeMeo, G. A., Tanko, D. J. (2006). *Evaporation from Lake Mead, Arizona and Nevada, 1997-99*. US Geological Survey.

Westerink, J. J., Gray, W. G. (1991). Progress in surface water modeling. *Reviews of Geophysics*, *29*(S1), 210–217.

Wood, E. F. (1991). Global scale hydrology: Advances in land surface modeling. *Reviews of Geophysics*, *29*(S1), 193–201.

Xu, H. (2006). Modification of normalised difference water index (NDWI) to enhance open water features in remotely sensed imagery. *International Journal of Remote Sensing*, *27*(14), 3025–3033. https://doi.org/10.1080/01431160600589179

Yang, T., Li, Q., Ahmad, S., Zhou, H., Li, L. (2019). Changes in Snow Phenology from 1979 to 2016 over the Tianshan Mountains, Central Asia. *Remote Sensing*, *11*(5), 499. https://doi.org/10.3390/rs11050499

Zhai, K., Wu, X., Qin, Y., Du, P. (2015). Comparison of surface water extraction performances of different classic water indices using OLI and TM imageries in different situations. *Geo-Spatial Information Science*, *18*(1), 32–42. https://doi.org/10.1080/10095020.2015.1017911

Zhang, H., Gorelick, S. M., Zimba, P. V, Zhang, X. (2017). A remote sensing method for estimating regional reservoir area and evaporative loss. *Journal of Hydrology*, *555*, 213–227. https://doi.org/10.1016/j.jhydrol.2017.10.007

Zhang, J., Xu, K., Yang, Y., Qi, L., Hayashi, S., Watanabe, M. (2006). Measuring Water Storage Fluctuations in Lake Dongting, China, by Topex/Poseidon Satellite Altimetry. *Environmental Monitoring and Assessment*, *115*(1–3), 23–37. https://doi.org/10.1007/s10661-006-5233-9

Zhang, S., Gao, H., Naz, B. S. (2014). Monitoring reservoir storage in South Asia from multisatellite remote sensing. *Water Resources Research*, *50*(11), 8927–8943. https://doi.org/10.1002/2014WR015829

Zhou, T., Nijssen, B., Gao, H., Lettenmaier, D. P. (2016). The contribution of reservoirs to global land surface water storage variations. *Journal of Hydrometeorology*, *17*(1), 309–325. https://doi.org/https://doi.org/10.1175/JHM-D-15-0002.1

**Curriculum Vitae**

**Sailuj Shakya**

---

Date: May 2019

Graduate College
University of Nevada, Las Vegas
Department of Civil and Environmental Engineering and Construction

Email address: e.sailuz.shakya@gmail.com

Education

University of Nevada, Las Vegas
M.S.E. Civil and Environmental Engineering, May 2019

Tribhuwan University, Kathmandu, Nepal
B.E. Civil Engineering, May 2014

Thesis Title: Estimation of Stage-area-storage relationships in reservoirs and Stage-discharge relationships in rivers using remotely sensed data.

Thesis Examination Committee:

Co-chairperson, Dr. Sajjad Ahmad
Co-chairperson, Dr. Haroon Stephen
Committee Member Dr. David James
Graduate College Representative, Dr. Pushkin Kachroo